A Microscopic Study of Cohesin

James David Peter Rhodes

Brasenose College

Department of Biochemistry

University of Oxford

A thesis submitted for the degree of

Doctor of Philosophy

Trinity 2017

Abstract

Cohesin is a ring-shaped Smc (Structural Maintenance of Chromosomes) complex that mediates DNA-DNA interactions between chromosomes (sister chromatid cohesion) and within chromosomes (looping). The mechanisms behind loop formation and cohesion establishment are not known despite cohesin's discovery 20 years ago. In this thesis findings are presented from two projects: one examining the establishment of sister chromatid cohesion and the other the formation of DNA loops by cohesin.

Cohesin can remain associated with chromosomes during DNA replication – Sister chromatid cohesion is established at the DNA replication fork. It is not known whether cohesin that is loaded ahead of the fork is used to build cohesion or if it is dislodged and cohesion is built from cohesin rings in the soluble pool. To address this the objective was to determine whether cohesin removal from chromatin is a necessary aspect of DNA replication. Cohesin was fluorescently labelled in a cell line in which cohesin's normal releasing activity was abrogated and cohesin's association with chromatin was followed across S phase. It was found that cohesin could remain in defined subnuclear areas demonstrating that the complex can remain bound to DNA despite replication fork passage. This finding is consistent with the conversion of cohesin that is loaded ahead of the replication fork into its cohesive state.

The cohesin loading factor Scc2 hops between cohesin rings – The human genome is organised into a series of megabase scale domains that interact with themselves more than sequences outside of the domain. Interactions inside theses Topologically Associating Domains (TADs) depend on the cohesin complex and are postulated to form by progressive loop enlargement through cohesin's lumen (loop extrustion). If this is the mechanism then cohesin must be able to translocate vast distances. Recent evidence suggests that Smc complexes are motor proteins and their translocation depends on ATP

hydrolysis. Cohesin's ATPase is stimulated by Scc2 (Nipbl) however this protein is thought to be involved exclusively during the cohesin loading reaction. Consistently, little colocalisation is detected between cohesin and Scc2 as measured by chromatin immunoprecipitation followed by massively parallel sequencing (ChIP-Seq). The aim of this project was to determine whether cohesin and Scc2 interact on DNA after the loading reaction. Using fluorescence recovery after photobleaching (FRAP) and single particle tracking it has been shown that Scc2 turns over rapidly on chromatin indicative of an association independent of cohesin loading, a process that is infrequent due to cohesin's long residence time. It was also found that stabilisation of cohesin on DNA leads to increased Scc2 chromosomal association and cohesin depletion leads to reduced association. These findings provide evidence for a post-loading association between cohesin and Scc2. Intriguingly, Scc2 was also found to spread across chromatin and cohesin vermicelli very slowly consistent with hopping between cohesin rings. Fluorescence analysis of Scc2 and Scc1 indicate that Scc2 is substoichiometric to cohesin. It was therefore proposed that due to an abundance of binding sites for Scc2, a low diffusion coefficient and a high on-rate, that Scc2 hops between cohesin rings performing a function distinct from loading.

Acknowledgments

I would first like to thank Kim Nasmyth for his supervision over the last four years. I am extremely grateful for his patience and encouragement. The academic environment in the group is as stimulating as it is unforgiving and collaborating with Kim has been a formative experience.

I would also like to thank Ahmed Rattani who mentored me in the early days. Thank you to Jon Godwin for the training, administration of the mouse colony and all the procedures you performed on my behalf. To Ricardo Nunes Bastos for help with gene editing. I am also grateful to Lana Strmecki for performing all the administrative duties of a supervisor. I want to thank all the people in the department who helped me in any way or provided reagents. Thank you to Benjamin Rowland, Judith Haarhuis and Luke Lavis who provided critical materials and advice. I am also grateful to Stephan Uphoff for showing me how to perform single particle tracking and for a fruitful collaboration.

I also want to thank my family for their support during my DPhil. It has been lovely living so close to home and I'm always looking forward to us all getting back together. To Margot, it has been an amazing experience getting to know you over the last year. I am very grateful to Beth Watts for looking after me and for proofreading this thesis.

Finally thank you to the friends who have been there for me over the last four years. To the guys in the lab, particularly Sarah Dixon and Fred Beckouët, you made it a fun place to work. I am especially grateful to the Alderney guys for having me to stay with you in London every weekend during my second year and the White Rabbit lot for all the good and sometimes very strange times. You have all been a wonderful distraction.

To Mum and Dad

Table of Contents

Chapter I Introduction

The Eukaryotic Cell Cycle

The growth and division of cells is central to the reproduction and development of all living organisms. The eukaryotic cell cycle can be divided into two main stages (Fig. 1-1) (Morgan, 2007). Interphase is the period when the cell's contents are synthesised and replicated, and mitosis (M phase) is when the cell and its contents are divided into two daughter cells. Interphase can be subdivided into G1 (Gap 1), S phase (Synthesis) and G2 (Gap 2). Throughout interphase the cell generates new components but only during S phase is the genome replicated. The length of these phases varies greatly between organisms and cell types but interphase always lasts longer than mitosis.

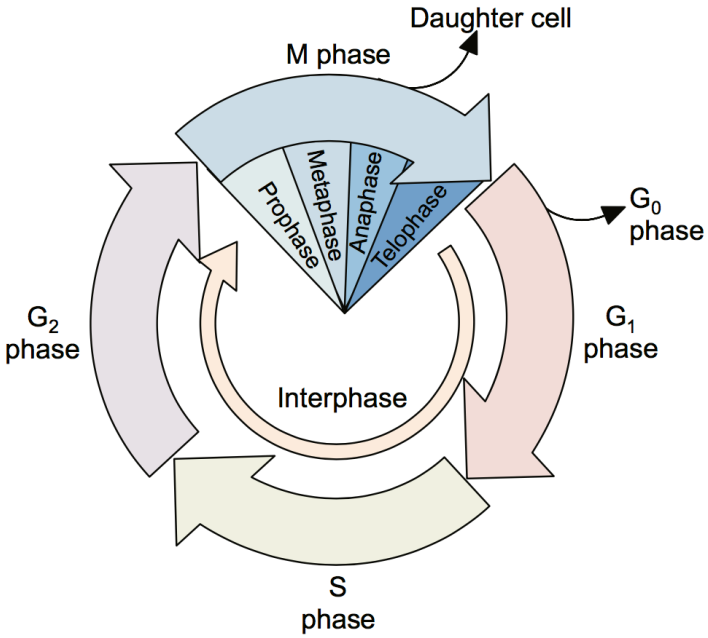

Figure 1-1 The Eukaryotic Cell Cycle The cell cycle is divided into interphase and M phase. G1, S and G2 constitute interphase when cellular components are synthesised and the genome is duplicated. During M phase the cell and the genome is divided and the daughter cells re-enter the cell cycle at G1. M phase is divided into prophase, metaphase, anaphase and telophase. Illustration made by Naomi Petela.

Mitosis is divided into four stages. During prophase the nuclear envelope breaks down and chromosomes metamorphose into rod-shaped structures that are easily transported around

the cell. This process is known as chromosome condensation. Metaphase involves the transport of the condensed chromosomes to the centre of the cell. Once all the chromosomes are aligned, the cell enters anaphase at which point sister chromatid disjunction occurs and sister chromatids are transported to opposite sides of the cell. The cell then enters telophase where the cell divides (cytokinesis) and nuclear membranes reform around the segregated chromosomes. At this point segregated chromosomes decondense and the cell cycle restarts in G1.

The cell cycle is controlled by a series of molecular switches which ensure the sequential progression from one stage to the next. The switches are controlled by two families of protein: cyclins and cyclin-dependent kinases (CDKs) (Evans et al., 1983; Lee and Nurse, 1987). Cyclins activate CDKs and changes in cyclin concentration dictate CDK activity. CDKs, in turn, phosphorylate a vast range of substrates and it is this phosphorylation that governs cell cycle progression (Morgan, 2007). Introduction of both positive and negative feedback loops introduces 'bistability' into the system. This ensures that once a threshold CDK activity has been reached the activity only increases and the cells progress unidirectionally into the next stage of the cell cycle (Novak et al., 2007).

DNA Replication

In order to maintain the correct number of genes in a cell, the genome must be replicated once and only once per cell cycle. For this reason DNA replication in eukaryotic cells is a tightly regulated event, which can be divided into three processes: initiation, elongation and termination. Initiation involves the assembly of the pre-replication complex (pre-RC). This happens exclusively when CDK activity is low, at the end of mitosis and G1, ensuring that DNA is not re-replicated (Dutta and Bell, 1997). Pre-RC formation begins with the loading of the Origin of Replication Complex (ORC 1-6) to specific DNA sequences called

origins of replication (Bell and Stillman, 1992; Stillman, 1993). Cdc6 is recruited to ORC, which in turn recruits the licensing factor Cdt1, and the MCM helicase (Grallert and Nurse, 1996; Liang et al., 1995; Nishitani et al., 2000). This chromatin-associated complex is the pre-RC. DNA replication initiates when cells transition from G1 to S phase. At this point MCM helicase is phosphorylated by Cdc7-Dbf4 kinase (DDK) and CDK resulting in the recruitment of key members of the replisome including DNA polymerases and Proliferating Cell Nuclear Antigen (PCNA) (Bell and Dutta, 2002). The complex has now become a replisome and the origin is said to have fired. The MCM-Cdc45-GINS complex unwinds the DNA and DNA polymerase ε and DNA polymerase δ replicate the leading and lagging strands respectively (Gambus et al., 2006). Many components of the replisome contribute to the processivity of the replication fork, including PCNA which improves the stability of the interaction between DNA polymerase and DNA (Bravo et al., 1987). To account for the enormous size of eukaryotic chromosomes multiple replisomes progress bi-directionally and simultaneously on each chromosome. If no other roadblock is reached, elongation continues until the replisome reaches a sequence of replicated DNA or it collides with another replisome approaching in the opposite direction (Bell and Dutta, 2002). When this happens replication stops and the resultant nicks between the replicons are joined by a DNA ligase. The product of DNA replication is two copies of each chromosome that can be packaged and delivered into daughter cells.

Sister Chromatid Cohesion

Most bacteria replicate and segregate their genetic content simultaneously (Webb et al., 1997). By using this mechanism the cell does not risk placing both sister chromosomes in the same daughter cell, leaving the other with no DNA. In eukaryotic cells, however, there is a gap (G2) between DNA replication and chromosome segregation. How then does the

cell know which chromosomes to put in which daughter cell? The eukaryotic cell has evolved a mechanism to solve this conundrum. Sister chromatids are held tightly together from their replication until cell division. This connection is called sister chromatid cohesion and it allows the cell to recognise pairs of chromosomes which, in turn, means they can be divided between daughter cells when the time comes.

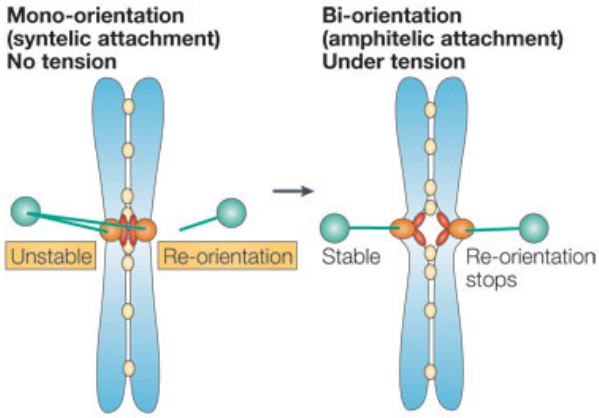

Figure 1-2 Bi-orientation of sister kinetochores If microtubules emanating from the same side of the cell attaches to both sister kinetochores (mono-orientation) the attachments are destabilised. This error-correction continues until sister kinetochores are being pulled away from each other (bi-orientation). Illustration from (Tanaka et al., 2005).

During metaphase microtubules emanating from both sides of the cell bind to kinetochores located at the centromeres of chromosomes (Fig. 1-2). The aim is to attach microtubules from one side of the cell to one sister kinetochore and microtubules emanating from the opposite side of cell to the other sister kinetochore (bi-orientation). Incorrect attachments occur (mono-oriented) but because they do not generate tension across the centromere they are destabilised. This process continues until every chromosome is bi-oriented, at which point sister chromatid cohesion is destroyed and sister chromatids are pulled to opposite sides of the cell. Sister chromatid cohesion is essential for this process for two reasons: first it provides resistance to the pulling forces of the microtubules so chromatids can be recognised as sisters, and second, by resisting the pulling forces tension is generated across centromeres when bi-oriented. By using tension across all centromeres as the trigger for

anaphase onset the cell ensures that when it divides each daughter will inherit a full complement of the genome.

The Cohesin Complex

The connection between sister chromatids has been observed since Walter Flemming first stained chromosomes (Flemming, 1879). However, the physical nature of these attachments remained enigmatic for over a century. It was first suggested that DNA catenation generated during DNA replication could hold sister chromatids together. However, sister minichromosomes could be separated by incubation in SDS, indicating a central role for proteins in sister chromatid cohesion (Koshland and Hartwell, 1987). A series of genetic screens in budding yeast revealed several genes that were required for sister chromatid cohesion (Guacci et al., 1997; Michaelis et al., 1997; Toth et al., 1999). Four of these proteins, Smc1, Smc3, Scc1 (Rad21) and Scc3 (SA1/2) were later shown to form a stable complex that was named “cohesin” (Toth et al., 1999).

Smc1 and Smc3 are members of the structural maintenance of chromosomes (Smc) family of proteins, which are found in all living organisms from bacteria to humans (Niki et al., 1991; Strunnikov et al., 1993). These proteins have diverse functions in DNA metabolism including sister chromatid cohesion, chromosome condensation and DNA repair (Nasmyth and Haering, 2005). Smc proteins fold back on themselves to form long rods with most of the length making an anti-parallel coiled coil (Fig. 1-3a) (Haering et al., 2002; Niki et al., 1992). There is a globular domain at each end of the coiled coil. At one end is the 'hinge' domain, which is composed of the central part of the polypeptide chain (Fig. 1-3b). Smc proteins dimerise via their hinge domains, with bacterial Smc proteins forming homodimers and eukaryotic Smc proteins forming heterodimers. At the other end of the Smc coiled coil is the head domain, which is composed of the N- and C-terminal regions.

When two Smc heads domains dimerise they form an ATP Binding Cassette (ABC)-type ATPase.

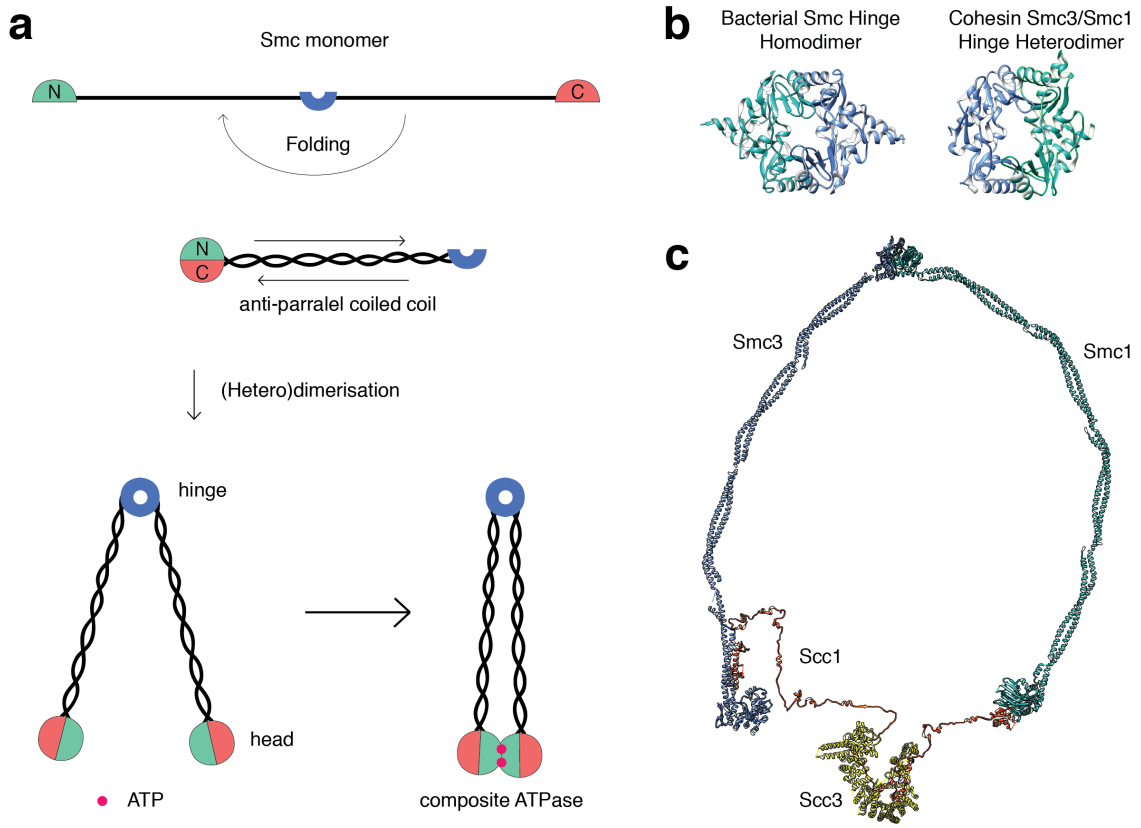

Figure 1-3 Architecture of the cohesin complex a) Smc proteins have part of their head domain at the N-terminus and part at the C-terminus. The Smc folds back on itself at the hinge domain allowing the head domain to fold. The head and hinge domains are separated by a 50 nm long coiled coil. Smc proteins dimerise via the hinge making a stable V-shaped heterodimer. Head domains transiently dimerise in the presence of ATP forming two active ATPases **b)** Smc hinge domains form toroidal dimers: Left: *T. maritima* Smc hinge homodimer (Green and blue are two molecules of the same protein) (PDB: 1gxl) Right: Heterodimer of Smc3 (blue) and Smc1 (green) hinge domains from *M. musculus* (PDB: 2wd5) **c)** A model of the core cohesin complex based on crystal structures. Smc3 (blue), Smc1 (green) and Scc1 (orange) form a ring while Scc3 (yellow) binds to Scc1. Modified from a model made by Kim Nasmyth.

When Smc1 and Smc3 dimerise via their hinge domain they form a V-shaped heterodimer (Fig. 1-3a). Scc1 binds to Smc3's coiled coil via its N-terminal domain and Smc1's head domain via its C-terminal domain thereby creating an enormous closed ring (Fig. 1-3c) (Gligoris et al., 2014; Gruber et al., 2003; Haering et al., 2004). Scc3 binds to Scc1 and provides a regulatory platform for other interacting proteins (Fig. 1-3c) (Hara et al., 2014; Toth et al., 1999).

The Cohesin Cycle and its Regulatory Proteins

Loading of cohesin onto chromosomes begins in telophase (Sumara et al., 2000; Watrin et al., 2006). Cohesin's initial association with chromatin depends on a separate complex of Scc2 (Nipbl) and Scc4 (Mau2), known as the loading complex (Fig. 1-4) (Ciosk et al., 2000; Gillespie and Hirano, 2004) (Fig. 1-4). Once on the DNA, cohesin can be released by Wapl and Pds5 (Fig. 1-4) (Kueng et al., 2006; Ouyang et al., 2016) which open the Smc3-Scc1 interface (Beckouët et al., 2016; Chan et al., 2012). The equilibrium between loading and release gives cohesin a mean residence time on DNA of approximately 20 minutes (Gerlich et al., 2006; Hansen et al., 2017).

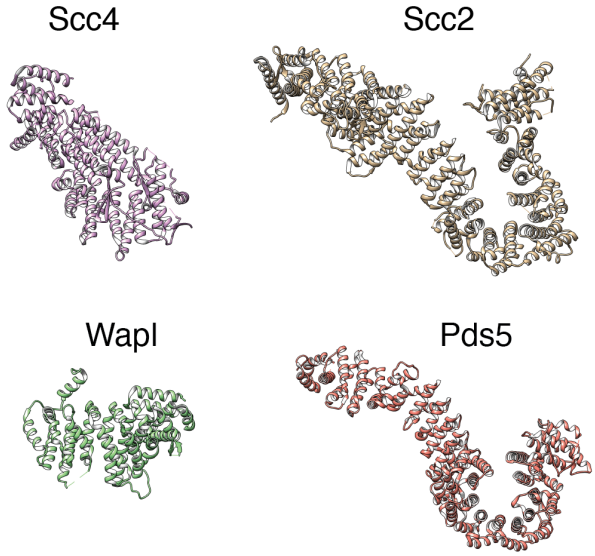

Figure 1-4 Cohesin interacting partners Scc4 (PDB: 4xdn) and Scc2 (C-terminal domain PDB: 5t8v) form a stable complex, which is required for cohesin's association with DNA. Wapl (C-terminal domain PDB: 4k6j) and Pds5 (C-terminal domain PDB: 5hdt) promote cohesin release. Pds5 is also required for establishment and maintenance of sister chromatid cohesion.

During DNA replication a fraction of cohesin becomes stabilised by acetylation of a pair of lysines on Smc3 by Esco1/2 and an interaction with sororin (Rankin et al., 2005; Rolef Ben-Shahar et al., 2008; Rowland et al., 2009; Unal et al., 2008). Sororin is an unstructured protein that is only found in animal species (Nishiyama et al., 2010). When sororin binds to acetylated cohesin it displaces Wapl-Pds5 allowing it to permanently hold

sister chromatids together throughout G2 (Ladurner et al., 2016; Nishiyama et al., 2010; Ouyang et al., 2016). As well as collaborating with Wapl in cohesin release Pds5 is also required for establishment and maintenance of cohesion (Chan et al., 2013; Panizza et al., 2000). The mechanisms behind Pds5's dual function in release and establishment remain unclear. When the cell enters prophase mitotic kinases phosphorylate residues on sororin and Scc3 resulting in sororin's dissociation from cohesin and therefore Wapl-dependent release of cohesin from DNA (Dreier et al., 2011; Nishiyama et al., 2013). Critically, cohesin at centromeres is spared from release by Sgol1-PP2A which dephosphorylates sororin (Kitajima et al., 2004; Liu et al., 2013; McGuinness et al., 2005) and Scc3 and competes with Wapl for a binding site on cohesin (Hara et al., 2014). During prophase the nuclear envelope breaks down, chromosomes are condensed and microtubules start the process of bi-orientation of sister kinetochores. Cohesin persists at centromeres until all chromosomes are bi-oriented. At this point the spindle assembly checkpoint is silenced and the Anaphase Promoting Complex or Cyclosome (APC/C) becomes active (Musacchio, 2015). The APC/C ubiquitinylates securin and cyclin B leading to their destruction by the 26S proteasome (Cohen-Fix et al., 1996; King et al., 1995; Shirayama et al., 1999; Sudakin et al., 1995). This in turn leads to the activation of a cysteine protease called separase, which cleaves cohesin at two sites on Scc1 (Ciosk et al., 1998; Uhlmann et al., 1999; 2000). Cleavage releases sister chromatids from cohesin's embrace and allows their subsequent disjunction. The lysines on Smc3 are then deacetylated by Hos1 (HDAC8) permitting subsequent release of the Scc1 cleavage product and recycling of the Smc proteins (Beckouët et al., 2010; Borges et al., 2010).

Topology of Cohesin's Interaction With Individual DNA Fibres

The discovery that the cohesin complex forms a closed ring led to the proposal that cohesin's stable association with DNA takes the form of a topological embrace rather than an electrostatic interaction (Haering et al., 2002). That is to say DNA sits within the cohesin ring. This hypothesis is called the ring model.

Several lines of evidence support this model. Firstly, when loaded onto a plasmid the interaction between cohesin and DNA is abolished upon linearisation of either cohesin or the DNA (Davidson et al., 2016; Ivanov and Nasmyth, 2005; Murayama and Uhlmann, 2014). This suggests that there is no inherent attraction between the two and that cohesin can slide off linear DNA. Further evidence came from the finding that covalent circularisation of the cohesin ring using engineered cysteine pairs in the three interfaces makes the interaction between cohesin and a circular minichromosome resistant to protein denaturation (Gligoris et al., 2014; Haering et al., 2008). The only possible explanation for this result is that cohesin can topologically entrap DNA. The fact that releasing activity requires opening of an interface (Beckouët et al., 2016; Buheitel and Stemmann, 2013; Chan et al., 2012; Eichinger et al., 2013), that cohesin can diffuse on DNA (Davidson et al., 2016; Kanke et al., 2016; Stigler et al., 2016) and that transcription pushes cohesin to the 3' end of genes *in vivo* (Busslinger et al., 2017; Lengronne et al., 2004) are all consistent with the idea that cohesin holds DNA within its lumen.

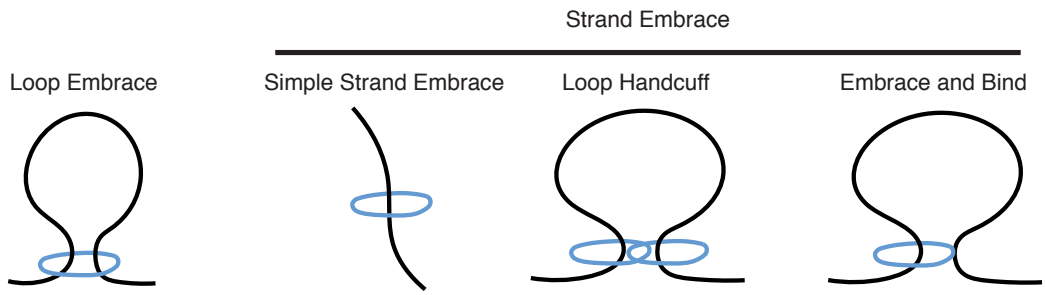

Figure 1-5 Models of cohesin association with individual DNA fibres Loop Embrace Cohesin may interact with DNA by holding a loop within its lumen. This would not require opening of an interface to load. **Strand Embrace** In these three models an interface must be opened so that DNA can pass into the lumen. **Simple Strand Embrace** Cohesin passes through the ring once without forming a loop. This is the classical view of cohesin's association with DNA. **Loop Handcuff** Two cohesin rings each entrapping the DNA interact thereby forming a loop. Translocation in opposite directions would increase the size of this loop. **Embrace and Bind** Cohesin entraps the DNA and binds to DNA in cis by electrostatic interactions thereby creating a loop. Unidirectional translocation would result in progressive enlargement of the loop.

Since the discovery that cohesin is involved in DNA looping (Parelho et al., 2008), a revisiting of the entrapment model has begun. Two types of entrapment can be imagined. In the first, *Loop Embrace*, a single fibre of DNA passes through cohesin, bends around and passes back through the same ring forming a loop (Fig. 1-5). This model of association with DNA is not strictly topological, as it would slide off the loop if cohesin were not also binding to DNA. Critically, this model does not require opening of an interface for loading, as the loop can be inserted into the lumen. The second type of model is *Strand Embrace* whereby DNA passes through individual cohesin rings once. Several variations of this model can be imagined that would result in loop formation (Fig. 1-5). These result in a true topological entrapment of DNA that cannot slide off long or circular DNA.

Both *Loop* and *Strand Embrace* are consistent with the notion that DNA sits inside the cohesin ring. Similarly, all of the experiments listed in this section do not distinguish between these models, with one exception. The cohesin rings, which entrap minichromosomes in the cysteine crosslinking experiments (Gligoris et al., 2014), must interact with DNA by *Strand Embrace*. The reason being that cohesin engaged in *Loop Embrace* would slide off small plasmids when treated with SDS even when the ring has

been chemically circularised. As mentioned, such conditions render the association between cohesin and a circular minichromosome resistant to protein denaturation (Gligoris et al., 2014). However, this does not disprove the existence of *Loop Embrace*. It only proves the existence of *Strand Embrace* and only on a plasmid in yeast.

The entrapment of DNA by Smc protein complexes has also been demonstrated for condensin (Cuylen et al., 2011) and for *Bacillus subtilis* Smc proteins (Wilhelm et al., 2015). This points to DNA entrapment as a common mechanism of Smc protein complexes.

Cohesin loading: The Entry Gate

Biochemical and electron microscopy demonstrate that cohesin forms a stable ring in the absence of DNA (Anderson et al., 2002; Gruber et al., 2003). Therefore, cohesin probably arrives at the DNA as a closed ring and complex formation on the DNA is probably not the mechanism of cohesin loading. To permit *Strand Embrace* either DNA breaks must occur allowing cohesin to slide on before being repaired or one of cohesin's interfaces must open to allow the DNA to pass in. It seems unlikely that DNA breakage would be the mechanism of cohesin loading given the fast turnover of cohesin in some organisms (Chan et al., 2012). This would undoubtedly lead to mutagenesis and genomic instability. Transient opening of one of cohesin's three interfaces therefore seems the most plausible mechanism. The identity of an 'entry' gate is controversial. Smc3-Scc1 and Smc1-Scc1 fusions, which functionally close those interfaces, were not defective in loading (Gruber et al., 2006). However, if the Smc1-Smc3 hinge interface was closed using rapamycin-induced protein dimerisation domains cohesin does not load onto DNA (Gruber et al., 2006). These results suggested that the hinge opens to allow DNA into the ring.

It has been argued that these modified proteins may have unknown defects which have confounded the results (Uhlmann, 2016). The Smc3-Scc1 interface has also been proposed as an entry gate. The evidence for this unified entry and exit gate is that Wapl-Pds5 promotes loading *in vitro* (Murayama and Uhlmann, 2015) and this complex is known to open the Smc3-Scc1 interface (Beckouët et al., 2016). Consistently, chemical crosslinking of the hinge interface with engineered cysteines does not inhibit loading of a Xenopus cohesin tetramer in Xenopus egg extracts (Madhusudhan Srinivasan - Personal Communication). It is also possible there may be redundancy between the interfaces and neither is essential for loading. Additionally, if cohesin interacts with DNA via *Loop Embrace* an entry gate is no longer an absolute requirement. It is conceptually possible for a loop of DNA to be introduced directly through the lumen (Nasmyth, 2001). The recent finding in yeast that mutant cohesin which is unable to entrap DNA by *Strand Embrace*, can load onto DNA and translocate just like wild type supports this new model (Madhusudhan Srinivasan - Personal Communication).

Cohesin Loading: The Loading Complex

Cohesin loading depends on Scc2 and Scc4, which form a heterodimer known as the cohesin loading complex or Kollerin (Fig. 1-4) (Ciosk et al., 2000; Watrin et al., 2006). Loading can occur in the absence of Scc4 both in human cells (Haarhuis et al., 2017) and in yeast (Maria Demidova - Personal Communication). On the other hand no circumstances have been found where Scc2 is dispensable. For this reason Scc2 is considered to be the critical component of the loading complex but how it loads cohesin onto the DNA is not well understood. Scc2 is a large protein (316 kDa in humans) and is monophyletic with Pds5 and Scc3, which are part of the HAWK family of proteins (HEAT repeat containing proteins Associated With Kleisins). This family of proteins is composed

of the key regulators of both cohesin and condensin (Wells et al., 2017) and all have large hook-shaped domains (Hara et al., 2014; Kikuchi et al., 2016; Lee et al., 2016; Roig et al., 2014). The N-terminus of Scc2 binds to Scc4 to form a heterodimer (Hinshaw et al., 2015). The C-terminal domain is composed of an array of Huntingtin, elongation factor 3 (EF3), protein phosphatase 2A (PP2A), and the yeast kinase TOR1 (HEAT) repeats (Kikuchi et al., 2016). Mutation analyses indicate that the hook-shaped C-terminus is the critical domain for Scc2's role in cohesin loading (Kikuchi et al., 2016) (Jean Metson – Personal Communication). The other requirement for the loading onto DNA is ATP hydrolysis by cohesin.

Smc Complexes form an ATP-binding cassette (ABC)-type ATPase

The ATP Binding Cassette is a highly conserved ATPase domain, which is historically considered one of the defining features of an ABC transporter (Hopfner and Tainer, 2003). ABC transporters are a large family of membrane-spanning proteins that transport their ligands across membranes (Rees et al., 2009). However, it has become clear that this domain is not restricted to this family and is found in the double-strand break repair protein Rad50, the DNA mismatch repair protein MutS and all Smc proteins (Aravind et al., 1999).

At one apex of Smc proteins there is a highly conserved ABC-type ATPase domain (Fig. 1-6a) (Niki et al., 1991). The composite active sites contain Walker A and B motifs from one Smc head domain and the signature motif from the opposing Smc head domain. When the ATPase domains come together in the presence of ATP they sandwich two ATP molecules between them (Hopfner et al., 2000).

ATP is held in the correct position in the ATP binding cassette by hydrogen bonds between its α- and β- phosphates and the Walker A motif, and its γ- phosphate and the signature

motif (Lammens et al., 2004). A glutamate residue in the Walker B motif is critical for the positioning of the ATP and the subsequent attack of water on the γ-phosphate that results in hydrolysis (Lammens et al., 2004). A large contact area is created between Smc head domains by ATP binding therefore ATP binding and subsequent hydrolysis is the main determinant of head domain engagement and opening.

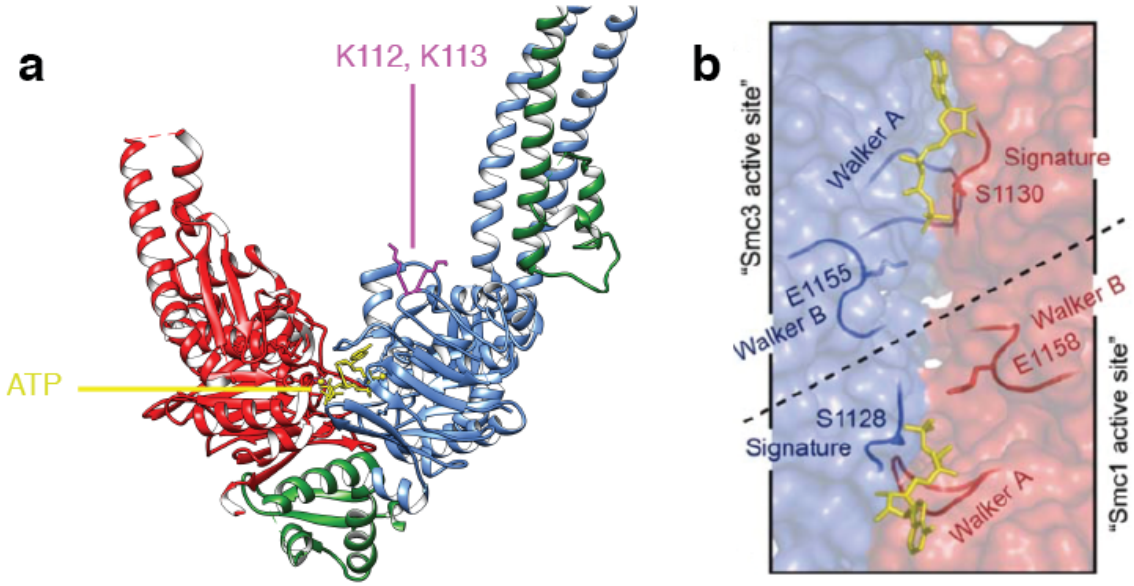

Figure 1-6 Model of cohesin's ABC-type ATPase formed by dimerisation of Smc3 and Smc1 head domains a) Model of cohesin's head domains (hd) in their engaged state based on crystal structures of Smc3-Scc1 (Gligoris et al., 2014) (PDB: 4ux3) and Smc1-Scc1 (Haering et al., 2004) (PDB: 1w1w) interfaces. Smc3 (blue), Smc1 (red), Scc1 (green) and ATP (yellow) are shown. Acetylation of Smc3 K112 and K113 (magenta) is sufficient to block release in budding yeast **b)** Smc3 (blue) and Smc1 (red) head domains. Smc3 and Smc1 sandwich two molecules of ATP (yellow). ATP is bound by the Walker A motif of one head and the signature motif of the other. Adapted from (Arumugam et al., 2003).

Mutation of cohesin's ATPase, which severely reduces hydrolysis, abrogates stable cohesin loading and leads to its accumulation at the loading site in yeast (Hu et al., 2011). Such accumulation is dependent on Scc2 and the mutant cohesin has a very fast turnover. This indicates that Scc2 has recruited cohesin to the loading site but the cohesin cannot be stabilised on the DNA. Similar findings have been found in human cells (Ladurner et al., 2014). These findings, taken with those in the previous section, have led to a two-step model for cohesin loading. First, Scc2 brings a cohesin complex to the DNA. Second, the

presence of both Scc2 and DNA stimulates cohesin's ATPase, which leads to ring opening and topological loading. How Scc2 brings cohesin to the DNA and how ATP hydrolysis by cohesin leads to stable association with DNA is not known.

Additional contributions of cohesin's ATPase

The ATPase has been implicated in two more of cohesin's functions. Yeast lose sister chromatid cohesion when Eco1 is inactivated because it inhibits cohesin release. By searching for suppressors of the lethal *Eco1* deletion, inhibitors and promoters of release have been identified (Beckouët et al., 2016; Rolef Ben-Shahar et al., 2008; Rowland et al., 2009; Unal et al., 2008). Recently, a series of mutations in the ATPase of Smc1 (but not Smc3) have been found that reduce cohesin's ATPase activity and loading but also inhibit cohesin release (Elbatsh et al., 2016). This is the first evidence that cohesin's ATPase has a role in cohesin unloading from the DNA. It was subsequently found that ATPase catalytically dead mutants of cohesin are not defective in release (Beckouët et al., 2016). Together these results show that an early step in the hydrolysis cycle, most likely ATP binding/head engagement, is required for cohesin release, but hydrolysis of the bound ATP is not needed.

It has also recently been suggested that the ABC-type ATPases of Smc proteins are involved in one-dimensional movement of the complexes on DNA. This would provide a mechanism for how cohesin moves from sites of loading to its final resting places (Lengronne et al., 2004; Parelho et al., 2008). The only evidence for ATPase driven translocation has come from the laboratory of Christian Haering. When endogenous condensin was purified from yeast, fluorescently labelled and incubated on stretched DNA, the condensin was found to move unidirectionally at a velocity of 60 bp per second (Terakawa et al., 2017). What is more, this directional movement was completely

abolished upon inactivation of condensin's ATPase even though it still associated with the DNA. This exciting finding, if true of cohesin, would explain several of its poorly understood functions in transcription, meiosis and DNA repair. Frustratingly, this behaviour has not been observed for purified cohesin despite several attempts (Davidson et al., 2016; Kanke et al., 2016; Stigler et al., 2016). Whether this is a technical problem related to the purification of over-expressed proteins (endogenous condensin was used), or if cohesin operates by a different mechanism is a question of the utmost importance.

The Topology of Cohesin's Interaction With Sister Chromatids

How cohesin holds sister chromatids together is also controversial. Several models have been proposed but they fall into two categories. In the first, a single cohesin ring entraps both sister chromatids. In the second, two cohesin rings, each entrapping one chromatid, interact thereby holding sister chromatids together. The strongest evidence in favour of the *Single Ring* model is that sister minichromosomes that normally run as individual molecules on an agarose gel (after denaturation), run as a dimer when cohesin is chemically circularised (Gligoris et al., 2014; Haering et al., 2008). Nevertheless, it is still argued that cohesin does not hold sister chromatids within a single ring (Huang et al., 2005; Zhang et al., 2008).

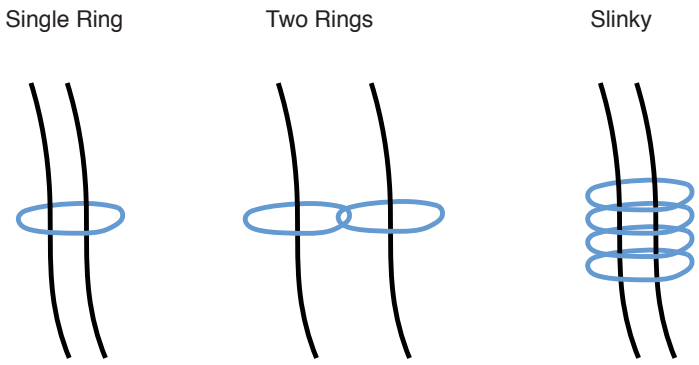

Figure 1-7 Models for the topology of sister chromatid cohesion Single Ring Replicated sister chromatids are entrapped within a single cohesin ring **Two Rings** Each sister chromatid is entrapped within a single cohesin ring. Cohesion is generated by interaction between the two rings. This may be via another subunit (Scc3 or Pds5) or via a topological interaction between the two cohesin rings **Slinky** Multiple rings collaborate to form the cohesive structure however sister chromatids are held within individual cohesin rings

Arguments for collaboration between cohesin complexes stem from the requirement of proteins other than the core trimeric ring to maintain cohesion (Skibbens, 2009). It is suggested that Pds5 or Scc3 may mediate the interaction between two cohesin rings. The strongest evidence for communication between cohesin rings comes from the finding that two different mutants of Scc1 in yeast, which are lethal when expressed individually, are viable when expressed together (Eng et al., 2015). Defects in chromosome binding, condensation and cohesion are all restored indicating that cohesin rings act as multimers in these processes. However, this finding does not exclude the possibility that sisters are entrapped within a single ring. It is conceivable that multiple cohesins each entrapping sister chromatids interact with each other forming a tube-like assembly (Fig. 1-7). This has been referred to as the Slinky model because the structure resembles the children's toy of the same name.

The Establishment of Sister Chromatid Cohesion

Several lines of evidence indicate that cohesion is established at the DNA replication fork. Cells that were depleted of cohesin could not build cohesion if cohesin was reintroduced in G2 (Uhlmann and Nasmyth, 1998). Smc3 acetylation was reduced in cells lacking the pre-

replication protein Cdc6 (Rolef Ben-Shahar et al., 2008). Delays in DNA replication generated by inhibition of the Cdc7 kinase resulted in corresponding delays in cohesion establishment (Beckouët et al., 2010). Furthermore, ChIP-Seq of sororin and replicated DNA (DNA immunoprecipitation - sequencing) in HeLa cells at different stages of S phase showed that cohesion was already established at sequences that had only recently been replicated (Ladurner et al., 2016).

The first step in understanding how cohesion is established at the replication fork is to find out whether it involves the conversion of cohesin that was loaded in front of the replication fork or whether soluble cohesin is loaded in a co-replicative pathway. Whether establishment of cohesion requires cohesin loading at the replication fork was tested by Lengronne and colleagues (Lengronne et al., 2006). Cells were arrested in early S phase using hydroxyurea (HU) to permit cohesin loading, before inactivating the loading complex using a thermosensitive allele of Scc2 and releasing the cells into S phase. Loading in G1 was sufficient for cohesion establishment and the authors concluded that Scc2-dependent cohesin loading at the replication fork is not a necessary feature of cohesion establishment. It has since been shown that in this HU arrest considerable DNA replication takes place before Scc2 inactivation (Nasmyth, 2017). Subsequent discoveries revealed that Wapl would remove G1-loaded cohesin within minutes of inactivating Scc2 (Chan et al., 2012; Gerlich et al., 2006; Kueng et al., 2006). It is still not known whether cohesion is generated from cohesin that is loaded in front of the replication fork.

The only proteins known to be absolutely required for cohesion in yeast are the cohesin complex (Smc1, Smc3, Scc1 and Scc3), the loading complex (Scc2 and Scc4), Eco1 and Pds5. These proteins have known roles: physically holding sister chromatids together (cohesin), placing cohesin on DNA (Scc2-4) and protecting cohesin from Wapl (Eco1 and

Pds5) (Chan et al., 2013). No other proteins that have a specific role in building cohesion at the replication fork emerged from early screens. Several other genes have now been identified which are not essential for viability but their deletion compromises establishment of cohesion. These include Ctf4, Ctf8, Dcc1, Ctf18, Tof1, Csm3, Chl1 and Mrc1 (Beckouët et al., 2010; Bermudez et al., 2003; Borges et al., 2013; Farina et al., 2008; Lengronne et al., 2006; Mayer et al., 2001; Skibbens et al., 1999). All of these proteins are involved in DNA replication. Whether they are directly involved in the positioning of cohesin around sister chromatids or whether their role is indirect, for instance maintaining the correct shape and dynamics of the replisome is not known. These experiments do, however, provide genetic evidence that cohesion not only depends on DNA replication but that cohesion is established at the replication fork.

Cohesin and CTCF in Regulation of Gene Expression

Shortly after the discovery of cohesin it was already implicated in transcriptional regulation (Donze et al., 1999; Rollins et al., 1999). Two roles have been proposed for cohesin in regulating gene expression. The first is the formation of long-range interactions between gene regulatory elements. Support for this function in mammals comes primarily from the finding that cohesin binds to enhancers and promoters (Kagey et al., 2010) and that depletion of cohesin results in a loss of interaction between them (Hadjur et al., 2009). More recent transcriptome-wide experiments have revealed that surprisingly few genes are down regulated after cohesin deletion (Busslinger et al., 2017; Rao et al., 2017). It would seem that while some genes require cohesin for their promoter to interact with their enhancer this is not an absolute requirement of transcription of all protein-coding genes.

The second role in which cohesin has been implicated is transcriptional insulation. This refers to the separation of an enhancer from a promoter despite their proximity on the

genome. This is supported by the finding that cohesin and the only known insulator in mammals, CTCF, colocalised in ChIP-Seq experiments (Parelho et al., 2008). CTCF is an insulator because when it binds between an enhancer and promoter, the enhancer no longer activates the promoter. When plasmids are transfected in which a promoter is separated from an enhancer by a CTCF site, the reporter (e.g. luciferase) is expressed at low levels in wild type cells. However, when CTCF is depleted the reporter protein becomes highly expressed because insulation between the enhancer and promoter is abrogated (Ishihara et al., 2006). Surprising, when cohesin subunits were depleted, expression of the reporter protein increased just like when CTCF was depleted (Parelho et al., 2008; Wendt et al., 2008). These observations indicated that cohesin somehow cooperates with CTCF in transcriptional insulation.

Topologically Associated Domains (TADs)

The mammalian genome is organised as a series of megabase scale domains within which sequences interact with each other more frequently than with sequences outside (Dixon et al., 2012; Nora et al., 2012). TADs are usually flanked by CTCF sites facing in a convergent orientation (Rao et al., 2014). This, together with the finding that cohesin is also found at these flanking sequences, led to the proposal of the 'hand-cuff' model (Dixon et al., 2016; Vietri Rudan and Hadjur, 2015). In this model, two TAD-flanking CTCF molecules dimerise to form a loop, which cohesin then stabilises. The contact enrichment at the flanks of TADs (corner of boxes in Hi-C) represents a stable loop. The contacts within the box simply reveal an increased probability of interacting with sequences in the same stable loop.

The 'loop extrusion' model has since been proposed to explain the TAD boxes in Hi-C (Fudenberg et al., 2016; Sanborn et al., 2015). In this model, a cohesin binds to DNA, a

small loop is created and this loop is progressively enlarged (Alipour and Marko, 2012; Nasmyth, 2001) until it reaches a CTCF site in a specific orientation. Hi-C maps generated by modelling loop extrusion closely resemble experimental results (Fudenberg et al., 2016) supporting this model. Further evidence comes from Hi-C experiments in WaplΔ haploid cancer cells. In these cells cohesin resides on the DNA for longer. Haarhuis and colleagues found that loops became bigger in the absence of Wapl, consistent with increased processivity of a loop extruding cohesin (Haarhuis et al., 2017).

Mammalian Cell Lines as an Experimental Model

Many animal cell types can be isolated and grown in plastic dishes when supplied with a liquid medium containing suitable levels of nutrients and salt. Healthy differentiated (non-stem) cells stop dividing after several rounds of division and enter a state called senescence. Sometimes cells lose the mechanisms that stop division and they continue to proliferate and the cell becomes immortalised. *In vivo* this results in cancer. When these cells are isolated from the body they continue to grow indefinitely and they are referred to as a cancer cell line.

Cell lines are an excellent model system for certain areas of cell biology. They are easy to culture, grow rapidly and can be isolated from many different organs allowing the study of different biological phenomena. Many cellular mechanisms were elucidated using yeast and bacteria but some processes are unique or very different in human cells. By experimenting on cultured animal cells it is possible to study these processes while minimising our dependence on live animal models.

Studying chromosome biology in these cancer cell lines has its risks. Many cancers are caused by errors in DNA metabolism, including DNA damage repair, transcriptional regulation, telomere shortening and chromosome instability. Therefore, by studying these

processes in cancer cell lines there is a risk of making incorrect conclusions about the equivalent processes in wild type animals. Caution must therefore be exercised when selecting a cell line for specific studies, and suitable controls must be performed.

GFP, HaloTag and SNAP-Tag

In the 1850s cytologists began experimenting with organic dyes to differentially label parts of the cell. While these dyes revealed a great deal about subcellular structures, cytologists were not able to specifically label a chosen protein. The discovery that proteins could be specifically stained using fluorescently labelled antibodies revolutionised cytology and for the first time allowed scientists to determine the location of their protein in an organism or cell (Coons and Berliner, 1942). However, in order to perform immunofluorescence the cells must be fixed using a crosslinking reagent. While fixation is suitable for many experiments, cellular processes are usually not static and by studying snapshots information may be lost.

A solution to this problem was discovered in the jellyfish *Aequorea victoria*. Osamu Shimomura isolated a protein from the jellyfish which glowed under UV light (Shimomura et al., 1962). It is now known as Green Fluorescent Protein (GFP) and, when genetically fused to another protein, makes it visible above millions of invisible proteins (Chalfie et al., 1994). By tagging a protein with GFP many of the problems associated with antibody staining were circumvented. GFP allowed observation of protein localisation in living cells and by performing time-lapse microscopy with GFP, dynamic processes became observable for the first time. These advances led to a revolution in cell biology and fluorescence microscopy of GFP is one of the most powerful tools in the cell biologist's tool kit.

While engineering of GFP led to improvements in brightness and stability many organic dyes were still much brighter. New techniques, especially detection of individual molecules of protein, depended on brighter fluorophores. Many organic dyes were brighter than enhanced GFP, but the problem still remained of how to conjugate dyes to proteins without the need for antibodies. Several strategies have been devised to combine the specificity of protein tagging with the improved photophysics of fluorescent dyes. Enzyme-based self-labelling tags, including HaloTag and SNAP-tag, have above all strategies contributed to the advancement of super resolution imaging and tracking of individual proteins in living cells.

The HaloTag is a mutant haloalkane dehalogenase enzyme from *Rhodococcus rhodochrous* (Los et al., 2008). When the HaloTag interacts with its ligand, an alkyl-enzyme intermediate is formed. The wild type protein would then catalyse the hydrolysis of the ligand, thereby releasing the enzyme. However, this reaction is lost in the mutant dehalogenase thus resulting in a covalent adduct with high stability. The SNAP-Tag is a mutant of a human DNA repair protein called O^6-alkylguanine-DNA-alkyltransferase (hAGT) (Keppler et al., 2003). hAGT removes an alkyl group from DNA and transfers it to one of its cysteine residues. However, it can also readily react with the nucleobase O^6-benzylguanine (BG) therefore when the SNAP-Tag reacts with BG the two become irreversibly linked.

A cell permeable fluorescent dye can be conjugated to either the HaloTag ligand or BG. If cells expressing HaloTag or SNAP-Tag respectively are incubated in the presence of these compounds the Halo or SNAP-Tag will be fluorescently labelled. The ability to conjugate fluorescent dyes to proteins via the HaloTag and SNAP-Tag has led to an explosion in the number of single molecule imaging studies (Chen et al., 2014; Mazza et al., 2012). This

has been further encouraged by the development of brighter (Grimm et al., 2015) and photoactivatable dyes (Grimm et al., 2016).

Fluorescence Recovery After Photobleaching (FRAP)

The dynamics of proteins are key to the cellular activities they control. Studying these dynamics has become more straightforward since the invention of fluorescent tags and fluorescence microscopy. The most commonly used method to measure the dynamics of proteins is FRAP (Sprague et al., 2004). In its most simple form FRAP involves photobleaching a small area of fluorescence with a high intensity laser and subsequently recording a series of images. The intensity of the pixels in the bleached area can be measured using a computer program (often ImageJ). Immediately after photobleaching the fluorescence intensity should drop to almost background intensity. If the protein of interest is moving then the fluorescence intensity in the bleached zone will recover as bleached molecules move out, and unbleached molecules move in. The rate of recovery depends on the diffusion coefficient of unbound molecules, the residence time of any immobile populations and the relative size of mobile and immobile fractions. By fitting mathematical models to the fluorescence recovery curves it is possible to extract numbers for these variables. However, the size and shape of the bleach area (Mueller et al., 2008), the fluorophore used (Morisaki and McNally, 2014), new synthesis of fluorescent protein (Kimura and Cook, 2001), choice of mathematical model (Mazza et al., 2012) and expression level of the fusion protein (Hansen et al., 2017) are all known to affect the results generated by FRAP.

Single Particle Tracking

An alternative method to measure the dynamics of proteins is by tracking individual molecules. Proteins can be labelled with bright fluorophores with Halo or SNAP tags (as

described above) and individual fluorophores can readily be detected by a microscope with a powerful laser and a sensitive camera. The coordinates of these individual molecules can be recorded. If the labelling density is sufficiently sparse then the coordinates of a molecule on subsequent frames can be linked to create a 'track'. Due to the high laser power required to observe fast moving molecules, fluorophores are only fluorescent for short periods and track lengths tend to be short (<200ms). Nevertheless, by determining the distance between localisations and relating this to the time between acquisitions the diffusion coefficients of individual molecules can be estimated. This method provides a more direct measurement of the fraction of molecules bound to DNA and diffusion coefficient of mobile molecules than bulk techniques such as FRAP.

Chapter II Cohesin can remain associated with chromosomes during DNA replication

The results described in this chapter have been published as:

Rhodes, J., Haarhuis, J., Grimm, J., Rowland, B., Lavis, L., & Nasmyth, K. Cohesin Can Remain Associated With Chromosomes During DNA Replication. *Cell Rep* ***20,*** *(2017)*

Introduction

The cohesin complex holds sister chromatids together from their replication in S phase to their segregation in mitosis. The establishment of sister chromatid cohesion is coupled to inhibition of cohesin turnover which is essential for the persistence of cohesion. In yeast acetylation of cohesin by Eco1 appears to be sufficient to stop release (Rolef Ben-Shahar et al., 2008; Rowland et al., 2009; Unal et al., 2008) however in animals cohesin must also bind to sororin (Rankin et al., 2005). Both modifications inhibit release of cohesin from DNA by Wapl (Nishiyama et al., 2010; Rowland et al., 2009). While the stabilisation of cohesin is well studied it is not known how two sister chromatids become entrapped within a cohesin ring.

It is assumed that cohesion establishment must occur close to the replication fork to make use of the proximity of the nascent sister DNAs. If not established immediately the sister chromatids would drift apart from each other (Schmitz et al., 2007). In the absence of DNA damage sister chromatid cohesion can only be generated during S phase indicating some form of interaction with DNA replication (Uhlmann and Nasmyth, 1998). What is more, inhibiting DNA replication delays cohesin acetylation, providing further evidence that cohesion is generated in a co-replicative process (Beckouët et al., 2010; Rolef Ben-Shahar et al., 2008).

Three models have been proposed for the establishment of cohesion at the replication fork (Fig. 2-1). In the first, the DNA replication machinery approaches a cohesin ring entrapping unreplicated DNA and passes through the ring, leaving sister chromatids trapped within cohesin. The second model posits that as the replication fork reaches a cohesin complex, the ring opens, dissociates transiently from the DNA and rebinds around sisters chromatids behind the fork. In the third model, the process of DNA replication

removes cohesin from the chromosome as it does with most other DNA binding proteins. A different cohesin molecule is then loaded *de novo* from the soluble pool behind the replication fork. The first step in revealing the mechanism is to determine whether cohesion establishment uses cohesin complexes that are loaded in front of the replication fork or whether cohesin is loaded at the replication fork.

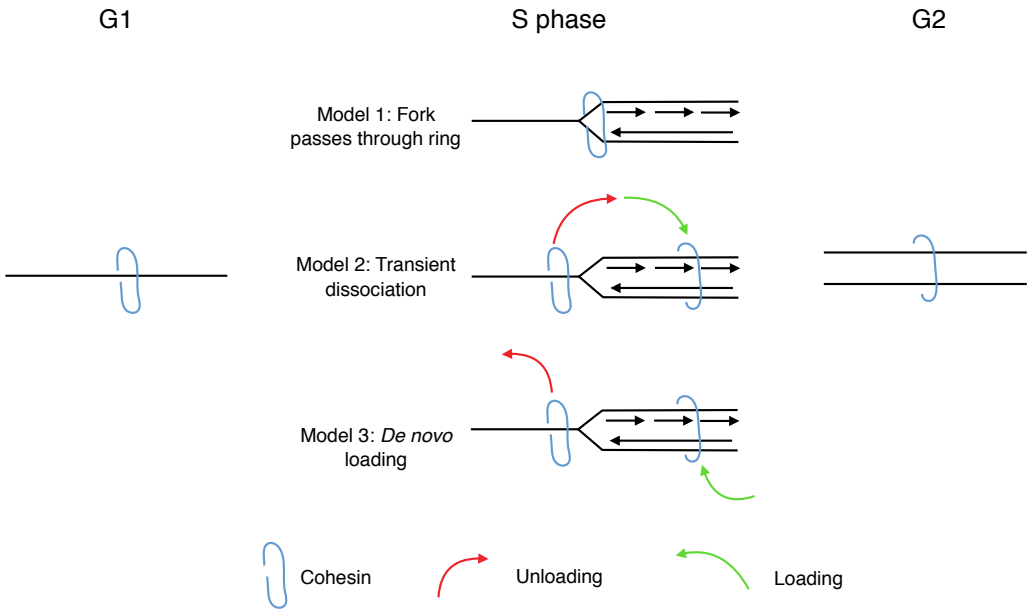

Figure 2-1 Models for the establishment of sister chromatid cohesion. (1) The replication machinery passes through the cohesin ring **(2)** When the replication fork makes contact with cohesin, the ring transiently opens, remains associated with the replisome and reloads around sister chromatids behind the fork. **(3)** Cohesin is removed from chromosomes by DNA replication and cohesin is loaded *de novo* around sister chromatids after fork passage.

If cohesin were loaded at the replication fork then the loading complex (Scc2-Scc4) would be essential for this process. Lengronne and colleagues (2006) attempted to determine whether cohesion establishment requires loading when there is already cohesin on the DNA. Budding yeast cells were arrested in early S phase with hydroxyurea (HU). The result should be a cell that is poised to replicate its DNA with cohesin already loaded. Scc2 was then inactivated and the cells were released from HU arrest and DNA replication proceeded. Lengronne and colleagues found that these cells built cohesion efficiently and that Scc2 dependent loading is not required during establishment of sister chromatid

cohesion. The authors concluded therefore that cohesion could be built from cohesin that is loaded in front of the replication fork.

Subsequently, Wapl-dependent cohesin release was discovered casting doubt on these experiments (Gerlich et al., 2006; Kueng et al., 2006). If yeast cohesin has a half-life on DNA of 2 minutes (Chan et al., 2012) Scc2 should be required just to keep cohesin on the DNA. The experiments were repeated but using shorter arrests in HU and found that Scc2 is required for cohesion if arrested for less time (Nasmyth, 2017). The requirement of Scc2 is most likely for its canonical role in loading which is continually required to counteract Wapl-dependent release.

The reason that Lengronne and colleagues did not see a requirement for Scc2 is that there is still considerable DNA replication and cohesion establishment in HU. In their experiment they arrested the cells for 60 minutes in HU. This is enough time to replicate a sufficient amount of the genome that chromosomes will be held together even if the rest is replicated without cohesin (Nasmyth, 2017).

Whether cohesion can be derived from cohesin that is loaded in front of the replication fork is therefore still not known. The above experiment was later attempted in a yeast cells in which Wapl has been inactivated. This should have removed the need for continual Scc2 loading and the experiment could be done with a very short HU arrest. Surprisingly, even in a *wpl*Δ yeast cell, cohesin falls off the DNA when Scc2 is inactivated (Madhusudhan Srinivasan - Personal Communication). A different approach was therefore needed to determine whether cohesive cohesin is derived from cohesin loaded in front of the fork or during fork progression.

Thesis Objectives

Three models for cohesion establishment have been described above. If cohesion is generated from cohesin that is loaded in front of the replication fork (models 1 and 2) then some cohesin must remain associated with chromatin during fork passage. Alternatively, cohesin may be removed from DNA at the replication fork and the cohesive pool loaded *de novo* (model 3). If this is the case then cohesin should be removed from chromatin at the same time as DNA is replicated. The primary objective of this project was to determine whether cohesin is removed from chromatin by DNA replication. The aim was to do this by performing FRAP on cohesin during S phase.

As cohesin has a natural turnover on chromatin it is not possible to probe DNA replication-induced removal of cohesin in wild type cells. Therefore the first objective of my thesis was to generate a cell line in which Wapl, the protein responsible for cohesin turnover, was inactivated. In this cell line it was also necessary to fluorescently label cohesin and monitor the stages of the cell cycle in the same cell.

Current FRAP techniques are not suitable for long time-lapses as new molecules of the fluorescent protein are synthesised or mature after photobleaching. This results in fluorescence recovery independent of the protein dynamics under study. In the past this artefact has been mitigated by performing experiments in the presence of cyclohexamide, a potent inhibitor of protein synthesis. While this treatment does stop synthesis of new fluorescent protein it also inhibits production of all other proteins. This means that cells can no longer progress through the cell cycle. As it was necessary to perform FRAP over long time periods and the cells needed to undergo DNA replication, traditional FRAP with fluorescent proteins and cyclohexamide was not suitable. Therefore, the second aim of my

thesis was to develop a method to determine protein-chromatin interactions over long time periods.

The final aim of this project was to use this cell line and the new technique to determine whether cohesin is necessarily removed from chromatin by DNA replication.

Results

Generating Scc1-Halo U2OS Cells

In order to observe cohesin's association with chromatin by microscopy a fluorescently labelled cohesin complex was required. During the course of this project CRISPR/Cas9-mediated genetic engineering was invented (Mali et al., 2013). A cell line was therefore established in which the endogenous Scc1 subunit of cohesin was homozygously tagged with a protein, which would allow us to visualise it. The HaloTag was chosen as the tag so that cohesin could be conjugated to a range of organic fluorescent dyes. U2OS cells were used because it was possible to delete Wapl in this cell line (Benjamin Rowland - Personal Communication).

To conjugate Scc1 with the HaloTag, a plasmid encoding the *Streptococcus pyogenes* (*Sp*) Cas9 endonuclease and a guide RNA (gRNA) complementary to the 3' end of the *SCC1* gene was co-transfected with a donor cassette encoding the HaloTag and a sequence homologous to the 3' end of *SCC1* (Yang et al., 2013). Donor plasmids were generated containing 1 Kb sequences homologous to the 3' region of the *SCC1* gene either side of the HaloTag. A 12 amino acid linker (3xGGGS) was included between Scc1 and the HaloTag. The sequence in the donor cassette complementary to the gRNA was mutated to avoid cutting of the donor template. If these mutations were in the coding region they were designed so that they did not alter the peptide sequence (silent mutation). Several days after transfection the cells were stained with the JF549-HaloTag ligand and Scc1-Halo^{JF549}

positive cells were enriched by Fluorescence Activated Cell Sorting (FACS). These cells were then plated for colony picking. PCR genotyping led to the identification of two homozygous Scc1-Halo clones (clone 6 and 17). Homozygous introduction of the tag was confirmed by Western blotting (Fig. 2-2a) and Sanger sequencing.

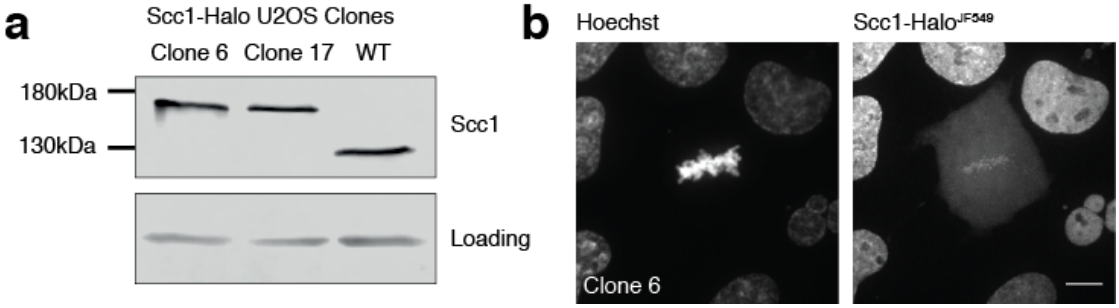

Figure 2-2 Scc1 can be tagged homozygously in U2OS cells a) Immunoblot of nuclear extract from Scc1-Halo U2OS clones with an antibody against Scc1. A non-specific band was used as the loading control **b)** Microscopy images of Scc1-Halo clone 6 labelled with JF549-HaloTag ligand and Hoechst. Scale bar, 5 μm.

As cohesin is essential for cell division, the isolation of homozygous Scc1-Halo cell lines indicated that the fusion protein was functional. To confirm this, Scc1-Halo (clone 6) cells were stained with the JF549-HaloTag ligand and imaged with a confocal microscope to determine cellular localisation. Scc1-Halo^{JF549} localised to the nucleus in interphase and to centromeres in metaphase (Fig. 2-2b). This pattern is consistent with previous studies using GFP-Scc1 (Gerlich et al., 2006) and immunofluorescence (Sumara et al., 2000). This demonstrated that cohesin containing Scc1-Halo could be loaded, hold sister chromatids together, released by Wapl and protected from Wapl at centromeres by Sgol1-PP2A. Scc1-Halo clone 6 was therefore selected for further modification.

Inactivation of Wapl in Scc1-Halo U2OS cells

Genes can be deleted by targeting Cas9 to a coding sequence near the 5' end of a gene. When Cas9-induced double-strand breaks are repaired by non-homologous end joining they create a mutation (most frequently a deletion) (Wang et al., 2013). If this deletion results in a frameshift then a non-functional truncation is produced. Alternatively, a part of

the gene can be deleted using two gRNAs. A third approach is to co-transfect Cas9 with a gRNA and a second plasmid encoding a selection cassette (Blomen et al., 2015). The selection cassette is sometimes introduced at the site of the double-strand break resulting in a truncated protein of interest fused to an antibiotic resistance cassette. This third approach was used by Dr Judith Haarhuis to delete Wapl in the Hap1 and U2OS cells (Haarhuis et al., 2017). All three approaches were used to delete Wapl in Scc1-Halo U2OS cells however no Scc1-Halo *WAPLΔ* clones were identified despite multiple attempts and extensive colony screening. It is possible that *WAPLΔ* clones were generated but grew slower than the wild type clones making them difficult to isolate.

The gRNA of *Sp*Cas9 is 20bp followed by NGG. These three nucleotides are known as the PAM sequence and vary between Cas9 homologs. *Sp*Cas9 cuts 3 bp upstream of the PAM sequence. It is therefore possible to generate a mutation at a specific base pair in the genome if there is a PAM sequence 3 bp either side of it. Amino acids that are essential for the function of Wapl in human cells have been identified (Ouyang et al., 2013). M1116 is in the αB helix of HEAT repeat 7 near the C-terminus of Wapl (Fig. 2-3a) and mutation to alanine in HeLa cells abrogates cohesin release without abolishing Wapl's interaction with cohesin or Pds5 (Ouyang et al., 2013). The codon for methionine 1116, which is located in exon 17 of the *WAPL* gene, has a PAM sequence 3 bp downstream (Fig. 2-3b). If Cas9 was expressed with a gRNA complimentary to this sequence all alleles of M1116 should be mutated.

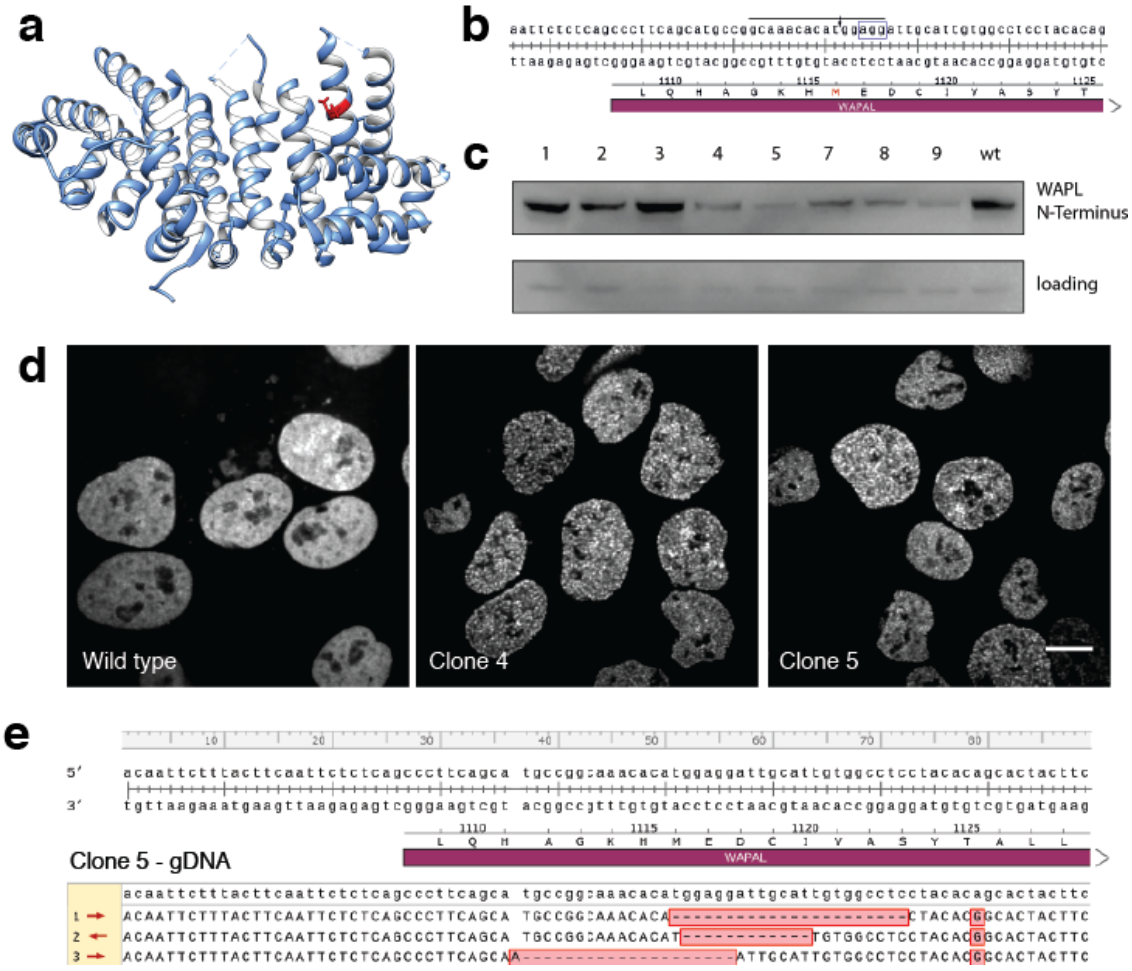

Figure 2-3 Inactivation of Wapl by targeting Cas9 to the WAPL M1116 codon a) Crystal structure of Wapl C-terminal domain demonstrating the position of M1116 (red) **b)** Surrounding DNA and amino acid sequence of Wapl at M1116. Black line illustrates position of gRNA and arrow shows where Cas9 would make a double-strand break **c)** Immunoblot of nuclear extract from eight clones of Scc1-Halo U2OS cells transfected with Cas9 and a gRNA targeting *WAPL*^{M1116}. Clone 6 stopped growing **d)** Live cell microscopy images of Scc1-Halo^{JF549} in WAPL^{+} and two clones (4 and 5) that had been transfected with Cas9 and a gRNA targeting *WAPL*^{M1116}. Scale bar, 5 μm **e)** DNA sequence of *WAPL*^{M1116} and surrounding region in clone 5 hereafter referred to as *WAPL*$^{1116\text{-}1119\Delta}$.

A plasmid encoding *Sp*Cas9 and a gRNA targeting the codon of *WAPL* M1116 was transfected into Scc1-Halo U2OS cells and transfected cells were selected with puromycin for two days. Colonies were isolated and screened for Wapl deletion by Western blotting with an antibody against the N-terminus of Wapl (Fig. 2-3c). None of the eight isolated clones had a complete loss of the Wapl band although several appeared to have reduced expression. Wapl inactivation was determined by staining Scc1-Halo with the JF549-HaloTag ligand and checking for changes in Scc1 distribution. Two colonies (clones 4 and

5) were identified in which the Scc1-Halo^{JF549} formed vermicelli (Fig. 2-3d). Clone 5 had the lowest Wapl levels and was therefore selected for further analysis. To check the DNA sequence at the cut site in clone 5, exon 17 was amplified by PCR and cloned into pUC19. 15 clones were purified and the sequences were determined by Sanger sequencing. This procedure allowed sequence analysis of individual alleles and revealed the presence of three different deletions in exon 17 (Fig. 2-3e). Two of these mutations cause a frameshift (19 and 22 bp deletions) and are predicted to result in a truncated protein. The third mutation was a 12 bp, non-frameshift deletion that results in the deletion of M1116, E1117, D1118 and C1119. Due to the existence of this remaining allele this cell line is referred to as *WAPL*$^{1116\text{-}1119\Delta}$. All three mutant alleles result in the deletion of critical residues for Wapl function.

To confirm that Wapl had been inactivated in clone 5, the prophase pathway was assessed. As expected the majority of cohesin is found in the cytoplasm in wild type metaphase cells (Fig. 2-4a). The cohesin that remains associated with chromosomes is at centromeres. However, in *WAPL*$^{1116\text{-}1119\Delta}$ cells the vast majority of cohesin remains associated with chromosomes and no enrichment at the centromeres is detectable. Wapl-dependent release of cohesin is therefore abrogated in Scc1-Halo *WAPL*$^{1116\text{-}1119\Delta}$ U2OS cells. Interestingly time-lapse video microscopy of these cells revealed that the fluorescence intensity drops rapidly after anaphase (Fig. 2-4b). This may represent degradation of the C-terminal product by the Ubr-dependent N end pathway (Rao et al., 2001). In this respect the cohesin cycle in *WAPL*$^{1116\text{-}1119\Delta}$ resembles that of budding yeast, which do not have a prophase pathway (Uhlmann et al., 1999). For this reason, telophase and G1 cells had much less functional cohesin than they had in G2. This presented a challenge for future FRAP experiments, which would only make use of Scc1-Halo that is loaded in this early stage.

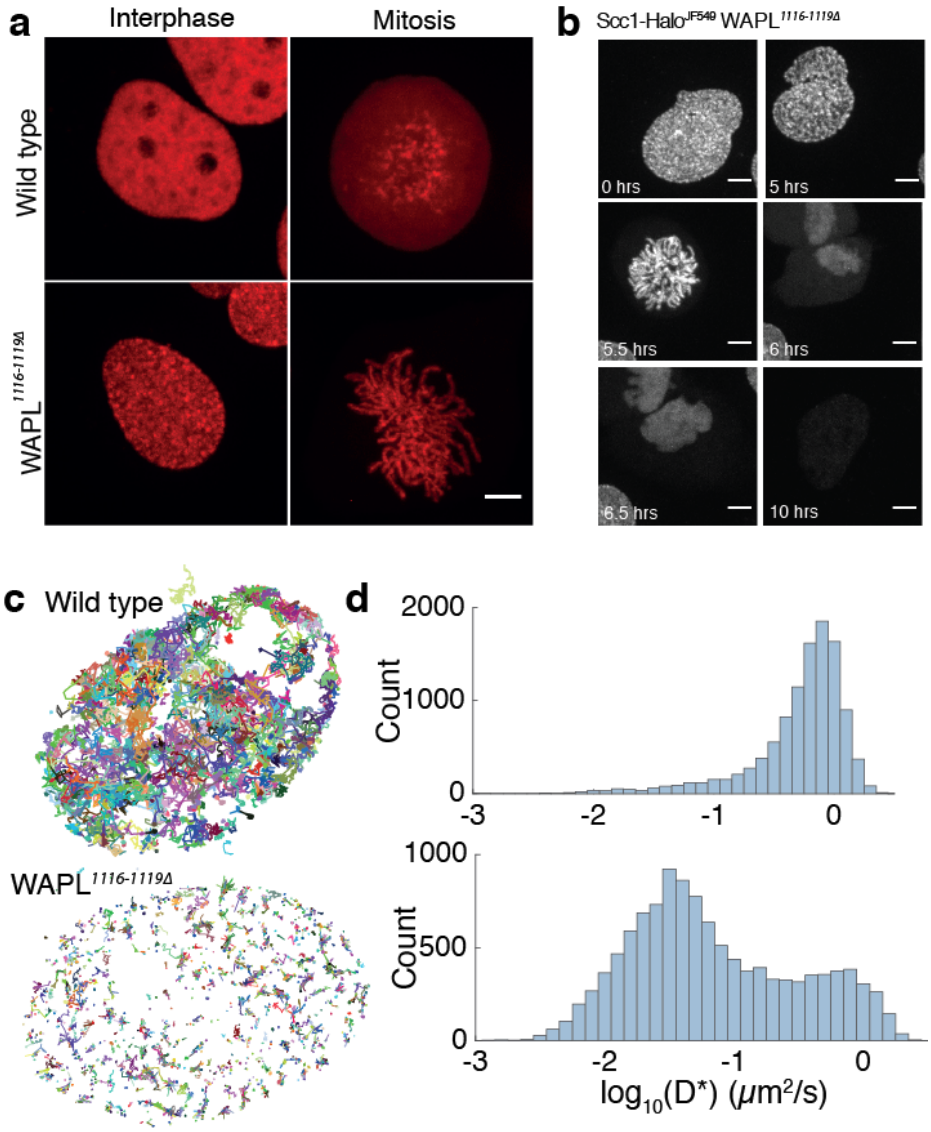

Figure 2-4 Cohesin release is abolished in Scc1-Halo *WAPL*$^{1116\text{-}1119\Delta}$ U2OS cells a) Live cell microscopy images of wild type or Scc1-Halo *WAPL*$^{1116\text{-}1119\Delta}$ U2OS cells in interphase and mitosis. Scale bar, 5 μm **b)** Still microscopy images from time-lapse video of Scc1-Halo *WAPL*$^{1116\text{-}1119\Delta}$ U2OS cells in mitosis and G1. Cells were imaged in the presence of HaloTag blocking ligand (see below). Scale bar, 5 μm **c)** Tracks of single Scc1-Halo^{JF549} molecules in wild type or *WAPL*$^{1116\text{-}1119\Delta}$ Scc1-Halo U2OS cells **d)** Histograms showing the number of molecules observed moving at different apparent diffusion coefficients n=10 cells.

To provide further evidence that cohesin release is abolished in *WAPL*$^{1116\text{-}1119\Delta}$ cells single particle tracking of individual Scc1-Halo^{JF549} molecules was performed in wild type and *WAPL*$^{1116\text{-}1119\Delta}$ cells (Fig. 2-4c). This revealed a large increase in the number of Scc1-Halo^{JF549} molecules that are stably associated with chromatin in *WAPL*$^{1116\text{-}1119\Delta}$ cells compared to wild type (Fig. 2-4d). This is consistent with inactivation of the Wapl-dependent cohesin release pathway.

Residual fluorescent ligand labels new HaloTag proteins

Having shown that the prophase pathway was abrogated and the fraction of cohesin associated with chromatin vastly increased, the aim was to directly show whether cohesin release was completely abolished in interphase. To do this, FRAP was used. If *WAPL*$^{1116\text{-}1119\Delta}$ U2OS cells were truly defective in releasing activity then there should be no fluorescence recovery in the bleached area. Scc1-Halo was again labelled with JF549 in *WAPL*$^{1116\text{-}1119\Delta}$ cells. Scc1-Halo^{JF549} signal was highly enriched on the chromatin in vermicelli. Half of the nucleus was then photobleached using the 568 nm laser. Once the unbleached soluble fraction had dispersed around the nucleus, a time-lapse recording of the cells was recorded.

Surprisingly, the fluorescence in the bleached half of the nucleus recovered substantially over this time period (Fig. 2-5a). This indicated that either cohesin was not stably associated with the DNA and therefore *WAPL*$^{1116\text{-}1119\Delta}$ possessed residual releasing activity. Alternatively, there was a technical problem with the FRAP procedure. Two observations indicated that the latter possibility was true. First, the mean fluorescence intensity of the whole nucleus increased by 53% over the recovery period. If the fluorescence recovery in the bleached half was due to the turnover of cohesin the total fluorescence intensity should remain the same (or decrease due to photobleaching). The second observation was that fluorescence also recovered in nuclei in which all nuclear Scc1-Halo^{JF549} was photobleached (Fig. 2-5b).

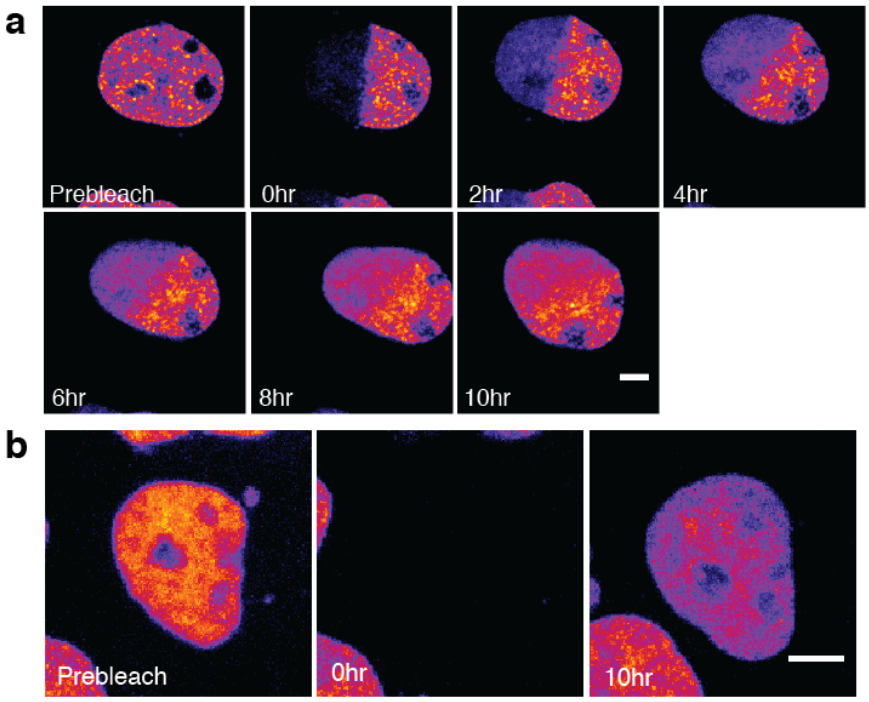

Figure 2-5 Residual HaloTag ligand labels newly synthesised Scc1-Halo a) Average intensity projections of z-stacks from Scc1-Halo half nuclear FRAP experiments. Scale bar, 5 µm **b)** Average intensity projections of z-stacks from Scc1-Halo whole nuclear FRAP experiments. Scale bar, 5 µm

Two possibilities were considered. First, when the Scc1-Halo^{JF549} was irradiated with high laser power the dye molecules were not permanently photobleached. The ability to revert from a dark state to a fluorescent one is clearly a property of the JF549 dye despite reports to the contrary (Morisaki and McNally, 2014). This 'blinking' behaviour is observed when JF549 is exposed to high laser power on a photoactivated localisation microscopy (PALM) microscope (Hansen et al., 2017). Therefore the recovery observed in the nuclear FRAP could be due to reversion of dyes to a bright state.

The second possible reason for the increase in nuclear fluorescence in bleached nuclei is that the signal is from newly labelled Scc1-Halo proteins. It was assumed that after fluorescent labelling of Scc1-Halo, repeated washing and incubation of cells would leave such a low concentration of JF549 in the medium that new Scc1-Halo would remain unlabelled. However, it was possible that the JF549 was binding to newly

synthesised/folded Scc1-Halo molecules. The objective was therefore to inhibit relabeling of the HaloTag to determine if this was the cause of the fluorescence recovery.

Chromatin association of proteins can be observed over long time periods using pulse chase FRAP

It was reasoned that by incubating the cells with a high concentration of a non-fluorescent HaloTag ligand, the JF549 ligand would be outcompeted and new Scc1-Halo proteins would be permanently labelled with the non-fluorescent ligand and remain dark (Fig. 2-6a). HaloTag ligands are available with several different reactive groups including the N-hydroxysuccinimide (NHS) ester. Addition of this ligand to the medium would result in the conjugation of the ligand to any free amine in the medium or cell surface. The NHS group was therefore reacted with tris, which contains an amine group, to produce the non-reactive tris-HaloTag Ligand.

To test the efficacy of the tris-HaloTag ligand in blocking labelling of HaloTag proteins, Scc1-Halo U2OS cells were labelled with JF549 ligand then transferred to the microscope after the addition of tris ligand or DMSO. A prebleach image was acquired then total JF549 nuclear fluorescence was photobleached. A recovery image was then acquired 16 hours later (Fig. 2-6b). The fluorescence intensity recovered to 45% when the cells were incubated in the absence of the tris-HaloTag ligand. Importantly, when the post bleach recovery was performed in the presence of the tris-HaloTag ligand the nuclear fluorescence recovered by only 1% (Fig. 2-6c). Because the tris-HaloTag ligand is able to inhibit labelling of the newly synthesised HaloTag protein it is subsequently referred to as the HaloTag blocking ligand. The ability to block relabeling of the HaloTag means that it should be possible to observe chromatin association over very long time periods for the first time. This modification to the FRAP protocol was named pulse chase or pcFRAP.

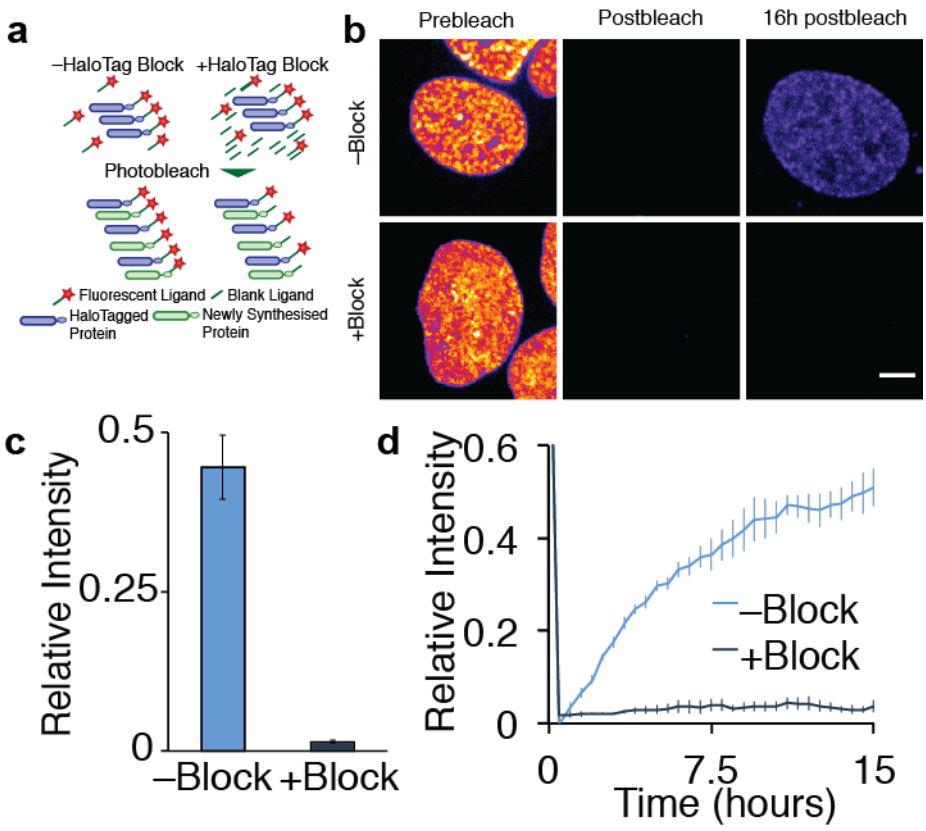

Figure 2-6 pulse chase FRAP blocks relabeling of newly synthesised protein a) Cartoon illustrating the inhibition of relabeling by incubating with a blocking ligand **b)** Average intensity projections of z-stacks from Scc1-Halo whole nuclear FRAP experiments. Scale bar, 5 μm **c)** Mean fluorescence intensity of Scc1-Halo^{JF549} nuclei 16 hours after bleaching of whole nucleus relative to prebleach intensity. Recovery was observed in the presence or absence of blocking HaloTag ligand. n=11 **d)** Graph depicting half nuclear FRAP for ^{JF549}SNAP-H3.3. n=6. Data are represented as mean ± SEM.

To demonstrate the utility of pcFRAP the chromatin association of histone H3.3 was measured. To this end H3.3 with an N-terminal SNAP-Tag was stably expressed in Scc1-Halo U2OS cells. Histone H3 is a very stable constituent of chromatin and this fusion protein would therefore allow us to observe chromatin movement over long time periods. SNAP-H3.3 U2OS cells were labelled with JF549-SNAP-Tag ligand, washed, and medium was added to the cells with or without SNAP-Cell Block. Half nuclear FRAP was then performed and fluorescence recovery measured for the subsequent 15 hours. When cells were imaged in the absence of SNAP-Cell Block, relative intensity between bleached and unbleached halves recovered to 45% (Fig. 2-6d). However, when the FRAP was performed in the presence of SNAP-Cell Block relative intensity recovered to only 4%. These results

show the benefit of pcFRAP for measuring chromatin association over long time periods. They also demonstrate that there is negligible turnover of histone H3.3 in our experiments. However, the SNAP-H3.3 is over expressed and so may not represent the dynamics of the endogenous protein.

Dual colour pcFRAP demonstrates little chromatin movement in Scc1-Halo SNAP-H3.3 U2OS cells

Determining whether cohesin is removed from chromatin by DNA replication depended not only on abrogation of Wapl-dependent release but also on low movement of chromatin and cohesin. If the unbleached region of chromatin mixes with the bleached region the signal will be dispersed which will resemble dissociation of cohesin from chromatin. To determine whether cohesin and chromatin are mobile in the nucleus SNAP-H3.3 was stably expressed in Scc1-Halo $WAPL^{1116\text{-}1119\Delta}$ U2OS cells. SNAP-H3.3 was labelled with JF646 and Scc1-Halo with JF549 and SNAP-Cell block and the HaloTag blocking ligand were added to the medium.

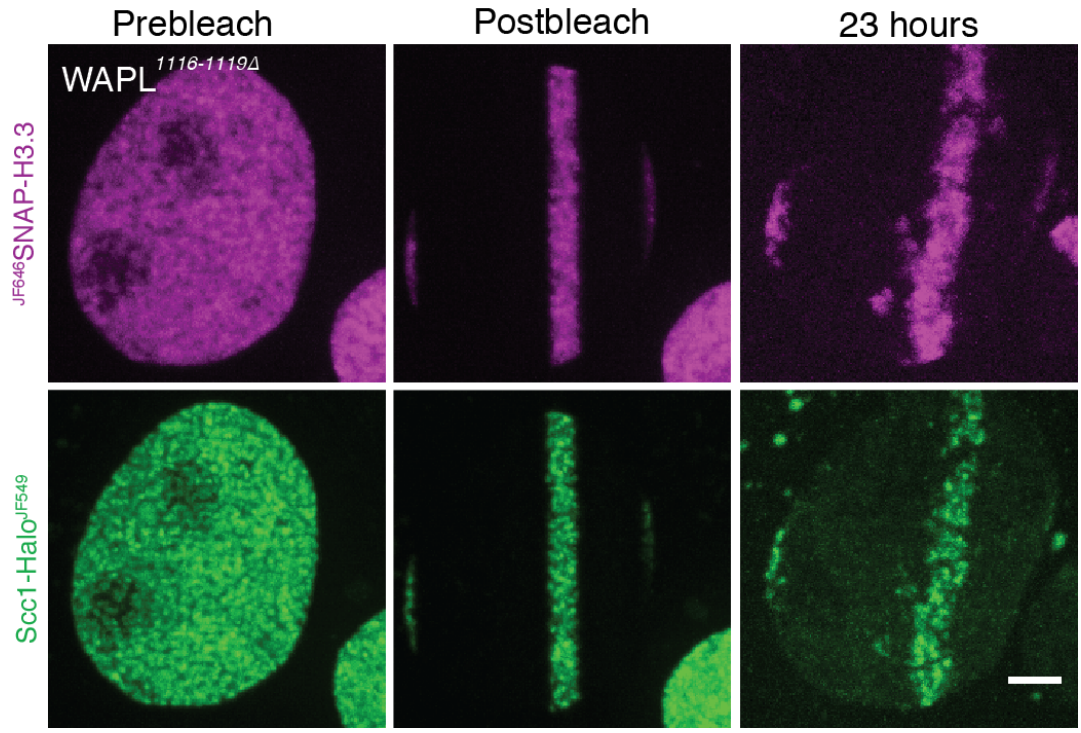

Figure 2-7 Limited movement of chromatin over long time periods Live cell microscopy images of Scc1-Halo^{JF549} ^{JF646}SNAP-H3.3 *WAPL*$^{1116-1119\Delta}$ U2OS cells before photobleaching with a 568 nm laser, immediately after photobleaching and 23 hours later. Scale bar, 5 µm. Contrast enhanced in 23 hours time point. n=10.

Fluorescence microscopy demonstrated that both ^{JF646}SNAP-H3.3 and Scc1-Halo^{JF549} could be imaged simultaneously without interference between the channels. The entire nucleus except a stripe across the middle was bleached. An image was acquired before bleaching, immediately and 23 hours after bleaching. This revealed that the majority of fluorescence associated with both proteins remained in the stripe across the middle of the nucleus (Fig. 2-7). Occasional patches of H3.3 fluorescence disjoined from the main body of fluorescence but importantly the Scc1-Halo^{JF549} associated with this region followed it. Two conclusions were made from this observation. First, that SNAP-H3.3 and Scc1-Halo can remain associated with chromatin for 23 hours in *WAPL*$^{1116-1119\Delta}$ U2OS cells. Second, that there is limited chromatin movement in interphase human cells consistent with previous studies (Gerlich et al., 2003; Walter et al., 2003). This low chromatin movement

meant that determining whether cohesin remains associated with DNA in S phase would be possible.

Cohesin localised to the interchromatid axis in mitosis

By co-staining Scc1-Halo and SNAP-H3.3 with bright organic dyes it was possible to determine the localisation of cohesin on condensed chromatids in metaphase. In wild type cells cohesin is found between sister chromatids at the centromere because it is holding them together. Cohesin vermicelli in WaplΔ cells have been suggested to represent intrachromatid loops. When chromosomes condense in prophase the cohesin holding loops would be spread over the entire chromatid. However, when Scc1-Halo and SNAP-H3.3 were co-stained the Scc1-Halo signal was located between the sister chromatids (Fig. 2-8a). To confirm this, cells were fixed and fluorescently labelled with an antibody against topoisomerase II (TopoII) to label the intrachromatid axis specifically (Fig. 2-8b).

Line profile analysis of TopoII and Scc1 fluorescence confirmed that Scc1 is found between sister chromatids (Fig. 2-8c). This raises the interesting possibility that the same cohesin that is holding loops (in interphase vermicelli) are also holding sister chromatids together. An alternative explanation is that cohesin loaded after replication translocates along DNA until it encounters a cohesive cohesin ring, which may be immovable (Kanke et al., 2016). This would therefore create a common axis of cohesive and loop forming cohesin.

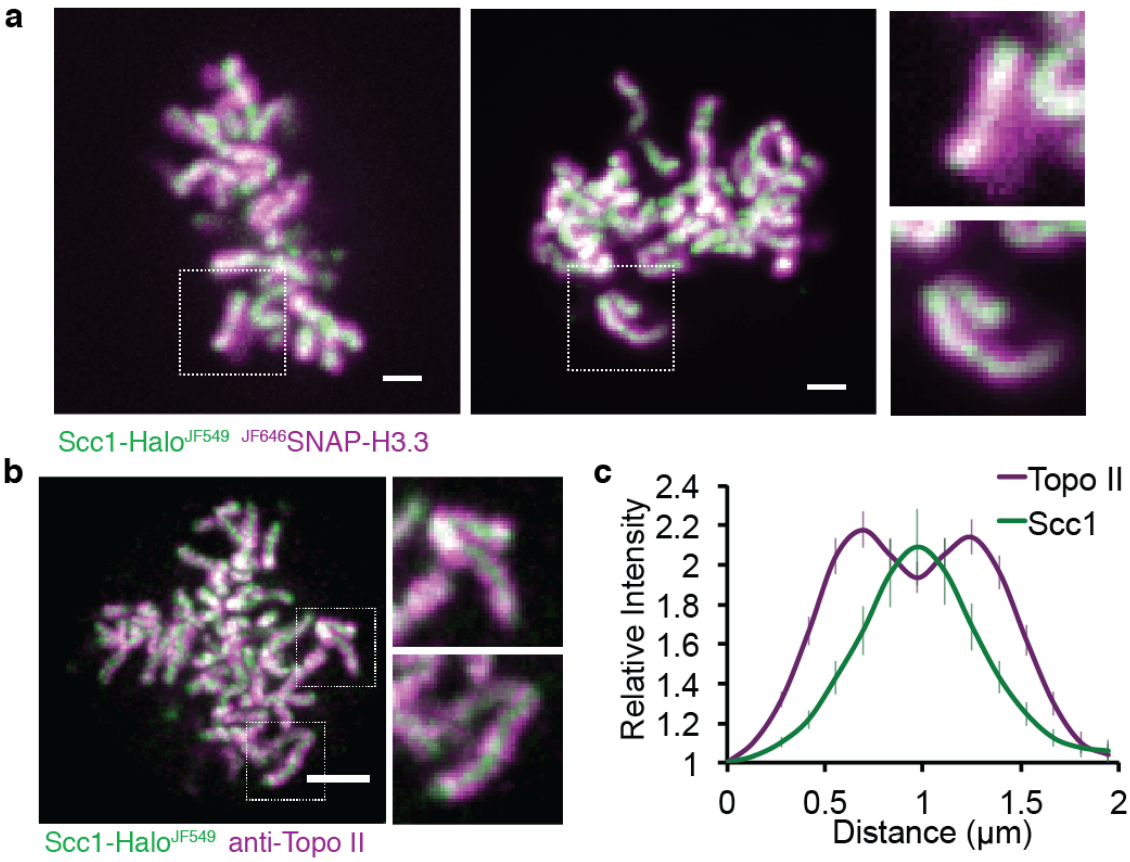

Figure 2-8 Scc1 localises to the inter chromatid axis in mitosis a) Live cell microscopy images of ^{JF646}SNAP-H3.3 Scc1-Halo^{JF549} *WAPL*$^{1116\text{-}1119\Delta}$ U2OS cells in mitosis **b)** Fixed cell microscopy images of Scc1-Halo^{JF549} *WAPL*$^{1116\text{-}1119\Delta}$ U2OS cells in mitosis co-stained with an antibody against topoisomerase II. Scale bar, 2 μm **c)** Fluorescence line profiles of Scc1-Halo^{JF549} and topoisomerase II across metaphase 30 chromosomes from 9 cells. Data are represented as mean ± SEM.

Cohesin can remain associated with chromosomes during DNA replication

While the above experiment demonstrated that cohesin could remain associated with chromatin for long periods in *WAPL*$^{1116\text{-}1119\Delta}$ cells, it did not address whether it is able to do so across S phase. To this end GFP-PCNA was stably expressed in Scc1-Halo *WAPL*$^{1116\text{-}1119\Delta}$ cells. Expression was confirmed by Western blotting (Fig. 2-9a) and live cell microscopy (Fig. 2-9b).

Scc1-Halo was labelled with JF549 and the HaloTag blocking ligand was added to the medium before mounting on the microscope. G1 cells were readily identified by a lack of nuclear GFP-PCNA foci, small nuclear size and proximity to a sister cell (having recently

divided). Because the prophase pathway was abrogated in *WAPL*$^{1116\text{-}1119\Delta}$ cells and therefore most cohesin cleaved at anaphase, very little cohesin was associated with chromatin in G1. The result being that the fluorescence intensity of Scc1-Halo^{JF549} was extremely low.

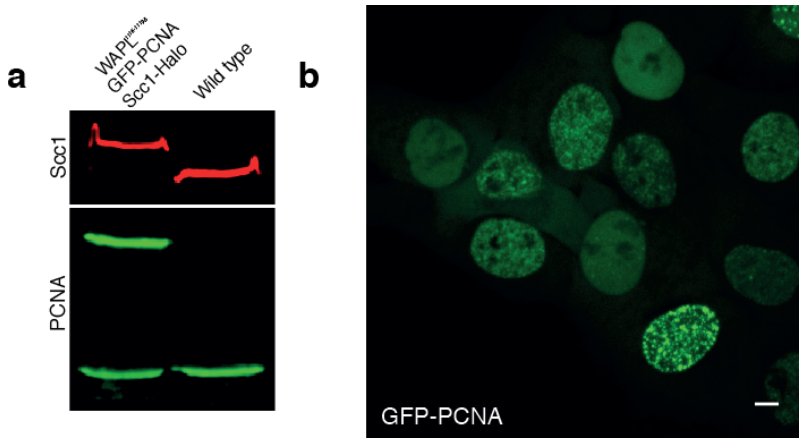

Figure 2-9 Stable expression of GFP-PCNA in Scc1-Halo *WAPL*$^{1116\text{-}1119\Delta}$ U2OS cells a) Immunoblot of nuclear extract from GFP-PCNA Scc1-Halo *WAPL*$^{1116\text{-}1119\Delta}$ or wild type U2OS cells with antibodies against Scc1 and PCNA **b)** Microscopy images of GFP-PCNA in GFP-PCNA Scc1-Halo *WAPL*$^{1116\text{-}1119\Delta}$ U2OS cells. Scale bar, 5 μm.

In G1 cells all Scc1-Halo^{JF549} was bleached except for a small region of chromatin bound protein at the side of the nucleus. Because the Scc1-Halo^{JF549} fluorescence was so weak only the GFP-PCNA was imaged between G1 and G2. S phase progression could be determined by GFP-PCNA distribution in the nucleus. In early and mid S phase many very small foci could be observed whereas in late S phase the foci were much larger and brighter. When the bleached cells had entered G2 phase (complete lack of GFP-PCNA foci) a recovery image of the Scc1-Halo^{JF549} was acquired. In all cases the subnuclear pattern of the Scc1-Halo^{JF549} fluorescence resembled that of the G1 nucleus.

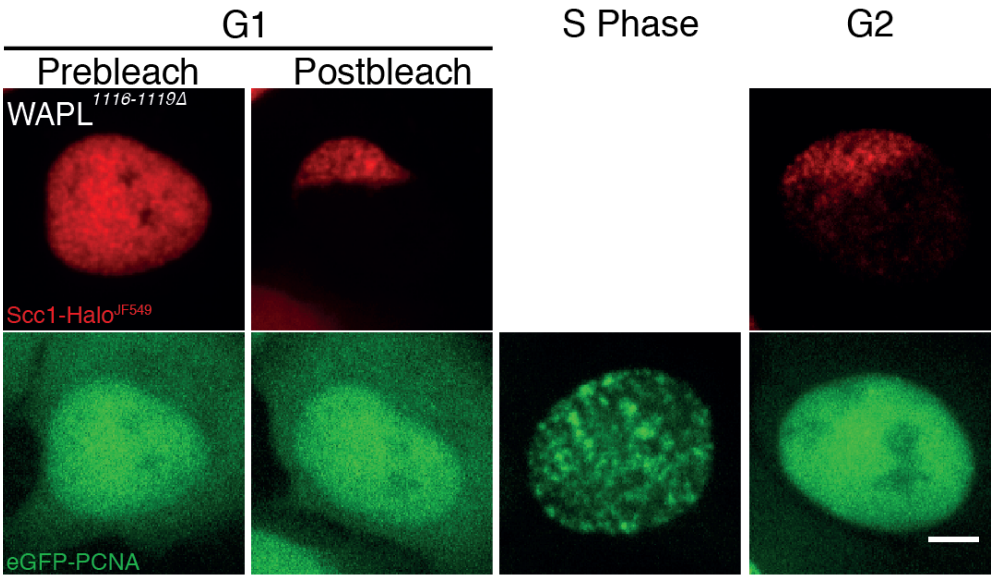

Figure 2-10 Cohesin can remain associated with DNA during S phase Live cell microscopy images of Scc1-Halo^{JF549} *WAPL*$^{1116-1119\Delta}$ eGFP-PCNA cells in G1 before photobleaching, in G1 after photobleaching, in S Phase and in G2. It was not possible to image Scc1-Halo^{JF549} between G1 and G2 because of low starting signal in G1. This fluorescence was lost easily by photobleaching from eGFP and JF549 acquisition. Contrast has been enhanced in Scc1-Halo^{JF549} channel in post bleach (after soluble fraction was bleached intentionally) and G2 (as there was a decrease in total nuclear signal). n=12. Scale bar, 5 μm.

It was concluded that DNA replication does not dislodge cohesin from DNA in a manner that results in its diffusion around the nucleus. This does not exclude the possibility that in a wild type cell Wapl releases cohesin in a co-replicative manner. Given that cohesion can be built in the complete absence of Wapl in yeast and mammalian cells this cannot be a necessary part of cohesion establishment. Nevertheless, cohesin, like histones H3 and H4, is capable of remaining associated with chromatin despite passage of the replisome.

Discussion

The aim of this project was to determine whether cohesin loaded onto chromosomes in telophase and G1 is necessarily displaced by the passage of the replication machinery. This information is important for understanding the mechanism of the establishment of sister chromatid cohesion. Cohesion could be derived from cohesin complexes loaded ahead of the replication fork and/or from cohesin loaded *de novo* after the replication fork. If

cohesion is generated from cohesin loaded ahead of the fork then it should be able to remain associated with chromatin despite replication fork passage.

The aim of this study was to determine whether dissociation of cohesin from chromatin is an obligatory feature of DNA replication. To this end the kleisin subunit of cohesin, Scc1, was tagged with the HaloTag in U2OS cells. Because Wapl-dependent releasing activity would mask any effect caused by DNA replication this activity was abrogated by mutating Wapl. Using this cell line it has been possible to observe subnuclear populations of cohesin and it has been demonstrated that they can persist from G1 to G2 despite the passage of the replication machinery. This shows that DNA replication itself does not cause cohesin to dissociate from the DNA in a manner that permits cohesin's diffusion through the nucleus.

While this finding does not exclude the possibility that cohesion is derived from the soluble pool of cohesin, it does indicate that G1-loaded cohesin is converted to the cohesive form. Whether this is achieved by passage of the replication fork through the cohesin ring or by transient opening of the ring remains one of the most important questions in the study of sister chromatid cohesion.

Since progress in answering this question *in vivo* has slowed, major steps have been made towards reconstituting this process *in vitro*. Firstly, using a large number of purified components of the replisome from budding yeast, John Diffley's research group are now able to efficiently replicate DNA *in vitro* (Kurat et al., 2017; Yeeles et al., 2015). Secondly, the budding yeast cohesin complex and its regulators have now been reconstituted (Chao et al., 2017). If these two systems were combined and the establishment of sister chromatid cohesion at the replication fork reconstituted it would be an incredibly powerful tool to probe the mechanism.

A different approach is to probe the reaction using single molecule imaging of purified cohesin in Xenopus egg extract. Xenopus egg extract contains all the constituents needed for the cell cycle and it is possible to replicate stretched lambda DNA while observing the dynamics of fluorescently labelled proteins added to the extract. Preliminary results tracking the movement of cohesin during fork passage have been reported (Kanke et al., 2016) however the data are not clear enough to make any conclusions.

Due to the low resolution of confocal imaging it was not possible to exclude the possibility that cohesin dissociates from the chromatin and re-associates nearby. However, in mouse cells the time between unloading and reloading is ~33 minutes (Hansen et al., 2017) meaning a replication specific mechanism for re-association would be required. If cohesin had redistributed throughout the nucleus in a replication dependent manner it would provide evidence that replication displaces cohesin. The finding to the contrary demonstrates that cohesin has the ability to remain in place despite replication fork passage.

Chapter III – The cohesin loading factor Scc2 hops between cohesin rings

The results described in this chapter have been published as:

Rhodes, J., Mazza, D., Nasmyth, K. & Uphoff, S. Scc2/Nipbl hops between chromosomal cohesin rings after loading. *Elife* 6, e30000 (2017).

Introduction

The spatial positioning of DNA has a direct role in the regulation of gene expression from bacteria (Oehler et al., 1990) to humans (Banerji et al., 1981). In eukaryotes, distal regulatory elements must be brought into proximity with their target promoters and kept away from inappropriate ones by a process known as insulation. Recent advances in measuring contacts between distant DNA sequences have revealed that the mammalian genome is organised into a series of regions within which sequences interact with each other more frequently than with sequences outside (Nora et al., 2012). These regions are called Topologically Associating Domains (TADs) or contact domains and range from several kilobases to over a megabase in length.

The CCTC-binding factor (CTCF) has been shown to act as an insulator in mammalian cells (Bell et al., 1999). In other words, an enhancer from one gene will not activate the promoter of a neighbouring gene when CTCF binds to the DNA between them. Over 85% of TADs are flanked by consensus sequences for the CTCF in a convergent orientation (Fig. 3-1) (Rao et al., 2014). These sequences interact with a higher frequency than those within the TAD and appear as spots at the corner of TAD boxes on Hi-C maps (Fig. 3-1). This suggests that spatial isolation of genes in TADs, as defined by CTCF, might be the mechanism of transcriptional insulation. Consistently, disruption of border CTCF sites results in the disruption of TAD boundaries (Sanborn et al., 2015) and the loss of transcriptional insulation (Flavahan et al., 2016). Additionally, degradation of CTCF leads to a massive reduction in boundary definition (Nora et al., 2017). How CTCF keeps DNA sequences spatially separated is an unanswered question, however there is mounting evidence that it involves cohesin. Firstly, cohesin and CTCF have been found to colocalise on DNA in ChIP-Seq experiments and CTCF is required for cohesin positioning at these

sites (Busslinger et al., 2017; Parelho et al., 2008). Secondly, depletion of cohesin results in a loss of transcriptional insulation on a reporter plasmid (Wendt et al., 2008). Thirdly, degradation of cohesin's Scc1 subunit leads to a complete loss of all interactions within TADs (Fig. 3-1) (Rao et al., 2017).

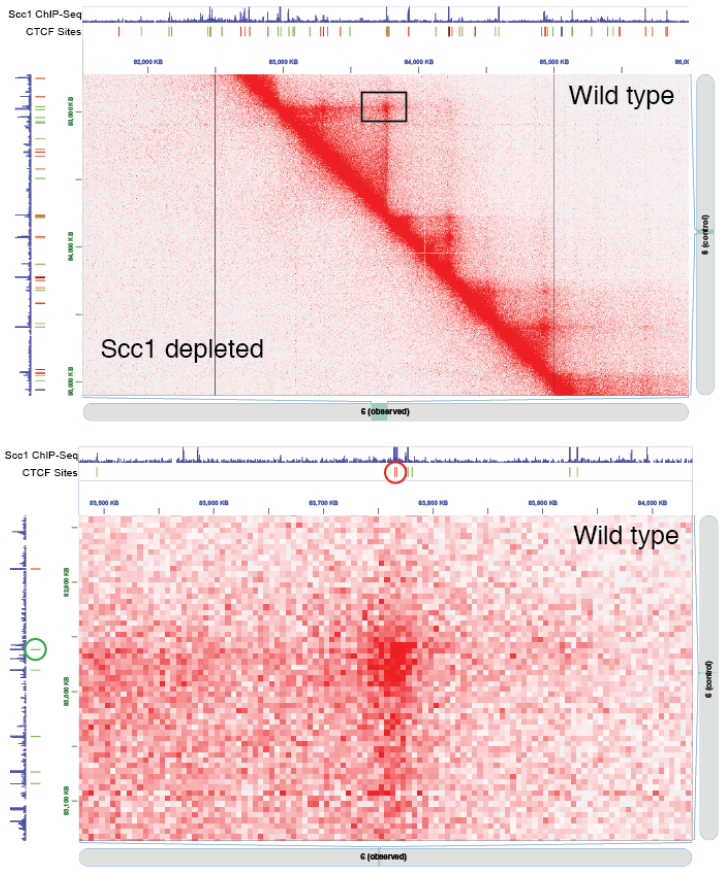

Figure 3-1 Cohesin is required for the formation of TADs Hi-C contact map of Scc1-mAID Tir1 HCT116 cells. ChIP-Seq of Scc1 in HCT116 cells and CTCF orientation (green=forward, red=reverse) are also displayed Top: with and without Scc1 degradation by addition of auxin. Bottom: Enlarged view of the box in top panel. Red and green circles show convergent CTCF site at the corner of a TAD. Data from (Rao et al., 2017).

The observations that the direction of CTCF sites is critical for their function as insulators, and that cohesin is essential for all the loops of DNA within a TAD, has led to the proposal that TADs are formed by loop extrusion (Fudenberg et al., 2016; Sanborn et al., 2015), a mechanism that was originally proposed for condensin (Alipour and Marko, 2012; Nasmyth, 2001). In the loop extrusion model, cohesin makes a small loop of DNA (Fig. 3-

2). This loop is then progressively enlarged until the cohesin ring reaches a CTCF site facing towards it. When this occurs extrusion from the CTCF side stops but continues from the other side until another convergent CTCF site has been reached.

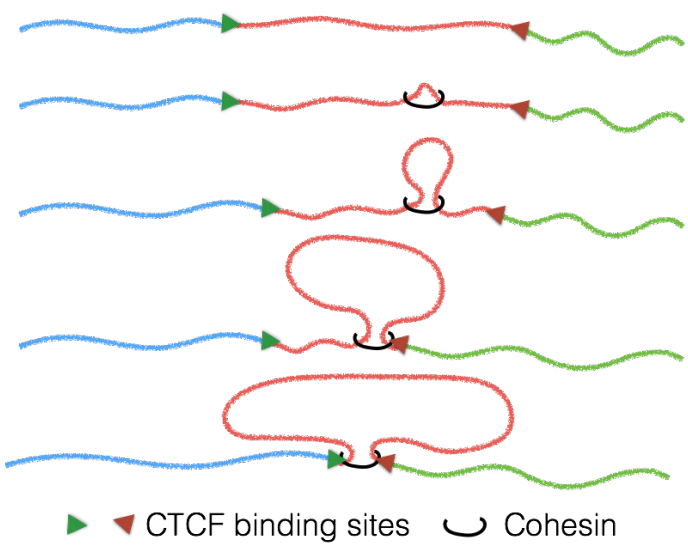

Figure 3-2 Illustration of loop extrusion Cohesin makes a small loop of DNA and progressively enlarges it. When cohesin reaches a DNA –bound CTCF facing towards it extrusion stops on that side but continues from the other direction. When a second convergent CTCF site is reached loop extrusion stops.

If loop extrusion by cohesin is the mechanism by which sequences within TADs interact then cohesin must be capable of travelling vast distances along DNA. There is increasing evidence that cohesin and other Smc complexes are able to do this. Bacterial Smc has been shown to bring the chromosome arms of the *Bacillus subtilis* chromosome together as it travels from Origin to Terminus (Wang et al., 2017), a journey of over two megabases. The yeast condensin complex travels along DNA *in vitro* in an ATPase dependent manner and can tether a second DNA strand while doing so (Terakawa et al., 2017). Several ChIP-Seq and *in vitro* single molecule imaging experiments indicate that cohesin is also capable of traveling along DNA (Busslinger et al., 2017; Hu et al., 2015; Lengronne et al., 2004; Stigler et al., 2016). However, unidirectional translocation by cohesin has not been directly observed.

Cohesin's association with chromosomes depends on the cohesin loading complex and hydrolysis of ATP by the Smc1 and Smc3 composite ABC-type ATPases (Arumugam et al., 2003; Ciosk et al., 2000). The cohesin loading complex is a heterodimer of Scc2 and Scc4 (Ciosk et al., 2000), but the Scc2 subunit is more important for cohesin loading as Scc4 can be deleted in yeast (Maria Demidova - Personal Communication) and in a human cancer cell line (Haarhuis et al., 2017). While essential for loading cohesin onto DNA, Scc2 is dispensable for the maintenance of sister chromatid cohesion in G2 (Ciosk et al., 2000). Until recently, it has been assumed that Scc2 only interacts with cohesin during the loading reaction. However, the recent findings that Scc2 itself stimulates cohesin's ATPase (Murayama and Uhlmann, 2014) including after cohesin has been loaded onto DNA (Çamdere et al., 2015), and that translocation of Smc complexes depends on their ATPase activity (Hu et al., 2011; Kanke et al., 2016; Terakawa et al., 2017) has led to a revisiting of this question.

Given that Scc2 stimulates the ATPase of DNA-bound cohesin rings, it may be driving the enlargement of DNA loops by loop extrusion. If this is the case then one should see cohesin and Scc2 colocalise on DNA. So far this has only been addressed by ChIP-Seq and the results from these experiments differ. Several studies have found that cohesin and Scc2 colocalise at enhancers and promoters (Fournier et al., 2016; Kagey et al., 2010) while others have detected no significant colocalisation and instead find Scc2 at active promoters independent of cohesin (Fig. 3-3) (van den Berg et al., 2016; Zuin et al., 2014).

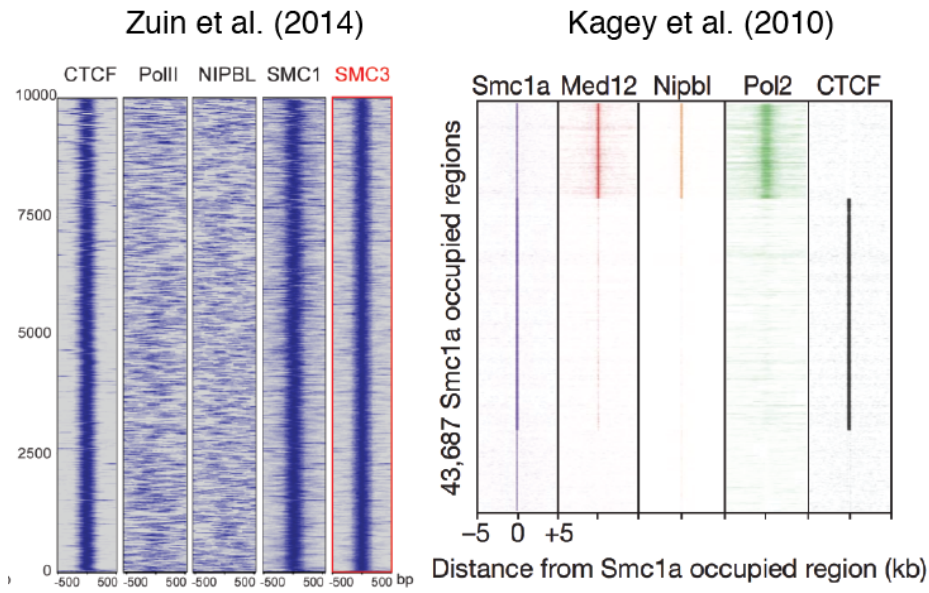

Figure 3-3 Two examples of published ChIP-Seq analyses of Scc2, cohesin and CTCF Heat maps plot ChIP-Seq signal of several proteins relative to peaks of cohesin (Smc3 and Smc1a). There is no overlap between Scc2 and cohesin at CTCF sites in either study.

Despite these differences, so far no ChIP-Seq study has seen any significant overlap of Scc2 with cohesin-CTCF co-occupied sites, despite this being where most cohesin peaks are found. It has therefore been concluded that Scc2 does not interact with cohesin after the loading reaction.

Cornelia de Lange Syndrome (CdLS) is a severe developmental disorder characterised by chraniofacial abnormalities and gastrointestinal and cardiac defects. An estimated 60% of CdLS probands have a mutation in the *SCC2* gene (Rohatgi et al., 2010). These usually result in a heterozygous deletion or loss of function. It is not known why mutation in *SCC2* causes CdLS. Surprisingly, patients have displayed clinically significant CdLS with reductions in Scc2 expression as small as 15% (Borck et al., 2006). Consistently, an Scc2 heterozygous knockout mouse model of CdLS had only 30% less Scc2 in its cells despite displaying high mortality rate and severe developmental defects (Kawauchi et al., 2009). It has been suggested that CdLS aetiology is linked to a cohesin-independent function of Scc2. This is partly because there are similar levels of chromosome-bound cohesin in

CdLS samples and chromosome segregation appears normal (Chien et al., 2011; Remeseiro et al., 2013). However, CdLS mutations are frequently found in other cohesin subunits (Boyle et al., 2016; Deardorff et al., 2012; Revenkova et al., 2009). Together these findings indicate a cause related to cohesin but not its canonical function in chromosome segregation. Additionally, as Scc2-dependent cohesin loading appears unchanged, it may be that, rather than its loading, cohesin's behaviour on the DNA is defective. Given that Scc2 stimulates cohesin's ATPase and Smc complexes translocate in an ATP dependent manner, Scc2 depletion could reduce cohesin processivity. If Scc2 is regulating cohesin's behaviour on DNA then they should reside at the same locations on the chromosome. However, as discussed above limited colocalisation has been detected genome wide leading to the assumption that Scc2 is exclusively involved in loading.

Results

Generating a Halo-Scc2 human cell line

Given that probing Scc2's interaction with chromatin with ChIP-Seq after paraformaldehyde fixation has yielded contradictory results, the objective of this project was to study Scc2 in native conditions and in living cells. To do this, the HaloTag system was used as it allows specific labelling of the protein of interest with a wide range of very bright organic dyes. Using CRISPR/Cas9-induced homologous recombination, the HaloTag and a 15 amino acid flexible linker was inserted at the 5 prime end of the *SCC2* gene in HeLa and HCT116 cells to generate an N-terminal fusion protein (Fig. 3-4a). In HeLa cells there are estimated to be seven or more copies of Scc2 (Rene Ladurner - Personal Communication). To increase the efficiency of identifying a cell line with as many alleles of Scc2 tagged as possible, a Blasticidin S-resistance gene was included in the donor plasmid (Fig. 3-4b). Individual Blasticidin-resistant colonies were isolated and

genotyped by PCR (Fig. 3-4c). All colonies had an insertion in at least one allele of Scc2 and in the HCT116 cells there were several colonies that were homozygous (Fig. 3-4c). However, in the HeLa cells no homozygous lines were obtained. The isolation of homozygous Halo-Scc2 HCT116 clones showed that Halo-Scc2 is functional and the reason homozygous HeLa clones were not obtained is most likely due to high copy number of *SCC2*. A heterozygous Halo-Scc2 was therefore used for further experiments.

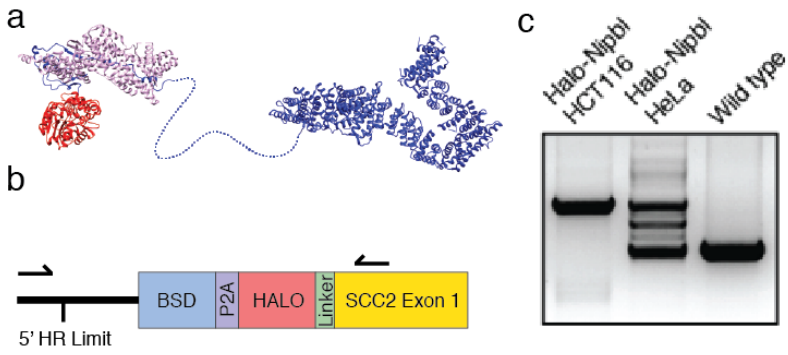

Figure 3-4 Tagging of Scc2 with HaloTag using CRISPR/Cas9 a) A model of Scc2 (blue)-Halo (red) in complex with Scc4 (pink) **b)** Schematic of BSD-P2A-HaloTag insertion at 5 prime end of SCC2. Black arrows represent PCR genotyping primers. **c)** PCR genotyping of Halo-Scc2 (Nipbl) HCT116 and HeLa cells

The cellular localisation of Scc2 has been determined by immunofluorescence in human cells (Watrin et al., 2006). Scc2 was found to be nuclear during interphase, cytoplasmic during mitosis and re-associates with chromatin in telophase. However, as recently demonstrated for several transcription factors, chromatin association of proteins can be missed by studying formaldehyde fixed cells (Teves et al., 2016). To verify that Scc2 does not associate with mitotic chromosomes, Halo-Scc2 HeLa cells were incubated transiently with the JF549-HaloTag ligand, thereby fluorescently labelling Scc2 ($Scc2^{JF549}$). Imaging fluorescently labelled Scc2 revealed its subcellular localisation, confirming that it dissociates from chromatin as the nuclear envelope breaks down (Fig. 3-5). This cell cycle dependent association with chromatin resembles that of cohesin which dissociates from

chromatin as cells enter mitosis via a mechanism known as the prophase pathway (Losada et al., 1998).

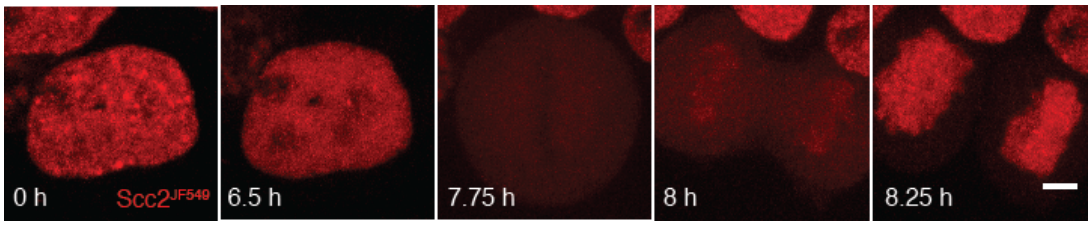

Figure 3-5 Sub-cellular localisation of HaloTagged Scc2 Live cell confocal microscopy images of Scc2^{JF549} HeLa cells in interphase and mitosis. 0 h = G2, 6.5 h = prophase, 7.75 h = metaphase, 8 h = telophase and 8.25 h = late telophase/G1.

Scc2 interacts dynamically with chromosomes before and after DNA replication

To compare Scc2's dynamics at different stages of interphase, Halo-Scc2 HeLa cells were synchronised in G1 or G2 by releasing cells for different periods of time from a double thymidine block. Most cells were in G2 six hours after release, having undergone S phase, whereas the majority of cells were in G1 15 hours after release, having undergone DNA replication and cell division (Fig. 3-6a). Halo-Scc2 was labelled with JF549 and the interaction between Scc2 and chromatin was measured by bleaching a 2.5 μm circle of JF549 and measuring FRAP for 10 minutes (Fig. 3-6b). The fluorescence in the bleached region completely recovered within 10 minutes demonstrating the absence of a permanently stable fraction (Fig. 3-6c).

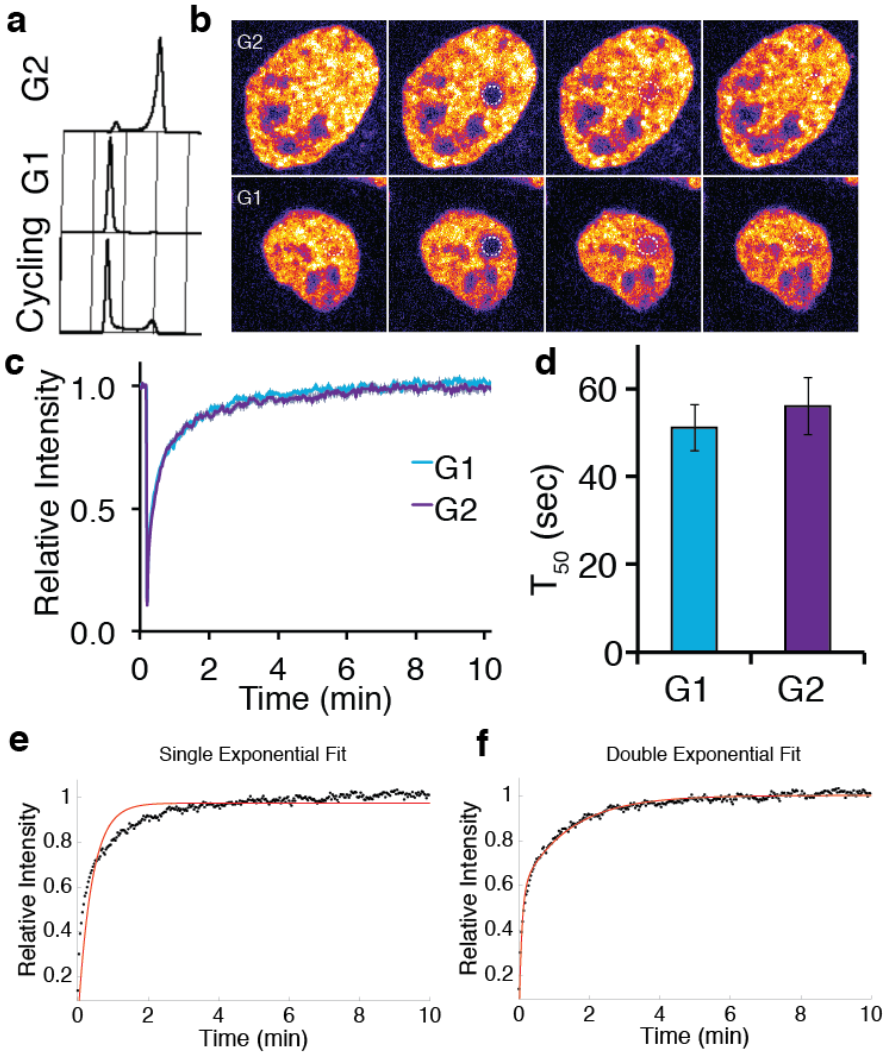

Figure 3-6 Scc2 interacts with chromatin with a half-life of less than one minute in G1 and G2 a) Fluorescence activated cell sorting (FACS) of propidium iodide-stained cells synchronised by double thymidine block **b)** Live cell microscopy images of wild type HeLa cells before and after bleaching a circle of $Scc2^{JF549}$ fluorescence. Dashed circle represents bleached region **c)** Recovery curves for G1 or G2 cells. **d)** Half-life of the chromatin associated $Scc2^{JF549}$ **e)** Single exponential fit and **f)** Double exponential fit of mean fluorescence recovery of G1 $Scc2^{JF549}$

To determine whether there is more than one population of Scc2 in the nucleus, single exponential curves were fitted to individual FRAP experiments. A single exponential function did not fit the recovery curves (R-square: G1=0.80, G2=0.84) (Fig. 3-6e). A double exponential function was then used and gave a better fit (R-square: G1=0. 0.98, G2=0.98) (Fig. 3-6f). This demonstrates that there are two or more populations of Scc2 in the nucleus with different mobilities. In G1 and G2, roughly half of Scc2 recovers with a half-life consistent with being unbound. In G1 53% (SEM = 2.7%) recovers with a half-life

of 2.88 s (SEM = 0.4 s), and in G2 57% (SEM = 3.7%) recovers with a half-life of 3.89 s (SEM = 0.51 s). The recovery of the second fraction is much slower and is associated with chromatin. In G1 45% (SEM = 3.0%) recovers with a half-life of 51.0 s (SEM = 5.2 s), and in G2 41% (SEM = 3.4%) recovers with a half-life of 56.08 s (SEM = 5.51 s) (Fig. 3-6d).

These data demonstrate that roughly half of Scc2 associates with chromatin and this interaction is much more frequent than that of cohesin (Gerlich et al., 2006). Although Scc2 turnover is faster than cohesin's, it is not fast when compared to many other DNA binding proteins. For example many transcription factors have residence times of several seconds (Chen et al., 2014; Mueller et al., 2008) and CTCF has a residence time of a minute (Hansen et al., 2017). The argument that Scc2 is not efficiently captured during ChIP-Seq because of fast turnover is therefore probably not valid.

Cohesin's nuclear dynamics are dramatically altered during the cell cycle. During S phase 30% of cohesin becomes stabilised and may be permanently associated with chromosomes (Gerlich et al., 2006). This is caused by the binding to cohesin by sororin (Nishiyama et al., 2010). Unlike cohesin, the fraction bound to chromatin and the rate of turnover is very similar between G1 and G2. One explanation for this is that while a stable fraction of cohesin appears in G2, the percentage of cohesin that dynamically associates with DNA does not change drastically between the two phases (Gerlich et al., 2006). If Scc2 does not bind to cohesive cohesin, then one would not expect its dynamics to be altered by cohesion establishment.

Scc2 colocalises with cohesin vermicelli in WaplΔ cells

Because a large fraction of both cohesin and Scc2 is unbound, and because the bound fractions are quite homogenous, it is difficult to determine, by fluorescence microscopy, whether Scc2 and cohesin colocalise. However, when Wapl is deleted, cohesin becomes

organised into axial structures called 'vermicelli' and the fraction of cohesin bound to the DNA is very high (Tedeschi et al., 2013). This presents an opportunity to establish whether Scc2 associates with chromosomal cohesin. To inactivate Wapl, a plasmid encoding *Sp*Cas9, puromycin resistance and a gRNA targeting the *WAPL* gene were transfected. The gRNA was designed so that, when expressed in human cells, it would make a double-strand break inside the codon of M1116 in *WAPL*, which is critical for its activity (Ouyang et al., 2013). This results in frameshift mutations in most copies of *WAPL* but also in-frame deletions at the M1116 codon. The plasmid was transfected in Halo-Scc2 HeLa cells and Cas9-expressing cells were selected for two days with puromycin. The Halo-Scc2 was labelled with JF549, fixed, and the cohesin subunit Scc1 was labelled by immunofluorescence. Whereas in wild type cells Scc1 was largely homogenous in the nucleus, in most WaplΔ cells Scc1 became reorganised into vermicelli (Fig. 3-7).

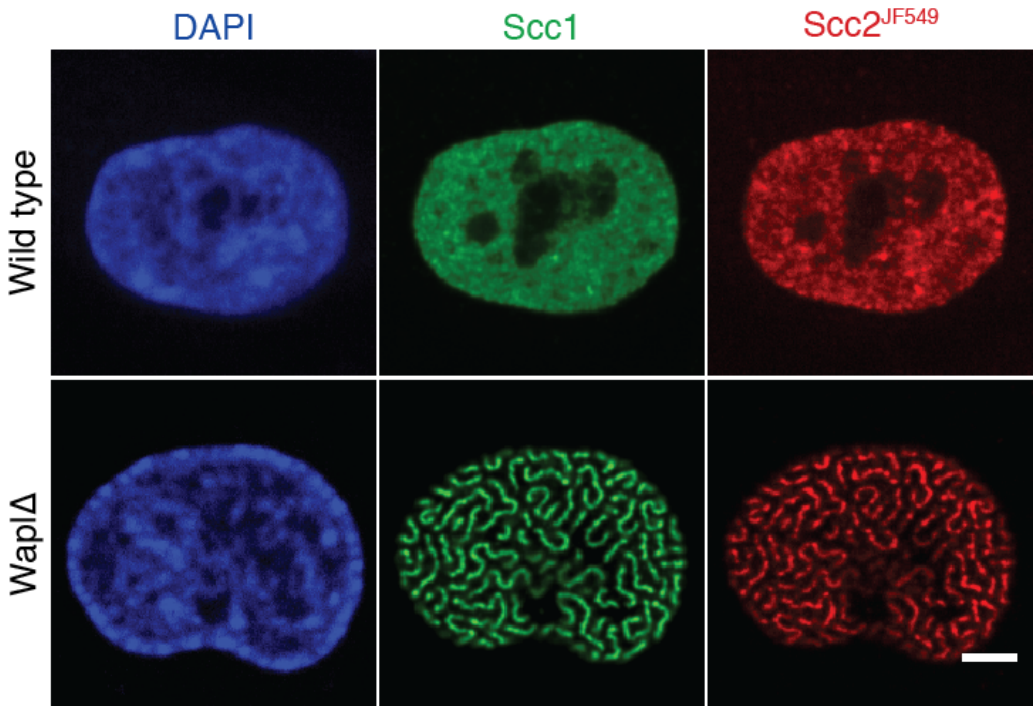

Figure 3-7 Scc2 forms vermicelli in WaplΔ HeLa cells Immunofluorescence microscopy images of wild type and WaplΔ Halo-Scc2 HeLa cells. Cohesin was stained with an antibody against Scc1 and Halo-Scc2 with JF549. Scale bar = 5 μm

Scc2^{JF549} also formed vermicelli and they colocalised with cohesin. Because most of the DNA was outside of the vermicelli the possibility that the colocalisation between cohesin and Scc2 was due to reorganisation of the chromatin was ruled out. Therefore, the finding that Scc2 colocalised with cohesin on vermicelli indicated that Scc2 interacted with cohesin that was stably associated with chromosomes.

Scc2 on vermicelli turns over with similar dynamics

Cohesin becomes stabilised on chromatin when Wapl is inactivated (Kueng et al., 2006). If Scc2's association with chromatin is mediated by an interaction with cohesin then Scc2 might bind more frequently to chromatin and turnover might be slower in WaplΔ cells. To determine whether Scc2's interaction with chromatin is altered by Wapl deletion, spot FRAP was performed on Scc2^{JF549} in WaplΔ HeLa cells (Fig. 3-8a).

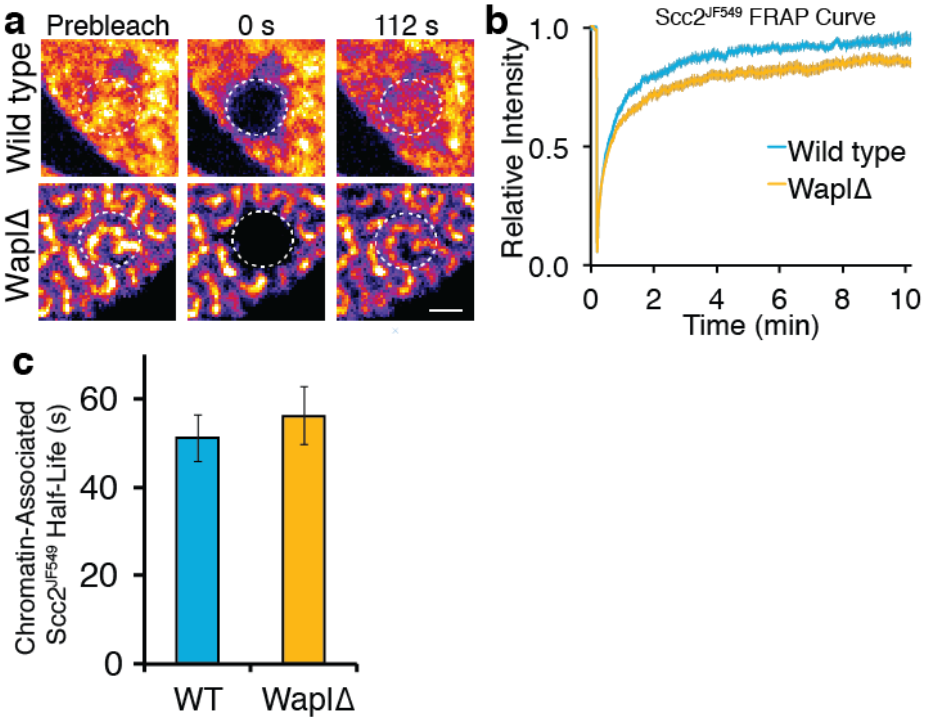

Figure 3-8 Scc2 turns over with similar dynamics on vermicelli a) Still images from spot FRAP experiments on Scc2^{JF549} in asynchronous wild type or WaplΔ HeLa cells. Dashed circle represents bleached region. Scale bar = 1 µm **b)** FRAP recovery curves from wild type and WaplΔ cells. Error bars denote SEM n=14 cells per condition. **c)** Mean half-life of chromatin bound Scc2^{JF549} derived from bi-exponential curve fitting of individual experiments from wild type or WaplΔ cells. Error bars denote standard error of the mean (SEM), n=14 cells per condition

Just as in wild type cells a single exponential model did not fit the recovery curve from Wapl∆ Scc2^{JF549} FRAP (R-square: WT=0.89, Wapl∆=0.84) but a bi-exponential function did (R-square: G1=0. 0.98, G2=0.98). This revealed that the bound fraction of Scc2^{JF549} was increased in Wapl∆ cells (Fig. 3-8b) and the fluorescence intensity in the bleached spot did not recover completely after ten minutes. Despite this the half-life of the chromatin-associated fraction was not significantly different (p=0.74). In WT 45.4% (SEM = 2%) recovers with a half-life of 49.6 s (SEM = 7.24 s) and in Wapl∆ 56.1% (SEM = 5%) recovers with a half-life of 52.6 s (SEM = 6.51 s).

In Wapl∆ cells there are fewer cohesin complexes in the soluble pool available for Scc2 to load onto the DNA. Therefore, if Scc2 only interacts with chromatin during the cohesin loading reaction then by inactivating Wapl the bound fraction should be diminished. Instead the chromatin associated fraction of Scc2 increased in Wapl∆ cells. The fact that an increase of chromatin associated cohesin and its reduced turnover also increased Scc2 binding demonstrates that Scc2 associates with cohesin after loading.

Scc2 dissociates from chromosomes in prophase independent of cohesin release

In mammalian cells most cohesin is released from chromosomes as cells enter mitosis via the non-proteolytic, prophase pathway. Sororin protects cohesive cohesin from Wapl-dependent release after DNA replication (Nishiyama et al., 2010; Rankin et al., 2005). Upon entry into mitosis, sororin and Scc3 are phosphorylated on multiple residues resulting in sororin's dissociation from cohesin (Nishiyama et al., 2013). This leaves cohesin vulnerable to Wapl and much of the cohesive cohesin dissociates from the chromosome arms. Sister chromatid cohesion is protected by the Sgol1-PP2A complex which dephosphorylates centromeric cohesin allowing it to maintain cohesion

(McGuinness et al., 2005). In the absence of Wapl the prophase pathway is inactive and cohesin remains associated with chromosome arms in metaphase. This therefore presented an opportunity to determine whether Scc2's dissociation from chromosome arms was dependent on cohesin release.

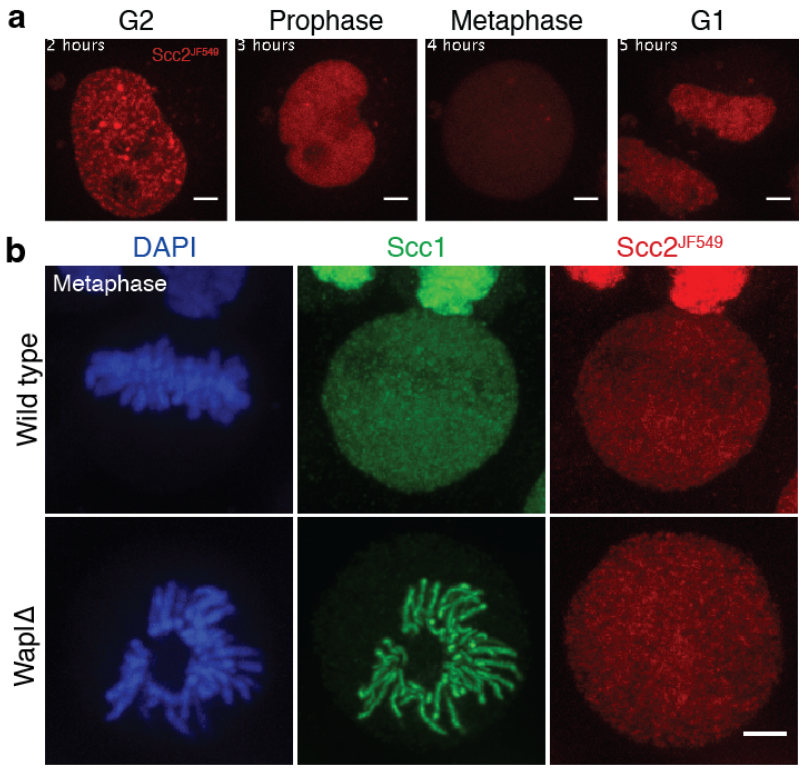

Figure 3-9 Dissociation of Scc2 from chromosomes in prophase does not depend on Wapl a) Live cell microscopy images of Scc2^{JF549} HeLa cell undergoing mitosis. **b)** Microscopy images of fixed Scc2^{JF549} HeLa cells labelled with DAPI (DNA) and an antibody against the cohesin subunit Scc1.

To address this, Wapl was again inactivated in Halo-Scc2 HeLa cells. Halo-Scc2 was labelled with JF549 and a time-lapse recording was acquired overnight. Scc2 vermicelli could be clearly seen in interphase cells. However, when cells entered prophase the Scc2^{JF549} rapidly unbound from chromosomes and became completely homogenous in the nucleus (Fig. 3-9a). Soon after nuclear envelope break down, Scc2^{JF549} was released into the cytoplasm and no enrichment could be detected on chromosomes. To verify that the prophase pathway had been inactivated in these cells, they were fixed and immuno-stained with an antibody against Scc1. This revealed that in wild type cells most cohesin is

removed from chromosomes, however, upon deletion of Wapl it is highly enriched on the chromosomes (Fig. 3-9b). The Scc2^{JF549} staining demonstrated that in the WaplΔ cells, when mitotic chromosomes are covered in cohesin, Scc2 is still absent from the DNA. It is possible that Scc2 dissociates from chromosomes due to phosphorylation of cohesin by mitotic kinases. However it is also possible that Pds5 displaces Scc2 from cohesin. It has been shown *in vitro* (Kikuchi et al., 2016) and *in vivo* (Naomi Petela - Personal Communication) that Pds5 and Scc2 compete for the same binding site.

Scc2 hops between chromosomal cohesins

During the course of these experiments it was noticed that in half nuclear FRAP Scc2 spreads slowly across the bleached zone. To demonstrate this, half nuclear FRAP was performed on Scc2^{JF549} and recovery images acquired for five minutes. Fluorescence recovery was then measured in bleached regions near (N) and far (F) from the unbleached region (Fig. 3-10a). The initial recovery for the region N was faster than for region F, which is to be expected for any protein with a free diffusing pool. However, the two regions did not equilibrate throughout the recovery (Fig. 3-10b).

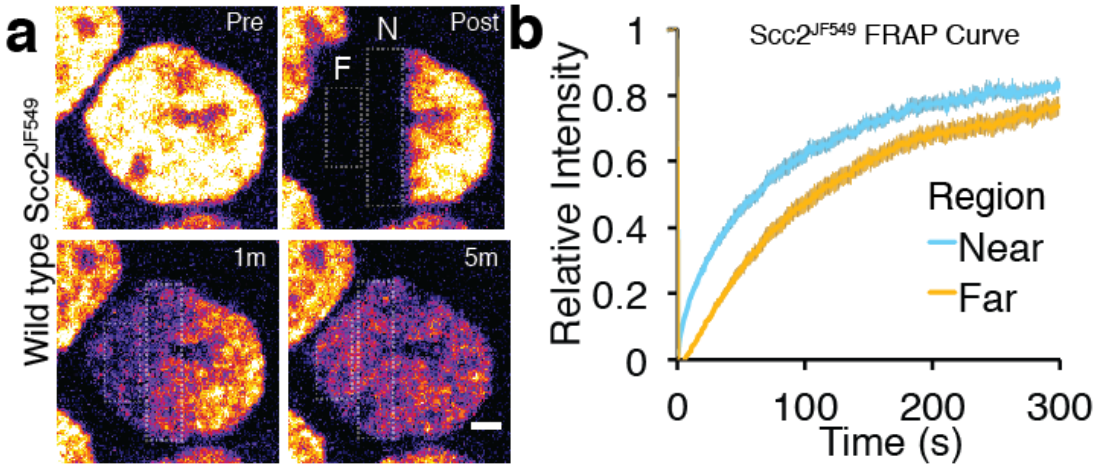

Figure 3-10 Scc2 spreads slows across chromatin a) Stills from half nuclear FRAP of Scc2^{JF549} in wild type HeLa cells. Dashed rectangle highlight a region Near (N) to and a region Far (F) from the unbleached half. Scale bar = 2.5 µm **b)** Half nuclear FRAP curves of Scc2^{JF549} in wild type HeLa cells. Recovery curves are shown from two zones within the bleached region. One zone is Near to the unbleached zone and the other is Far from the unbleached zone. Error bars denote SEM n=14 cells per condition.

There are two possible explanations for this spreading. One is that Scc2 has a very slow diffusion coefficient in the nucleus and the constant dissociation of Scc2 from the unbleached zone created a gradient of fluorescence. A second possibility is that Scc2^{JF549} was continually associating and dissociating from chromatin in a manner that disrupted its passage through the nucleus. Because Scc2^{JF549} is homogeneous in the nucleus it is not possible to distinguish between these two possibilities. However, given that Scc2^{JF549} forms vermicelli in WaplΔ cells, this pattern was used to differentiate between diffusion and hopping on cohesin. If Scc2 travels exclusively by diffusion without interruptions by cohesin then in half nuclear FRAP the spreading should remain homogenous. However, if Scc2 is hopping between cohesins then fluorescence may recover on vermicelli near to the bleached region before it can diffuse further away.

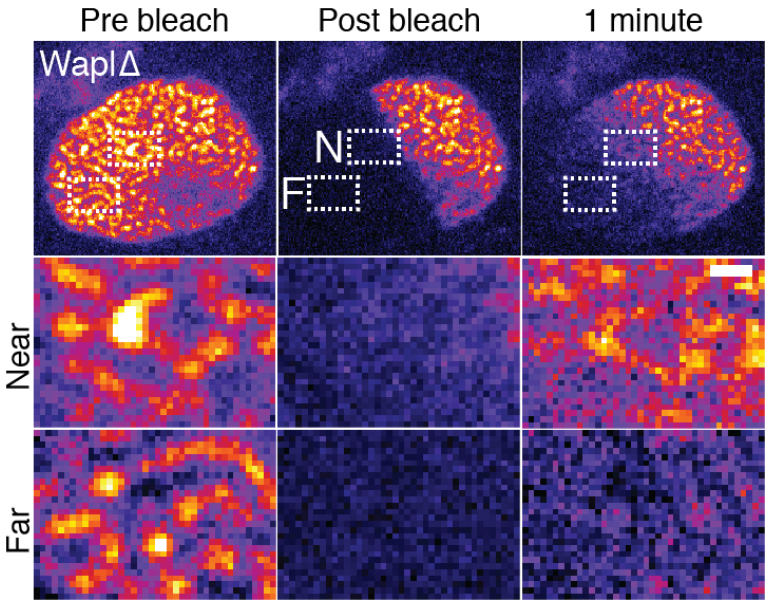

Figure 3-11 Scc2 hops between cohesin binding events Still images from a half-nuclear FRAP experiment of Scc2^{JF549} in WaplΔ HeLa cells. Dashed rectangles highlights a zone near (N) and a zone far (F) from the unbleached region shown in insets. Scale bar = 1 µm in inset.

Wapl was therefore deleted in Halo-Scc2 HeLa cells and Scc2^{JF549} became rearranged into vermicelli. Half of the nuclear JF549 fluorescence was bleached and recovery images were acquired for ten minutes. Strikingly, Scc2^{JF549} on bleached vermicelli close to the

unbleached region recovered before the region further away (Fig. 3-11). This demonstrates that, after unbinding, Scc2 rebinds another cohesin before diffusing an appreciable distance. This contrasts with cohesin and CTCF which spends 30 minutes and one minute respectively, diffusing between unbinding and rebinding (Hansen et al., 2017). Similar hopping behaviour has been observed for the histone linker H1 and the transcription factor Foxo (Misteli et al., 2000; Sekiya et al., 2009).

The dynamics of Scc2's chromatin association depend on cohesin

If Scc2 associates with chromatin mainly via an interaction with cohesin then removal of cohesin should have a major effect on Scc2 dynamics. Depletion of Scc1 must be achieved quickly and before the cells have the opportunity to divide, as mitosis in the absence of cohesin may have highly pleiotropic consequences. In order to deplete cohesin, Scc2 was tagged with the HaloTag in an HCT116 cell line expressing *Oryza sativa* Tir1, and Scc1 tagged with the mini Auxin Inducible Degron (mAID), and a fluorescent mClover tag (Fig. 3-4c) (Natsume et al., 2016). As previously reported, upon addition of auxin, Scc1-mAID-mClover was degraded within 1.5 hours as demonstrated by complete loss of nuclear mClover signal (Fig. 3-12a and b). Scc1 was also HaloTagged in HCT116 cells to enable comparison between recovery of Scc2 (Scc2-Scc4 = 386 kDa) and that of cohesin tetramers, which are larger (500 kDa). Half nuclear FRAP was then performed as, when compared to spot FRAP, it is easier to distinguish between freely diffusing molecules and those which move slowly by hopping.

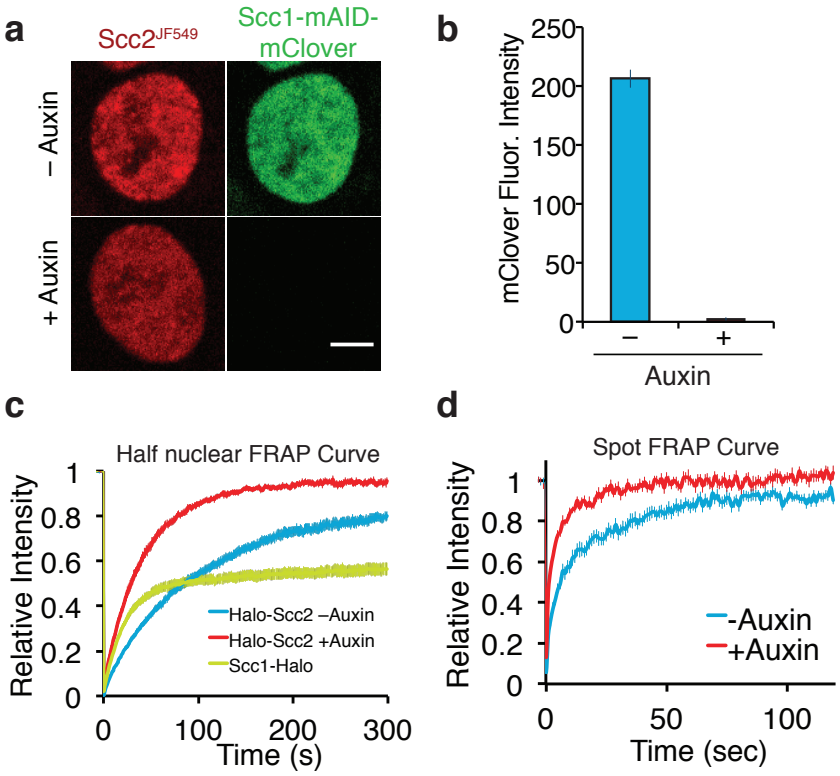

Figure 3-12 Depletion of Scc1 increases the rate of Scc2 FRAP recovery a) Live cell microscopy images of Scc1-mAID-mClover Tir1 Halo-Scc2 HCT116 cells with and without incubation in auxin for 1.5 hours. Scale bar, 5 μm **b)** nuclear fluorescence intensity of mClover with and without auxin treatment **c)** Half nuclear FRAP recovery curves of Halo-Scc2 with and without auxin treatment and Scc1-Halo. Error bars represent SEM n=10 **d)** Spot FRAP recovery curves from asynchronous HCT116 cells +/- Auxin. Error bars denote SEM n=13 cells per condition.

In untreated cells the Scc2^{JF549} fluorescence intensity in the bleached region recovered slowly, representing not just turnover but also frequent rebinding (which limits Scc2's movement in the nucleus). The initial recovery was slower than that of Scc1^{JF549}, despite cohesin being a larger complex than Scc2-Scc4 heterodimers. Strikingly, upon addition of auxin, and inactivation of cohesin, there was a large increase in the recovery rate of Scc2 into the bleached region (Fig. 3-12c). This suggests that Scc2's association with chromatin is largely dependent on an interaction with cohesin in wild type cells.

To determine whether there is still a bound fraction of Scc2^{JF549} after depletion of cohesin the experiment was repeated using spot FRAP rather than half nuclear FRAP (Fig. 3-12d). In the Scc1-depleted cells it was predicted that Scc2^{JF549} dynamics should now be

simplified. Therefore, spot FRAP was performed to permit modelling of the recovery curves (modelling was performed by Davide Mazza). In the absence of Scc1 the recovery curves for $Scc2^{JF549}$ were inconsistent with a single unbound population. Instead, upon depletion of cohesin 44% of $Scc2^{JF549}$ is bound to chromatin with a residence time of 22 seconds. The unbound fraction moves with a diffusion coefficient of 0.79 $\mu m^2/s$. This slow diffusion coefficient is consistent with a protein moving by effective diffusion (a mix of diffusion and non-specific interactions with DNA). Together these results suggest that in wild type cells Scc2 frequently binds to cohesin and this slows its movement around the nucleus. However, Scc2 can also bind to other targets on chromatin and, when cohesin is inactivated, a larger fraction of Scc2 associates with these other sites. Yet because Scc2's on rate is lower at these cohesin-independent sites, $Scc2^{JF549}$ can move more freely around the nucleus upon cohesin inactivation. Additionally, between specific binding events on chromatin Scc2 makes frequent but transient contact, further slowing Scc2 passage through the nucleus.

Single-molecule imaging of $Scc2^{JF549}$ demonstrates cohesin-dependent association with chromatin

Analysis of FRAP experiments demonstrated that Scc2 interacts with chromatin both via cohesin and independently of cohesin. Modelling of FRAP experiments in Scc1-depleted cells also revealed that while there is a significant unbound pool of Scc2, the diffusion coefficient of this fraction is consistent with effective diffusion. In other words, the movement of Scc2 in the nucleus is interrupted by frequent, non-specific and transient binding events. To test these hypotheses with an orthogonal and more direct approach, single-molecule imaging was employed to measure the movement of Scc2 molecules and quantify their interactions. The HaloTag ligand JF549 is sufficiently bright to detect single Halo-Scc2 molecules at 15 ms exposures and ~25 nm localisation precision inside nuclei

of living HCT116 cells (Fig. 3-13a). The dye blinks stochastically permitting the detection of thousands of molecules per cell over the course of a movie. These molecules remained fluorescent for an average of 9 frames (135 ms) before disappearing. This disappearance was due to blinking, photobleaching, or movement of the molecule out of the focal plane. Some molecules, however, lasted several seconds. The coordinates of individual molecules were determined and, by linking these localisations, a track could be generated for individual Scc2^{JF549} molecules (Fig. 3-13b). From each track the diffusion coefficient was determined and used to create maps of the bound and unbound Scc2 molecules in individual HCT116 cells (Fig. 3-13c).

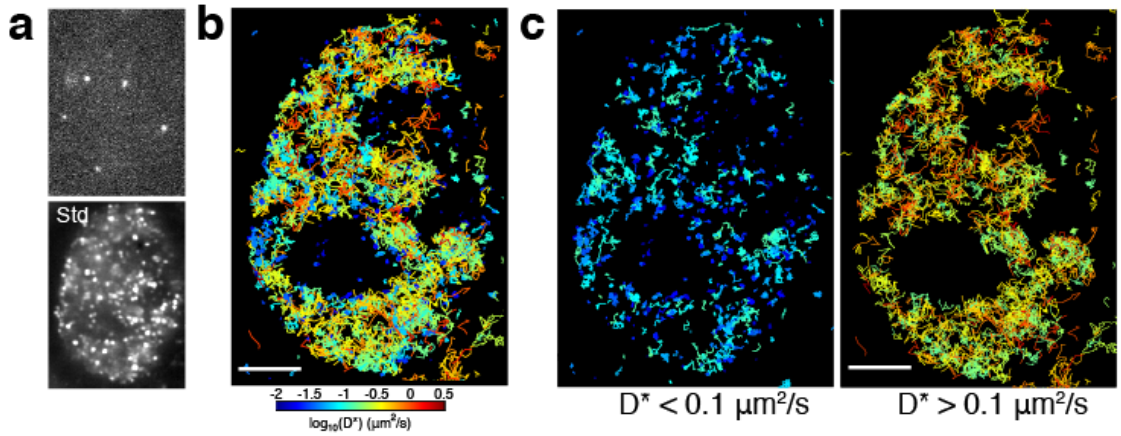

Figure 3-13 Trajectories and diffusion coefficients can be calculated for individual Scc2^{JF549} molecules using single molecule imaging a) Live cell microscopy image of Scc2^{JF549} in HCT116 cell. Spatial distribution of Scc2^{JF549} molecules shown by plotting standard deviation of pixel intensities from a recording of the same cell **b)** Trajectories of individual Scc2^{JF549} molecules from a single HCT116 nucleus. The colour of each track represents the diffusion coefficient **c)** Trajectories of the bound (left) and immobile (right) Scc2^{JF549} tracks. Data analysis performed by Stephan Uphoff.

The distribution of Scc2 tracks based on their diffusion coefficient revealed two distinct populations. The first displayed a diffusion coefficient consistent with chromatin association (37%) and the second were mobile and therefore unbound (63%) (Fig. 3-14a and b). The average apparent diffusion coefficient of the mobile molecules was 0.6 μm^2/s. This number is consistent with the results from the FRAP experiments.

The experiment was repeated for Scc1-Halo HCT116 cells allowing the comparison of fractions of bound and unbound molecules of Scc1 and Scc2. The distribution of diffusion coefficients of Scc1-Halo molecules also demonstrated two distinct populations and the fractions of bound and unbound molecules were remarkably similar to Scc2 (Fig. 3-14a and b).

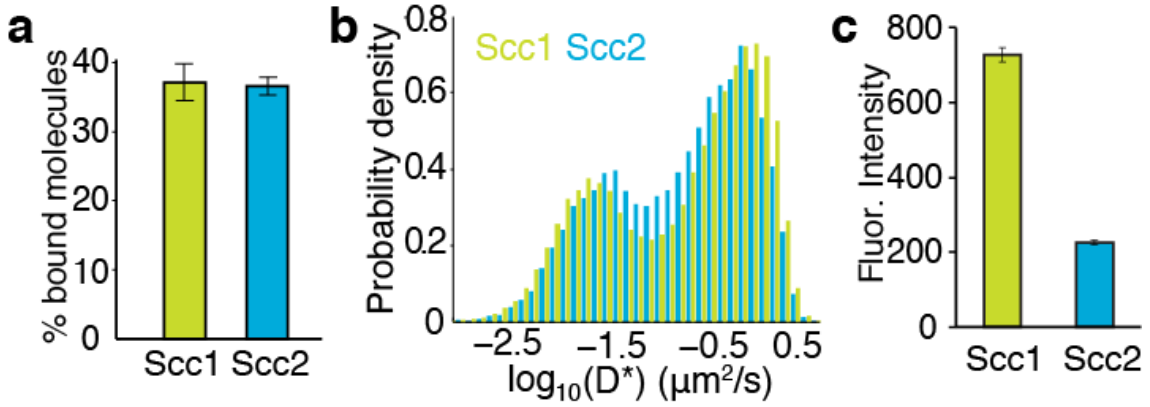

Figure 3-14 Comparison of Scc1 and Scc2 in HCT116 cells a) Histogram showing the fraction of Scc1 and Scc2 molecules that were bound to chromatin **b)** Log-scale distribution of apparent diffusion coefficients for Scc2 and Scc1 **c)** Nuclear fluorescence intensity above background of $Scc1^{JF549}$ and $Scc2^{JF549}$. n>10. Data analysis performed by Stephan Uphoff (a and b).

By tagging Scc1 and Scc2 with the HaloTag the relative stoichiometry of the two proteins could be compared. Scc1-Halo and Scc2-Halo HCT116 cell lines were stained with JF549 and confocal microscopy images were acquired. The nuclear fluorescence intensity was quantified revealing that there was three times more Scc1-Halo than Scc2-Halo in HCT116 cells (Fig. 3-14c). Given that roughly 40% of Scc1 molecules are associated with chromosomes, Scc2 is substoichiometric to chromosome-bound cohesin. Therefore, there is an excess of cohesin binding sites for Scc2 in the nucleus which may contribute to the spreading of Scc2 across chromatin seen in FRAP experiments.

Single molecule imaging confirms that chromosomal cohesin levels affect Scc2's chromatin association

To test the model that Scc2 interacts with pre-loaded cohesin, single molecule tracking was performed in cells in which the levels of chromosome-associated cohesin were altered. First, Scc2 molecules were tracked in HeLa cells in which Wapl had been deleted (Fig. 3-15a). In these cells most cohesin is chromosome-bound and it was found that the fraction of bound Scc2 molecules increased from 41% (wild type) to 55% (WaplΔ) (Fig. 3-15b and c). Therefore, increasing the fraction of cohesin that resides on chromosomes also increases the abundance of chromatin-bound Scc2. The experiment was then repeated in HCT116 cells in which cohesin could be removed from the DNA using an auxin degron on Scc1 (Fig. 3-15d). Elimination of cohesin from the DNA had the inverse effect; the fraction of Scc2 that was immobile decreased from 37% (no auxin) to 27% (1.5 hours after auxin addition) (Fig. 3-15e and f). Both observations are consistent with the notion that a significant fraction of Scc2 is bound to cohesin associated with chromosomes.

The Wapl deletion experiment is stronger evidence for a post-loading interaction than cohesin depletion. This is because Scc2 interacts with cohesin during the loading reaction and it is conceivable that Scc1 depletion may stop Scc2 interacting with chromatin by inactivating this process. In Wapl-deleted cells cohesin becomes stabilised on the DNA and a higher fraction is chromatin-bound because none is being released. Therefore the increased bound fraction of Scc2 in WaplΔ cells strongly supports the idea that Scc2 repeatedly revisits cohesin after the loading reaction has completed. There is no reason to think that there is a higher rate of cohesin loading. In fact one might expect the rate of loading to go down as the soluble pool of cohesin is depleted.

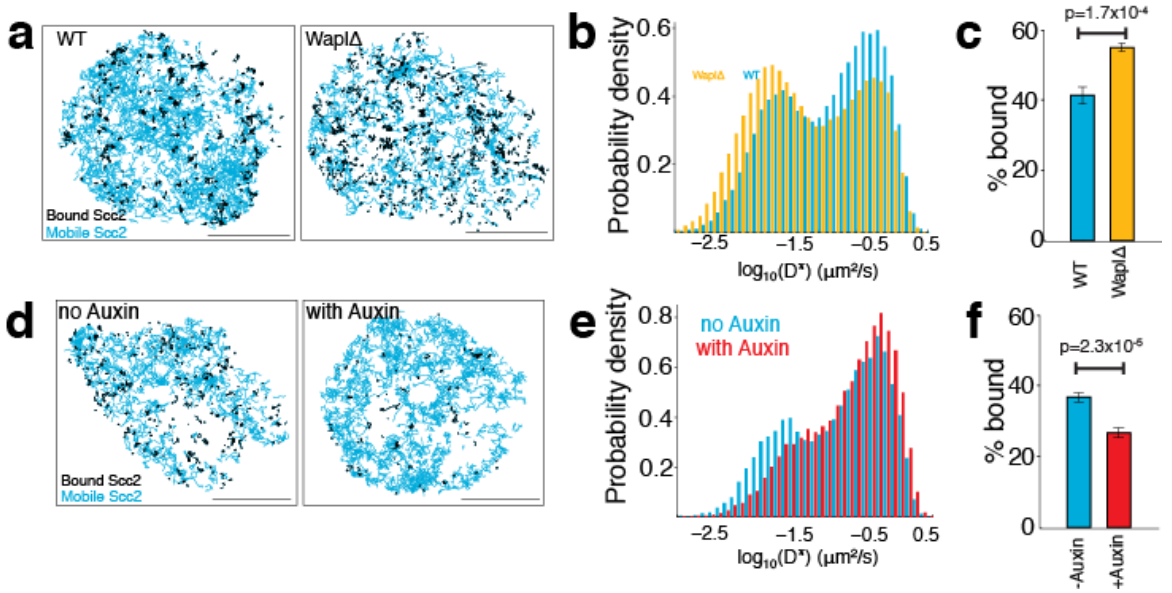

Figure 3-15 Chromosomal cohesin levels affect Scc2's association with chromatin a) Trajectories of individual Scc2^{JF549} molecules in wild type and WaplΔ HeLa cells **b)** Log-scale distribution of apparent diffusion coefficients for Scc2^{JF549} in wild type and WaplΔ HeLa cells **c)** fraction of chromatin-bound Scc2^{JF549} molecules in wild type and WaplΔ HeLa cells **d)** Trajectories of individual Scc2^{JF549} molecules in Scc1-mAID-mClover HCT116 cells with and without treatment with auxin **e)** Log-scale distribution of apparent diffusion coefficients for Scc2^{JF549} in these cells **f)** fraction of Scc2 molecules associated with chromatin with and without auxin treatment. Data analysis performed by Stephan Uphoff.

The fact that a significant fraction of Scc2 remains bound to DNA after cohesin depletion confirms that Scc2 binds to cohesin independent sites on chromatin (Zuin et al., 2014). This means that the decrease in Scc2's chromatin association upon cohesin depletion does not reflect the fraction that was originally bound to cohesin. Instead much of the Scc2 that was released from chromatin may have found other binding sites, which would then be visited more frequently by Scc2. Single particle tracking is not the best measure for the effect of Scc1 depletion on Scc2 dynamics because residence time is not a factor. Instead this change is better observed using half nuclear FRAP (Fig. 3-12) which takes into account the changes in residence time.

Additionally, these experiments showed that although the fraction of unbound molecules was decreased upon Wapl deletion and increased in Scc1 depletion, the apparent diffusion coefficient of Scc2 did not change. This indicated that the diffusion of mobile Scc2 is not

affected by changes in chromatin organisation induced by Wapl or cohesin perturbation or interactions with cohesin (soluble or chromatin bound).

Direct observation of Scc2's transient chromatin interactions

Scc2 spot FRAP in Scc1-depleted cells revealed that Scc2 has a low diffusion coefficient consistent with effective diffusion. If Scc2 frequently and transiently interacts with chromatin during its target search it should be possible to directly observe this by single molecule tracking. While most tracks last only several frames before moving out of focus or bleaching, some last several seconds. Tracks were found that lasted for a minimum of 10 frames and included steps with a high diffusion coefficient (mobile) and steps with a low diffusion coefficient (bound). By doing this it was possible to identify Scc2 tracks, in which the protein appears to jump between sub-second binding events on chromatin. This is direct evidence for the effective diffusion detected in FRAP experiments (Fig. 3-16). Furthermore, this type of track was found in Scc1-depleted cells confirming that the dynamics at this time scale are not determined by interactions with cohesin. These binding events were interpreted as cohesin-independent interactions at the 100 ms time scale that may be involved in target search.

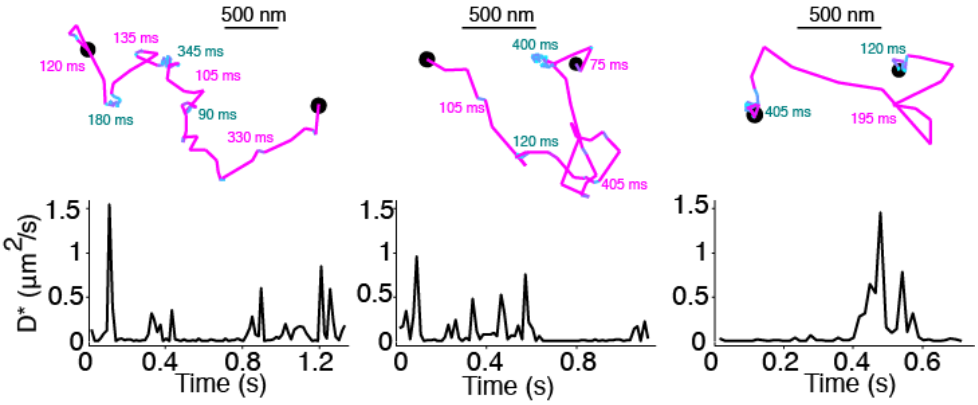

Figure 3-16 Direct observation of effective diffusion by Scc2 Individual trajectories of Scc2^{JF549} that contain both immobile and mobile phases. For each track the diffusion coefficient is plotted for the constituent steps. Data analysis performed by Stephan Uphoff.

Scc2 interacts with chromatin with a residence time of one minute

Measuring the length of Scc2's long-lived interaction with chromatin was not possible using the same experimental design because most JF549 molecules revert to a dark state within several milliseconds. To solve this problem cells were imaged with an exposure time of 1 s instead of 15 ms per frame. In 1 s exposures, mobile molecules were low intensity and blurred as the photons emitted by the JF549 were spread over more pixels. Increasing exposure time meant laser intensity could be reduced 30-fold, meaning molecules lasted much longer on average. It was therefore possible to determine how long, on average, molecules remained detectable. However, this information alone could not be used to calculate the residence time because dissociation kinetics was not the only factor causing the loss of $Scc2^{JF549}$ spots. Blinking, bleaching and cell movement were also causing loss of fluorescence. The results were corrected using $Scc1^{JF549}$ which is subject to the same biases but is known to reside stably on the DNA for tens of minutes (Gerlich et al., 2006). This correction factor was calculated by fitting a double exponential curve to the dwell time distribution of Scc1 and applying it to the corresponding dwell time distribution for Scc2. The dwell time distribution for Scc2 fitted a double exponential model (Fig. 3-17). 55% of Scc2 molecules were bound with a half-life of 1 s and 45% with a half-life of 47 s. The half-life calculated by tracking single molecules of Scc2 are very similar to those calculated using FRAP.

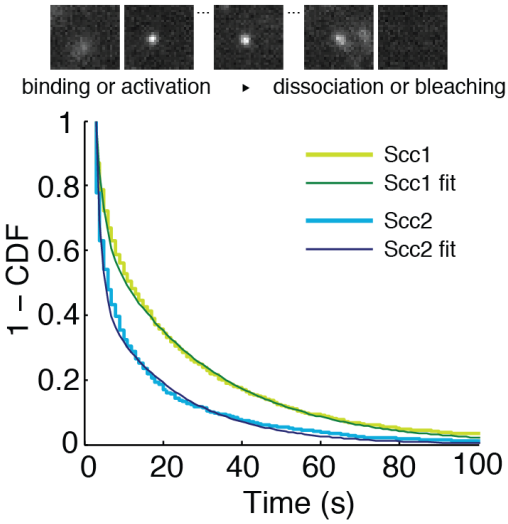

Figure 3-17 Scc2 binds to chromatin with a half-life of 47 s Example frames of Scc2^{JF549} at 1 s exposures. A bound molecule still produces a sharp spot but when it dissociates it blurs. Distributions (1 - cumulative distribution function) of measured dwell times of immobile Scc2 and Scc1 molecules and fitted curves. n>10.

These single molecule tracking experiments have helped explain the phenomenon of Scc2 spreading on chromatin. By resolving diffusing and chromatin bound molecules it has been shown in as direct a method as possible that Scc2 frequently interacts with cohesin on the DNA where it resides with a half-life of 47 s. Due to the high relative abundance of cohesin on the DNA Scc2 always has a binding site close by. It has also been shown that the diffusion of Scc2 is frequently punctuated by transient binding events, which slow its movement around the nucleus. This slow effective diffusion may contribute to the small distance that Scc2 can travel before it finds another cohesin ring to bind to.

Discussion

There is mounting evidence that the translocation of Smc complexes on DNA depends on their ATPase activity (Terekawa et al., 2017). Scc2 stimulates cohesin's ATPase activity *in vitro* (Murayama and Uhlmann, 2014) and promotes loop extension in mammalian cells (Haarhuis et al., 2017). If Scc2 determines cohesin's behaviour on DNA then they should interact after the cohesin loading reaction. However, several ChIP-Seq studies have found that there is no overlap between cohesin and Scc2 at CTCF sites where most cohesin peaks

are located (Kagey et al., 2010). In this study the aim was to resolve whether Scc2 interacts with cohesin once the loading reaction has been completed. This interaction was tested by introducing a HaloTag at the endogenous Scc2 locus and imaging these cells using fluorescence microscopy.

The ability to measure Scc2's chromatin association without the limitations of antibodies and chemical fixation permitted the observation that Scc2 binds frequently to cohesin that has completed the loading reaction (Fig. 3-18). Upon deletion of Wapl, cohesin is stable on the DNA and becomes arranged in axial structures called vermicelli. It was found that unlike most of the chromatin, Scc2 colocalises with these vermicelli.

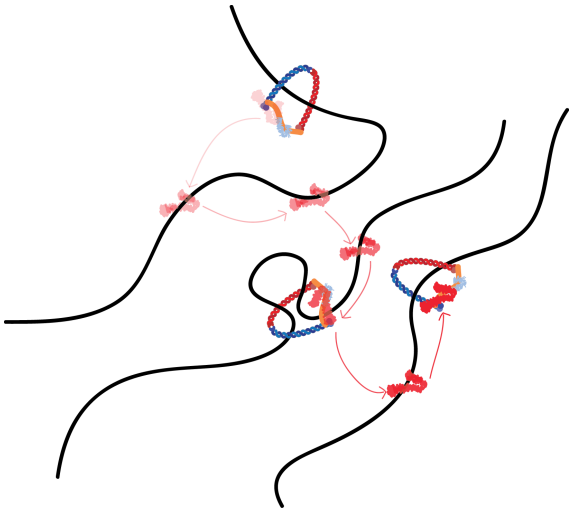

Figure 3-18 Model of Scc2 nuclear dynamics After unbinding from one cohesin ring Scc2 does not diffuse far before associating with the next. Diffusion is slowed by frequent non-specific interaction with chromatin. Scc2 also binds specifically to DNA perhaps while performing its function as a transcription factor.

In WaplΔ cells there is much less unbound cohesin because release has been abolished. If Scc2 interacted with cohesin exclusively during the loading reaction then Scc2 should bind less frequently to DNA in WaplΔ cells because there is less cohesin left to be loaded. The fact that Scc2 binds more frequently to chromatin when cohesin is overloaded is the best evidence that Scc2 interacts with cohesin outside of the loading reaction.

Consistent with this hypothesis, rapid degradation of Scc1 greatly increases Scc2's mobility and reduces the fraction of molecules, which are associated with chromatin. The drop in chromatin association is more modest than the increase in mobility because Scc2 has other chromatin binding sites, which it may bind more frequently in the absence of cohesin. However, these non-cohesin binding events have a faster turnover resulting in a big difference in FRAP.

The finding that Scc2's interaction with chromatin is predominantly via an association with cohesin raises the question why overlap between the two proteins has not been detected by ChIP-Seq. One possibility is that the epitope recognised by anti-Scc2 antibodies does not recognise the protein in its conformation at CTCF sites. However, several different antibodies have been used including one against a GFP-tagged Scc2, with all generating similar results, suggesting it is not due to antibody problems. Alternatively, the interaction may not be captured by formaldehyde crosslinking as demonstrated for some transcription factors (Teves et al., 2016). However, this is a problem for proteins with fast turnovers but it has been shown in this study that Scc2 resides on cohesin for approximately one minute. This is similar to CTCF itself and many other proteins whose genomic binding is captured very efficiently by ChIP-Seq. Inefficient crosslinking is probably not the reason why Scc2 is not detected at CTCF-cohesin sites.

The apparent exclusion of Scc2 from CTCF-cohesin sites may, therefore, be something much more interesting. By ChIP-Seq, cohesin peaks are detected at CTCF sites because ChIP-Seq experiments uses aggregate reads from millions of cells and CTCF sites are the sequences at which cohesin stops. It is possible however that, in a single cell, most cohesin rings are bound to DNA between CTCF sites but this is typically classed as 'background'. Scc2 may therefore bind to cohesin at most locations but not at CTCF sites. Could it be

that Scc2 is physically excluded from these positions? This could offer a possible explanation as to why cohesin stops translocating at CTCF sites and how CTCF acts as an insulator. If Scc2 is excluded from CTCF sites, cohesin's ATPase activity, and therefore its translocation, would likely be arrested. CTCF may function as an insulator by turning off cohesin's ATPase.

How might CTCF exclude Scc2 from the cohesin complex? It has recently been shown that Pds5 and Scc2 compete for the same binding site on Scc1 (Kikuchi et al., 2016) and that in Pds5-depleted HeLa cells loop anchors and physical insulation is lost (Wutz et al., 2017), just as in CTCF-depleted cells (Nora et al., 2017). It is conceivable that CTCF promotes Pds5's association with cohesin, which inhibits binding of Scc2 to cohesin, thereby shutting down the ATPase.

An alternative mechanism is that Esco1, which acetylates cohesin in G1 but does not contribute to sister chromatid cohesion (Alomer et al., 2017) is recruited by CTCF. Cohesin would then be acetylated at CTCF sites, which would inhibit cohesin's ATPase and potentially inhibit Scc2 binding to cohesin. In this model cohesin would remain in place even if CTCF dissociated from its binding site. Given that CTCF and Pds5 have a residence time of about one minute, a physical blockade would frequently allow cohesin to move past the site. Pds5 is known to promote cohesin acetylation (Chan et al., 2013) and this may explain why TADs disappear when Pds5 is depleted (Wutz et al., 2017).

CdLS is a severe developmental disorder that in the vast majority of cases is caused by mutations in the gene that encodes Scc2 (*NIPBL)*. Mutations are always heterozygous and result in a loss of function or deletion of one allele, leading to a reduction in the concentration of functional Scc2. Several studies have shown that, in cells that have one allele of *SCC2* deleted, mRNA levels are only reduced by 30% (Kawauchi et al., 2009). A

case has even been reported in which the patient displayed symptoms typical of CdLS but only had a 15% reduction in mRNA levels caused by a mutation in the 5' untranslated region of *SCC2* (Borck et al., 2006). Why small reductions in Scc2 concentration cause such severe developmental defects is not known.

In this study, several observations are presented, which are informative in answering this question. Scc2 interacts with cohesin after the loading reaction potentially stimulating its ATPase. Scc2 is substoichiometric relative to cohesin. Finally, Scc2 rapidly rebinds cohesin after dissociating. It is possible that the developmental defects observed in CdLS are caused by altered activity of cohesin on the DNA and not by defects in cohesin loading. If Scc2 concentration is rate limiting for cohesin's ATP-driven translocation and there is a limited concentration of Scc2 in the nucleus then small decreases in Scc2 levels may decrease cohesin's processivity on the DNA. This may decrease the frequency of interactions between enhancers and promoters and perturb insulation.

During the course of this study it was noticed that Scc2 has the ability to spread slowly through chromatin. FRAP and single molecule tracking it was shown that Scc2 moves through chromatin by hopping between cohesin complexes. This phenomenon probably arises because (i) Scc2 moves very slowly by effective diffusion, (ii) there is an abundance of cohesin rings for it to bind to and (iii) Scc2 has a high affinity for cohesin. The result is that after dissociating from one cohesin, Scc2 rapidly rebinds another cohesin before it is able to diffuse far through the nucleus. In these experiments, selective photobleaching was used to create a reservoir of fluorescent Scc2, which hops away from this source. However, situations can be imagined where a subnuclear structure or genomic locus could act as a source or landing pad for molecules. One example that has been proposed is the spreading of silenced chromatin by Polycomb complexes (Talbert and Henikoff, 2006). In this model

Polycomb Response Elements would act as a reservoir for Polycomb complexes, which would spread by local diffusion to nearby sequences creating a gradient of silencing histone modifications. Another example is Xist RNA, which is expressed from a single locus and appears to spread over the X chromosome so that only this chromosome is inactivated (Engreitz et al., 2013). Hopping would be an effective way of maintaining a high concentration of protein or RNA in certain nuclear locations and a low in concentration in others.

Chapter IV Materials and Methods

Antibodies

Scc1 (Upstate, 05-908, 1:100 for immunofluorescence), Scc1 (Abcam, ab154769, 1:1000 for Western blotting), PCNA (Abcam, ab29, 1:1000 for Western blotting), Wapl N-Terminus (Santa Cruz, sc-365189, 1:200 for Western blotting), anti-rabbit HRP (Sigma, #A4914); anti-mouse HRP (Jackson Immunoresearch, #115-035-068); Fluorescent secondary antibodies were all raised in donkey and conjugated to Alexa Fluor dyes (Molecular Probes).

Cell Lines and Cell Culture Conditions

Wild type U2OS cells were a gift from Benjamin Rowland. Wild type HeLa-S3 and HCT116 cell lines were a gift from Francis Barr. The Scc1-mAID-mClover TIR1 HCT116 cell line was a gift from Masato Kanemaki (Natsume et al., 2016).

HeLa and U2OS cells were cultured in Dulbecco's Modified Eagle Medium (DMEM) supplemented with 10% foetal bovine serum (FBS), penicillin (100 U/ml), streptomycin (100 μg/ml) and 2 mM L-Glutamine. HCT116 cells were cultured in McCoy's 5A (Modified) Medium supplemented with 10% FBS, penicillin (100 U/ml), streptomycin (100 μg/ml) and 2 mM L-Glutamine (All Gibco, San Diego, California, United States). Cell cultures were incubated at 37°C in 5% CO_2.

Plasmids

pSpCas9(BB)-2A-Puro (PX459) V2.0 was a gift from Feng Zhang (Addgene plasmid # 62988). Oligonucleotides encoding gRNAs were phosphorylated using Polynucleotide Kinase and annealed before ligation into the BbsI restriction site. Human H3.3 cDNA was a gift from Danette Daniels (Promega).

pEGFP-PCNA-IRES-puro2b was a gift from Daniel Gerlich (Addgene plasmid # 26461). pSNAPTag-H3.3-IRES-BSD and pEGFP-PCNA-IRES-BSD were generated by Gibson Assembly using linearised pEGFP-PCNA-IRES-puro2b (AgeI and XbaI) as the vector backbone.

A poly Glycine-Serine linker, BSD, GSG-P2A (self cleaving peptide) and the HaloTag were cloned into pUC19 between KpnI and SalI by Gibson Assembly to generate pUC19 NT-BSD-GSG-P2A-HaloTag. If this sequence is inserted after the start codon of a gene equimolar amounts of BSD and N-terminally HaloTagged protein of interest are expressed (Stewart-Ornstein and Lahav, 2016). The reverse was also assembled to make pUC19 CT-HaloTag-GSG-P2A-BSD for C-terminal tagging. HaloTag was amplified from pHTN (Promega) and SNAP-Tag cDNA from pH2B-SNAP.

Guide RNAs for CRISPR/Cas9

gRNAs for CRISPR/Cas9 were identified and checked for off-target binding using the MIT CRISPR design tool (Zhang Lab, MIT 2015). So that Cas9 would not cut the donor construct, where possible a gRNA was chosen whose binding is disrupted by the insertion of the tag. If such a gRNA was not identified then the highest scoring gRNA that binds closest to the insertion site was chosen. In this case, to prevent Cas9 cutting the donor construct, silent mutations were introduced, preferably mutating the PAM sequence (NGG at the 3' end of gRNA). The following oligonucleotides were cloned into pX459 linearised with BpiI (BbsI) (Thermo).

SCC1(Hs) 3'	ATAATATGGAACCTTGGTCC
SCC2(Hs) 5'	TCCAGAAATTCAGGATGAAT
WAPL M1116	GCATGCCGGCAAACACATGG

Donor Constructs for CRISPR/Cas9

The fluorescent tag (or tag-P2A-resistance marker) and a kilobase region either side of the start or stop codon of the target gene were amplified by PCR. Primers were designed to include 20 bp overlap with the neighbouring fragments and to insert a flexible linker (3xGGGSG) between the target protein and the tag. The homology arms and tag were cloned into pUC19 linearised with KpnI and SalI using Gibson Assembly (NEB). Donor constructs were verified by Sanger Sequencing (Source Bioscience).

Genome Editing

The day before transfection cells were seeded on 35 mm dishes. 500 ng of pX459 and 1500 ng of HR donor plasmid were co-transfected according to manufacturer's instructions. For HeLa and U2OS Transit-LT1 (Mirus) and for HCT116 cells Fugene-HD (Promega) was used as a transfection reagent. The day after transfection cells were re-plated sparsely to permit picking of individual colonies. For genome editing without a stable selection marker, transient expression of Cas9 was selected for two days with puromycin (2 μg/ml). When integrating P2A-BSD, cells were selected for a week with blasticidin (5 μg/ml). 10-14 days after replating, colonies were sufficiently large to pick and split into two replica 96-well plates. Clonal cell lines were genotyped by PCR with primers that bind outside of the homology arms.

Cell Cycle Synchronisation

Double thymidine block was used for enrichment of G1 and G2 HeLa cells. $7.5x10^4$ cells were seeded on 35 mm glass-bottomed dishes. The following day 2.5 mM thymidine (Sigma) was added to the cells. 18 hours later thymidine was removed by washing in CO_2 equilibrated medium. The cells were then left for 10 hours before a second addition of 2.5 mM thymidine. After 12 hours the thymidine was removed by washing and returned to

the incubator. After six hours most cells were in G2 and after 16 hours cells had divided and were in G1.

Preparation of protein extracts

For whole cell extract a confluent 100 mm plate was trypsinised and resuspended in culture medium. The cell suspension was centrifuged at 1000g and the supernatant discarded. The cell pellet was resuspended in 5 ml PBS and centrifuged again at 1000g. The supernatant was discarded and the pellet resuspended in 300 μl of RIPA buffer (Thermo). The cell suspension was rotated for one hour at 4ºC then centrifuged at 14000g for 30 minutes. The supernatant was transferred to a precooled tube for protein quantification. Protein extract concentration was measured using the Bradford Assay (Bradford, 1976)

Protein gel electrophoresis and Western blotting

Protein extracts were separated by electrophoresis through a polyacrylamide gel. Separated extracts were transferred onto PVDF membranes by semi dry transfer which was verified by Ponceau staining. Membranes were washed for five minutes in PBS then blocked in PBS with Tween-20 (0.1%) and milk (5%). Primary antibodies were diluted in the same solution and were incubated on the membrane for one hour at room temperature. The membrane was then washed three times for ten minutes in PBS with Tween-20 (0.1%). Secondary antibodies were diluted in PBS with Tween and milk and incubated on the membrane for one hour at room temperature. The membrane was washed three times for ten minutes in PBS with Tween-20 (0.1%) before developing. Enhanced chemiluminescence solution (GE Healthcare) was added to the membrane and it was imaged on a LI-COR Imager.

Immunofluorescence

~100,000 cells were seeded onto glass coverslips in 35 mm dishes two days prior to fixation. All subsequent steps were performed at room temperature. Cells were fixed in 2% paraformaldehyde (PFA) for 10 minutes. PFA was removed by repeatedly aspirating most fixative then adding IF wash buffer (PBS+0.1% Tween-20). The fixed cells were permeabilised in 0.1% Triton-X in PBS for 10 minutes. Coverslips were then placed cell side down on 50 μl drops of MaxBlock (Abcam) on parafilm for 30 minutes to reduce non-specific binding of antibodies. Primary antibodies were diluted in MaxBlock and coverslips were placed cell side down on 50 μl drops on parafilm and left for one hour. The unbound primary antibody was removed by repeated washing in IF wash buffer. Secondary antibodies were all diluted at 1 in 1000 in MaxBlock. Cover slips were placed cell side down in secondary antibody dilution for one hour. The cells were then washed a further five times in IF wash buffer to remove any residual unbound secondary antibody. Stained coverslips were fixed for a second time in 2% PFA before staining with DAPI (1 μg/ml in PBS) for 10 minutes. The coverslips were then mounted in VectaShield Mounting Medium and sealed with nail varnish.

Fluorescent labelling of HaloTag and SNAP-Tag fusion proteins

Two days before imaging, cells were seeded on glass bottom, 35 mm tissue culture dishes. Dishes were coated with 2.5 M glycine for 15 minutes beforehand to reduce binding of fluorescent ligands to the coverslip (van de Linde et al., 2011). To label Halo or SNAP-tagged proteins ligands were added to the medium for 15 minutes or 30 minutes respectively. The labelled cells were then washed five times with CO_2 and temperature equilibrated medium with an intervening 30 minutes incubation to allow unbound ligand to diffuse out of the cells.

Confocal Microscopy and FRAP

Live cell microscopy was performed in complete medium without phenol red. Confocal imaging was performed on a spinning disk confocal microscope (PerkinElmer UltraVIEW) with an EMCCD (Hamamatsu) mounted on an Olympus IX8 microscope with an Olympus 60 1.35 N.A objective. For live cell imaging the objective and stage were heated to 37ºC and the microscope was maintained in a chamber at 25ºC to minimize fluctuation of temperature. Cells were incubated in a humidified chamber and in 5% CO_2. Images were acquired using Volocity (Perkin Elmer). For spot FRAP, a minimum of ten prebleach acquisitions were made before a 2.5 μm circle was bleached using a 561 nm laser at 75% power for 30 ms. At least 10 cells were analysed per experiment.

FRAP Analysis

Fluorescence intensity measurements were made using ImageJ. Fluorescence intensity was measured in the bleached and unbleached regions and a region outside of a cell (background). The background intensity was subtracted from the bleached and unbleached intensities.

$$I_{CorrBleach} = I_{Bleach} - I_{Background}$$

$$I_{CorrUnbleach} = I_{Unbleach} - I_{Background}$$

The relative intensity between bleached and unbleached was calculated by dividing background corrected unbleached intensity by the background corrected bleached intensity.

$$\text{Relative Intensity} = I_{CorrBleach} / I_{CorrUnbleach}$$

The mean of the relative intensity of prebleach images was calculated and used to normalise all the values so that the relative intensity before bleaching had a mean of 1. The

mean normalised relative intensity for each time point for all repeats was calculated and plotted. For model fitting a custom MatLab script was used to fit a single or bi-exponential function to individual FRAP experiments. Significance was calculated using an unpaired *t*-test.

Single Molecule Imaging

A TIRF microscope was used with an Olympus 100x NA1.4 objective that was heated to 37ºC. A 561 nm laser (Toptica iChrome MLE) was focused into the back focal plane of the objective. To optimise the signal-to-noise ratio the position of the focal plane was moved. The nuclear florescence was pre-bleached until individual molecules were sufficiently infrequent that tracks did not overlap. For imaging both immobile and mobile molecules, images were acquired with continuous 561 nm excitation at a frame rate of 64.5 frames/s and an exposure time of 15 ms. Between 5000 and 20000 frames were acquired per movie. For binding time experiments, 300 frames were recorded under continuous 561 nm excitation at a frame rate of 1 frame/s and exposure time of 1 s.

Localisation and tracking analysis was performed in MATLAB (MathWorks) using custom software (STORMTracker) (Uphoff et al., 2014). An intensity threshold was used to detect molecules, and their localisations were determined by fitting an elliptical Gaussian Point Spread Function (PSF). Localisations within a radius of 0.48 μm that appeared in consecutive frames were linked to make tracks. Tracks made up of a minimum of four steps were used to calculate the apparent diffusion coefficients (D^*) from the mean-squared displacement (MSD) on a particle-by-particle basis: $D^* = MSD/(4\ dt)$, where dt is the time between frames. Apparent diffusion coefficient was used to classify mobile and immobile molecules after correcting for the localisation uncertainty of $\sigma = 25$

nm; Dcorrected = MSD/(4 dt) – σ ^2/dt. A molecule was deemed to be mobile if the D* was above 0.1 $\mu m^2/s$ and bound if it was below this number.

Binding times were estimated from single molecule imaging at 1 s exposures and a radius of 0.192 μm was used for tracking. Diffusing molecules were excluded from the analysis, by filtering tracks based on the apparent diffusion coefficient and the width of the fitted Gaussian function. Dwell times were calculated from the lengths of tracks of stationary molecules with diffraction-limited PSF. A double exponential decay function was fitted to the distribution of dwell times to compute the binding time constants. Binding times were corrected by using Scc1-Halo as a correction because it is known to reside stably on DNA (20-30 min) (Gerlich et al., 2006) for much longer than the time scale of the experiment (<60 s). Disappearance of Scc1 molecules was therefore deemed to be due to blinking, bleaching or movement out of the focal plane. The apparent dwell time constant (Scc1-Halo) was tBleach = 28.3 s. The following equation was used to calculate the binding times of Scc2 from the fitted dwell time constants: tBound = tDwell*tBleach / (tBleach - tDwell).

Bibliography

Alipour, E., and Marko, J.F. (2012). Self-organization of domain structures by DNA-loop-extruding enzymes. Nucleic Acids Res. *40*, 11202–11212.

Alomer, R.M., da Silva, E.M.L., Chen, J., Piekarz, K.M., McDonald, K., Sansam, C.G., Sansam, C.L., and Rankin, S. (2017). Esco1 and Esco2 regulate distinct cohesin functions during cell cycle progression. Proc. Natl. Acad. Sci. U.S.a. *114*, 9906–9911.

Anderson, D.E., Losada, A., Erickson, H.P., and Hirano, T. (2002). Condensin and cohesin display different arm conformations with characteristic hinge angles. J. Cell Biol. *156*, 419–424.

Aravind, L., Walker, D.R., and Koonin, E.V. (1999). Conserved domains in DNA repair proteins and evolution of repair systems. Nucleic Acids Res. *27*, 1223–1242.

Arumugam, P., Gruber, S., Tanaka, K., Haering, C.H., Mechtler, K., and Nasmyth, K. (2003). ATP hydrolysis is required for cohesin's association with chromosomes. Curr. Biol. *13*, 1941–1953.

Banerji, J., Rusconi, S., and Schaffner, W. (1981). Expression of a beta-globin gene is enhanced by remote SV40 DNA sequences. Cell *27*, 299–308.

Beckouët, F., Hu, B., Roig, M.B., Sutani, T., Komata, M., Uluocak, P., Katis, V.L., Shirahige, K., and Nasmyth, K. (2010). An Smc3 acetylation cycle is essential for establishment of sister chromatid cohesion. Mol. Cell *39*, 689–699.

Beckouët, F., Srinivasan, M., Roig, M.B., Chan, K.-L., Scheinost, J.C., Batty, P., Hu, B., Petela, N., Gligoris, T., Smith, A.C., et al. (2016). Releasing Activity Disengages Cohesin's Smc3/Scc1 Interface in a Process Blocked by Acetylation. Mol. Cell *61*, 563–574.

Bell, A.C., West, A.G., and Felsenfeld, G. (1999). The protein CTCF is required for the enhancer blocking activity of vertebrate insulators. Cell *98*, 387–396.

Bell, S.P., and Stillman, B. (1992). ATP-dependent recognition of eukaryotic origins of DNA replication by a multiprotein complex. Nature *357*, 128–134.

Bell, S.P., and Dutta, A. (2002). DNA replication in eukaryotic cells. Annu. Rev. Biochem. *71*, 333–374.

Bermudez, V.P., Maniwa, Y., Tappin, I., Ozato, K., Yokomori, K., and Hurwitz, J. (2003). The alternative Ctf18-Dcc1-Ctf8-replication factor C complex required for sister chromatid cohesion loads proliferating cell nuclear antigen onto DNA. Proc. Natl. Acad. Sci. U.S.a. *100*, 10237–10242.

Blomen, V.A., Májek, P., Jae, L.T., Bigenzahn, J.W., Nieuwenhuis, J., Staring, J., Sacco, R., van Diemen, F.R., Olk, N., Stukalov, A., et al. (2015). Gene essentiality and synthetic lethality in haploid human cells. Science *350*, 1092–1096.

Borck, G., Zarhrate, M., Cluzeau, C., Bal, E., Bonnefont, J.-P., Munnich, A., Cormier-Daire, V., and Colleaux, L. (2006). Father-to-daughter transmission of Cornelia de Lange syndrome caused by a mutation in the 5' untranslated region of the NIPBL Gene. Hum.

Mutat. *27*, 731–735.

Borges, V., Lehane, C., Lopez-Serra, L., Flynn, H., Skehel, M., Rolef Ben-Shahar, T., and Uhlmann, F. (2010). Hos1 deacetylates Smc3 to close the cohesin acetylation cycle. Mol. Cell *39*, 677–688.

Borges, V., Smith, D.J., Whitehouse, I., and Uhlmann, F. (2013). An Eco1-independent sister chromatid cohesion establishment pathway in S. cerevisiae. Chromosoma *122*, 121–134.

Boyle, M.I., Jespersgaard, C., Nazaryan, L., Bisgaard, A.-M., and Tümer, Z. (2016). A novel RAD21 variant associated with intrafamilial phenotypic variation in Cornelia de Lange syndrome - review of the literature. Clin. Genet.

Bradford, M.M. (1976). A rapid and sensitive method for the quantitation of microgram quantities of protein utilizing the principle of protein-dye binding. Anal. Biochem. *72*, 248–254.

Bravo, R., Frank, R., Blundell, P.A., and Macdonald-Bravo, H. (1987). Cyclin/PCNA is the auxiliary protein of DNA polymerase-delta. Nature *326*, 515–517.

Buheitel, J., and Stemmann, O. (2013). Prophase pathway-dependent removal of cohesin from human chromosomes requires opening of the Smc3-Scc1 gate. Embo J. *32*, 666–676.

Busslinger, G.A., Stocsits, R.R., van der Lelij, P., Axelsson, E., Tedeschi, A., Galjart, N., and Peters, J.-M. (2017). Cohesin is positioned in mammalian genomes by transcription, CTCF and Wapl. Nature *460*, 410.

Chalfie, M., Tu, Y., Euskirchen, G., Ward, W.W., and Prasher, D.C. (1994). Green fluorescent protein as a marker for gene expression. Science *263*, 802–805.

Chan, K.-L., Gligoris, T., Upcher, W., Kato, Y., Shirahige, K., Nasmyth, K., and Beckouët, F. (2013). Pds5 promotes and protects cohesin acetylation. Proc. Natl. Acad. Sci. U.S.a. *110*, 13020–13025.

Chan, K.-L., Roig, M.B., Hu, B., Beckouët, F., Metson, J., and Nasmyth, K. (2012). Cohesin's DNA exit gate is distinct from its entrance gate and is regulated by acetylation. Cell *150*, 961–974.

Chao, W.C.H., Murayama, Y., Muñoz, S., Jones, A.W., Wade, B.O., Purkiss, A.G., Hu, X.-W., Borg, A., Snijders, A.P., Uhlmann, F., et al. (2017). Structure of the cohesin loader Scc2. Nat Commun *8*, 13952.

Chen, J., Zhang, Z., Li, L., Chen, B.-C., Revyakin, A., Hajj, B., Legant, W., Dahan, M., Lionnet, T., Betzig, E., et al. (2014). Single-molecule dynamics of enhanceosome assembly in embryonic stem cells. Cell *156*, 1274–1285.

Chien, R., Zeng, W., Kawauchi, S., Bender, M.A., Santos, R., Gregson, H.C., Schmiesing, J.A., Newkirk, D.A., Kong, X., Ball, A.R., et al. (2011). Cohesin mediates chromatin interactions that regulate mammalian β-globin expression. J. Biol. Chem. *286*, 17870–17878.

Ciosk, R., Shirayama, M., Shevchenko, A., Tanaka, T., Toth, A., and Nasmyth, K. (2000). Cohesin's binding to chromosomes depends on a separate complex consisting of Scc2 and

Scc4 proteins. Mol. Cell *5*, 243–254.

Ciosk, R., Zachariae, W., Michaelis, C., Shevchenko, A., Mann, M., and Nasmyth, K. (1998). An ESP1/PDS1 complex regulates loss of sister chromatid cohesion at the metaphase to anaphase transition in yeast. Cell *93*, 1067–1076.

Cohen-Fix, O., Peters, J.M., Kirschner, M.W., and Koshland, D. (1996). Anaphase initiation in Saccharomyces cerevisiae is controlled by the APC-dependent degradation of the anaphase inhibitor Pds1p. Genes Dev. *10*, 3081–3093.

Coons, A., and Berliner, E. (1942). The Demonstration of Pneumococcal Antigen in Tissues by the Use of Fluorescent Antibody. The Journal of Immunology *45*, 159–170.

Cuylen, S., Metz, J., and Haering, C.H. (2011). Condensin structures chromosomal DNA through topological links. Nat. Struct. Mol. Biol. *18*, 894–901.

Çamdere, G., Guacci, V., Stricklin, J., and Koshland, D. (2015). The ATPases of cohesin interface with regulators to modulate cohesin-mediated DNA tethering. Elife *4*, 13115.

Davidson, I.F., Goetz, D., Zaczek, M.P., Molodtsov, M.I., Huis in 't Veld, P.J., Weissmann, F., Litos, G., Cisneros, D.A., Ocampo-Hafalla, M., Ladurner, R., et al. (2016). Rapid movement and transcriptional re-localization of human cohesin on DNA. Embo J. *35*, 2671–2685.

Deardorff, M.A., Bando, M., Nakato, R., Watrin, E., Itoh, T., Minamino, M., Saitoh, K., Komata, M., Katou, Y., Clark, D., et al. (2012). HDAC8 mutations in Cornelia de Lange syndrome affect the cohesin acetylation cycle. Nature *489*, 313–317.

Dixon, J.R., Gorkin, D.U., and Ren, B. (2016). Chromatin Domains: The Unit of Chromosome Organization. Mol. Cell *62*, 668–680.

Dixon, J.R., Selvaraj, S., Yue, F., Kim, A., Li, Y., Shen, Y., Hu, M., Liu, J.S., and Ren, B. (2012). Topological domains in mammalian genomes identified by analysis of chromatin interactions. Nature *485*, 376–380.

Donze, D., Adams, C.R., Rine, J., and Kamakaka, R.T. (1999). The boundaries of the silenced HMR domain in Saccharomyces cerevisiae. Genes Dev. *13*, 698–708.

Dreier, M.R., Bekier, M.E., and Taylor, W.R. (2011). Regulation of sororin by Cdk1-mediated phosphorylation. J. Cell. Sci. *124*, 2976–2987.

Dutta, A., and Bell, S.P. (1997). Initiation of DNA replication in eukaryotic cells. Annu. Rev. Cell Dev. Biol. *13*, 293–332.

Eichinger, C.S., Kurze, A., Oliveira, R.A., and Nasmyth, K. (2013). Disengaging the Smc3/kleisin interface releases cohesin from Drosophila chromosomes during interphase and mitosis. Embo J. *32*, 656–665.

Elbatsh, A.M.O., Haarhuis, J.H.I., Petela, N., Chapard, C., Fish, A., Celie, P.H., Stadnik, M., Ristic, D., Wyman, C., Medema, R.H., et al. (2016). Cohesin Releases DNA through Asymmetric ATPase-Driven Ring Opening. Mol. Cell *61*, 575–588.

Eng, T., Guacci, V., and Koshland, D. (2015). Interallelic complementation provides functional evidence for cohesin-cohesin interactions on DNA. Mol. Biol. Cell *26*, 4224–

4235.

Engreitz, J.M., Pandya-Jones, A., McDonel, P., Shishkin, A., Sirokman, K., Surka, C., Kadri, S., Xing, J., Goren, A., Lander, E.S., et al. (2013). The Xist lncRNA exploits three-dimensional genome architecture to spread across the X chromosome. Science *341*, 1237973–1237973.

Evans, T., Rosenthal, E.T., Youngblom, J., Distel, D., and Hunt, T. (1983). Cyclin: a protein specified by maternal mRNA in sea urchin eggs that is destroyed at each cleavage division. Cell *33*, 389–396.

Farina, A., Shin, J.-H., Kim, D.-H., Bermudez, V.P., Kelman, Z., Seo, Y.-S., and Hurwitz, J. (2008). Studies with the human cohesin establishment factor, ChlR1. Association of ChlR1 with Ctf18-RFC and Fen1. J. Biol. Chem. *283*, 20925–20936.

Flavahan, W.A., Drier, Y., Liau, B.B., Gillespie, S.M., Venteicher, A.S., Stemmer-Rachamimov, A.O., Suvà, M.L., and Bernstein, B.E. (2016). Insulator dysfunction and oncogene activation in IDH mutant gliomas. Nature *529*, 110–114.

Flemming, W. (1879). Beitrage zur Kenntniss der Zelle und ihrer Lebenserscheinungen. Archiv Für Mikroskopische Anatomie *16*, 302–436.

Fournier, M., Bourriquen, G., Lamaze, F.C., Côté, M.C., Fournier, É., Joly-Beauparlant, C., Caron, V., Gobeil, S., Droit, A., and Bilodeau, S. (2016). FOXA and master transcription factors recruit Mediator and Cohesin to the core transcriptional regulatory circuitry of cancer cells. Sci Rep *6*, 34962.

Fudenberg, G., Imakaev, M., Lu, C., Goloborodko, A., Abdennur, N., and Mirny, L.A. (2016). Formation of Chromosomal Domains by Loop Extrusion. Cell Rep *15*, 2038–2049.

Gambus, A., Jones, R.C., Sanchez-Diaz, A., Kanemaki, M., van Deursen, F., Edmondson, R.D., and Labib, K. (2006). GINS maintains association of Cdc45 with MCM in replisome progression complexes at eukaryotic DNA replication forks. Nat. Cell Biol. *8*, 358–366.

Gerlich, D., Beaudouin, J., Kalbfuss, B., Daigle, N., Eils, R., and Ellenberg, J. (2003). Global chromosome positions are transmitted through mitosis in mammalian cells. Cell *112*, 751–764.

Gerlich, D., Koch, B., Dupeux, F., Peters, J.-M., and Ellenberg, J. (2006). Live-cell imaging reveals a stable cohesin-chromatin interaction after but not before DNA replication. Curr. Biol. *16*, 1571–1578.

Gillespie, P.J., and Hirano, T. (2004). Scc2 couples replication licensing to sister chromatid cohesion in Xenopus egg extracts. Curr. Biol. *14*, 1598–1603.

Gligoris, T.G., Scheinost, J.C., Bürmann, F., Petela, N., Chan, K.-L., Uluocak, P., Beckouët, F., Gruber, S., Nasmyth, K., and Löwe, J. (2014). Closing the cohesin ring: structure and function of its Smc3-kleisin interface. Science *346*, 963–967.

Grallert, B., and Nurse, P. (1996). The ORC1 homolog orp1 in fission yeast plays a key role in regulating onset of S phase. Genes Dev. *10*, 2644–2654.

Grimm, J.B., English, B.P., Chen, J., Slaughter, J.P., Zhang, Z., Revyakin, A., Patel, R., Macklin, J.J., Normanno, D., Singer, R.H., et al. (2015). A general method to improve

fluorophores for live-cell and single-molecule microscopy. Nat Meth *12*, 244–50–3pfollowing250.

Grimm, J.B., English, B.P., Choi, H., Muthusamy, A.K., Mehl, B.P., Dong, P., Brown, T.A., Lippincott-Schwartz, J., Liu, Z., Lionnet, T., et al. (2016). Bright photoactivatable fluorophores for single-molecule imaging. Nat Meth *13*, 985–988.

Gruber, S., Arumugam, P., Katou, Y., Kuglitsch, D., Helmhart, W., Shirahige, K., and Nasmyth, K. (2006). Evidence that loading of cohesin onto chromosomes involves opening of its SMC hinge. Cell *127*, 523–537.

Gruber, S., Haering, C.H., and Nasmyth, K. (2003). Chromosomal cohesin forms a ring. Cell *112*, 765–777.

Guacci, V., Koshland, D., and Strunnikov, A. (1997). A direct link between sister chromatid cohesion and chromosome condensation revealed through the analysis of MCD1 in S. cerevisiae. Cell *91*, 47–57.

Haarhuis, J.H.I., van der Weide, R.H., Blomen, V.A., Yáñez-Cuna, J.O., Amendola, M., van Ruiten, M.S., Krijger, P.H.L., Teunissen, H., Medema, R.H., van Steensel, B., et al. (2017). The Cohesin Release Factor WAPL Restricts Chromatin Loop Extension. Cell *169*, 693–707.e14.

Hadjur, S., Williams, L.M., Ryan, N.K., Cobb, B.S., Sexton, T., Fraser, P., Fisher, A.G., and Merkenschlager, M. (2009). Cohesins form chromosomal cis-interactions at the developmentally regulated IFNG locus. Nature *460*, 410–413.

Haering, C.H., Farcas, A.-M., Arumugam, P., Metson, J., and Nasmyth, K. (2008). The cohesin ring concatenates sister DNA molecules. Nature *454*, 297–301.

Haering, C.H., Löwe, J., Hochwagen, A., and Nasmyth, K. (2002). Molecular architecture of SMC proteins and the yeast cohesin complex. Mol. Cell *9*, 773–788.

Haering, C.H., Schoffnegger, D., Nishino, T., Helmhart, W., Nasmyth, K., and Löwe, J. (2004). Structure and stability of cohesin's Smc1-kleisin interaction. Mol. Cell *15*, 951–964.

Hansen, A.S., Pustova, I., Cattoglio, C., Tjian, R., and Darzacq, X. (2017). CTCF and cohesin regulate chromatin loop stability with distinct dynamics. Elife *6*, 2848.

Hara, K., Zheng, G., Qu, Q., Liu, H., Ouyang, Z., Chen, Z., Tomchick, D.R., and Yu, H. (2014). Structure of cohesin subcomplex pinpoints direct shugoshin-Wapl antagonism in centromeric cohesion. Nat. Struct. Mol. Biol. *21*, 864–870.

Hinshaw, S.M., Makrantoni, V., Kerr, A., Marston, A.L., and Harrison, S.C. (2015). Structural evidence for Scc4-dependent localization of cohesin loading. Elife *4*, e06057.

Hopfner, K.P., Karcher, A., Shin, D.S., Craig, L., Arthur, L.M., Carney, J.P., and Tainer, J.A. (2000). Structural biology of Rad50 ATPase: ATP-driven conformational control in DNA double-strand break repair and the ABC-ATPase superfamily. Cell *101*, 789–800.

Hopfner, K.-P., and Tainer, J.A. (2003). Rad50/SMC proteins and ABC transporters: unifying concepts from high-resolution structures. Curr. Opin. Struct. Biol. *13*, 249–255.

Hu, B., Itoh, T., Mishra, A., Katoh, Y., Chan, K.-L., Upcher, W., Godlee, C., Roig, M.B., Shirahige, K., and Nasmyth, K. (2011). ATP hydrolysis is required for relocating cohesin from sites occupied by its Scc2/4 loading complex. Curr. Biol. *21*, 12–24.

Hu, B., Petela, N., Kurze, A., Chan, K.-L., Chapard, C., and Nasmyth, K. (2015). Biological chromodynamics: a general method for measuring protein occupancy across the genome by calibrating ChIP-seq. Nucleic Acids Res. *43*, e132.

Huang, C.E., Milutinovich, M., and Koshland, D. (2005). Rings, bracelet or snaps: fashionable alternatives for Smc complexes. Philos. Trans. R. Soc. Lond., B, Biol. Sci. *360*, 537–542.

Ishihara, K., Oshimura, M., and Nakao, M. (2006). CTCF-dependent chromatin insulator is linked to epigenetic remodeling. Mol. Cell *23*, 733–742.

Ivanov, D., and Nasmyth, K. (2005). A topological interaction between cohesin rings and a circular minichromosome. Cell *122*, 849–860.

Kagey, M.H., Newman, J.J., Bilodeau, S., Zhan, Y., Orlando, D.A., van Berkum, N.L., Ebmeier, C.C., Goossens, J., Rahl, P.B., Levine, S.S., et al. (2010). Mediator and cohesin connect gene expression and chromatin architecture. Nature *467*, 430–435.

Kanke, M., Tahara, E., Huis In't Veld, P.J., and Nishiyama, T. (2016). Cohesin acetylation and Wapl-Pds5 oppositely regulate translocation of cohesin along DNA. Embo J. *35*, 2686–2698.

Kawauchi, S., Calof, A.L., Santos, R., Lopez-Burks, M.E., Young, C.M., Hoang, M.P., Chua, A., Lao, T., Lechner, M.S., Daniel, J.A., et al. (2009). Multiple organ system defects and transcriptional dysregulation in the Nipbl(+/-) mouse, a model of Cornelia de Lange Syndrome. PLoS Genet. *5*, e1000650.

Keppler, A., Gendreizig, S., Gronemeyer, T., Pick, H., Vogel, H., and Johnsson, K. (2003). A general method for the covalent labeling of fusion proteins with small molecules in vivo. Nat. Biotechnol. *21*, 86–89.

Kikuchi, S., Borek, D.M., Otwinowski, Z., Tomchick, D.R., and Yu, H. (2016). Crystal structure of the cohesin loader Scc2 and insight into cohesinopathy. Proc. Natl. Acad. Sci. U.S.a. *113*, 12444–12449.

Kimura, H., and Cook, P.R. (2001). Kinetics of core histones in living human cells: little exchange of H3 and H4 and some rapid exchange of H2B. J. Cell Biol. *153*, 1341–1353.

King, R.W., Peters, J.M., Tugendreich, S., Rolfe, M., Hieter, P., and Kirschner, M.W. (1995). A 20S complex containing CDC27 and CDC16 catalyzes the mitosis-specific conjugation of ubiquitin to cyclin B. Cell *81*, 279–288.

Kitajima, T.S., Kawashima, S.A., and Watanabe, Y. (2004). The conserved kinetochore protein shugoshin protects centromeric cohesion during meiosis. Nature *427*, 510–517.

Koshland, D., and Hartwell, L.H. (1987). The structure of sister minichromosome DNA before anaphase in Saccharomyces cerevisiae. Science *238*, 1713–1716.

Kueng, S., Hegemann, B., Peters, B.H., Lipp, J.J., Schleiffer, A., Mechtler, K., and Peters, J.-M. (2006). Wapl controls the dynamic association of cohesin with chromatin. Cell *127*,

955–967.

Kurat, C.F., Yeeles, J.T.P., Patel, H., Early, A., and Diffley, J.F.X. (2017). Chromatin Controls DNA Replication Origin Selection, Lagging-Strand Synthesis, and Replication Fork Rates. Mol. Cell *65*, 117–130.

Ladurner, R., Bhaskara, V., Huis in 't Veld, P.J., Davidson, I.F., Kreidl, E., Petzold, G., and Peters, J.-M. (2014). Cohesin's ATPase activity couples cohesin loading onto DNA with Smc3 acetylation. Curr. Biol. *24*, 2228–2237.

Ladurner, R., Kreidl, E., Ivanov, M.P., Ekker, H., Idarraga-Amado, M.H., Busslinger, G.A., Wutz, G., Cisneros, D.A., and Peters, J.-M. (2016). Sororin actively maintains sister chromatid cohesion. Embo J. *35*, 635–653.

Lammens, A., Schele, A., and Hopfner, K.-P. (2004). Structural biochemistry of ATP-driven dimerization and DNA-stimulated activation of SMC ATPases. Curr. Biol. *14*, 1778–1782.

Lee, B.-G., Roig, M.B., Jansma, M., Petela, N., Metson, J., Nasmyth, K., and Löwe, J. (2016). Crystal Structure of the Cohesin Gatekeeper Pds5 and in Complex with Kleisin Scc1. Cell Rep *14*, 2108–2115.

Lee, M.G., and Nurse, P. (1987). Complementation used to clone a human homologue of the fission yeast cell cycle control gene cdc2. Nature *327*, 31–35.

Lengronne, A., Katou, Y., Mori, S., Yokobayashi, S., Kelly, G.P., Itoh, T., Watanabe, Y., Shirahige, K., and Uhlmann, F. (2004). Cohesin relocation from sites of chromosomal loading to places of convergent transcription. Nature *430*, 573–578.

Lengronne, A., McIntyre, J., Katou, Y., Kanoh, Y., Hopfner, K.-P., Shirahige, K., and Uhlmann, F. (2006). Establishment of sister chromatid cohesion at the S. cerevisiae replication fork. Mol. Cell *23*, 787–799.

Liang, C., Weinreich, M., and Stillman, B. (1995). ORC and Cdc6p interact and determine the frequency of initiation of DNA replication in the genome. Cell *81*, 667–676.

Liu, H., Rankin, S., and Yu, H. (2013). Phosphorylation-enabled binding of SGO1-PP2A to cohesin protects sororin and centromeric cohesion during mitosis. Nat. Cell Biol. *15*, 40–49.

Los, G.V., Encell, L.P., McDougall, M.G., Hartzell, D.D., Karassina, N., Zimprich, C., Wood, M.G., Learish, R., Ohana, R.F., Urh, M., et al. (2008). HaloTag: A Novel Protein Labeling Technology for Cell Imaging and Protein Analysis. ACS Chem. Biol. *3*, 373–382.

Losada, A., Hirano, M., and Hirano, T. (1998). Identification of Xenopus SMC protein complexes required for sister chromatid cohesion. Genes Dev. *12*, 1986–1997.

Mali, P., Yang, L., Esvelt, K.M., Aach, J., Guell, M., DiCarlo, J.E., Norville, J.E., and Church, G.M. (2013). RNA-guided human genome engineering via Cas9. Science *339*, 823–826.

Mayer, M.L., Gygi, S.P., Aebersold, R., and Hieter, P. (2001). Identification of RFC(Ctf18p, Ctf8p, Dcc1p): an alternative RFC complex required for sister chromatid

cohesion in S. cerevisiae. Mol. Cell *7*, 959–970.

Mazza, D., Abernathy, A., Golob, N., Morisaki, T., and McNally, J.G. (2012). A benchmark for chromatin binding measurements in live cells. Nucleic Acids Res. *40*, e119–e119.

McGuinness, B.E., Hirota, T., Kudo, N.R., Peters, J.-M., and Nasmyth, K. (2005). Shugoshin prevents dissociation of cohesin from centromeres during mitosis in vertebrate cells. PLoS Biol. *3*, e86.

Michaelis, C., Ciosk, R., and Nasmyth, K. (1997). Cohesins: chromosomal proteins that prevent premature separation of sister chromatids. Cell *91*, 35–45.

Misteli, T., Gunjan, A., Hock, R., Bustin, M., and Brown, D.T. (2000). Dynamic binding of histone H1 to chromatin in living cells. Nature *408*, 877–881.

Morgan, D. (2007). The Cell Cycle.

Morisaki, T., and McNally, J.G. (2014). Photoswitching-free FRAP analysis with a genetically encoded fluorescent tag. PLoS ONE *9*, e107730.

Mueller, F., Wach, P., and McNally, J.G. (2008). Evidence for a common mode of transcription factor interaction with chromatin as revealed by improved quantitative fluorescence recovery after photobleaching. Biophysical Journal *94*, 3323–3339.

Murayama, Y., and Uhlmann, F. (2014). Biochemical reconstitution of topological DNA binding by the cohesin ring. Nature *505*, 367–371.

Murayama, Y., and Uhlmann, F. (2015). DNA Entry into and Exit out of the Cohesin Ring by an Interlocking Gate Mechanism. Cell *163*, 1628–1640.

Musacchio, A. (2015). The Molecular Biology of Spindle Assembly Checkpoint Signaling Dynamics. Curr. Biol. *25*, R1002–R1018.

Nasmyth, K. (2001). Disseminating the genome: joining, resolving, and separating sister chromatids during mitosis and meiosis. Annu. Rev. Genet. *35*, 673–745.

Nasmyth, K. (2017). Scc2-Mediated Loading Of Cohesin Onto Chromosomes In G1 Yeast Cells Is Insufficient To Build Cohesion During S Phase.

Nasmyth, K., and Haering, C.H. (2005). The structure and function of SMC and kleisin complexes. Annu. Rev. Biochem. *74*, 595–648.

Natsume, T., Kiyomitsu, T., Saga, Y., and Kanemaki, M.T. (2016). Rapid Protein Depletion in Human Cells by Auxin-Inducible Degron Tagging with Short Homology Donors. Cell Rep *15*, 210–218.

Niki, H., Imamura, R., Kitaoka, M., Yamanaka, K., Ogura, T., and Hiraga, S. (1992). E.coli MukB protein involved in chromosome partition forms a homodimer with a rod-and-hinge structure having DNA binding and ATP/GTP binding activities. Embo J. *11*, 5101–5109.

Niki, H., Jaffé, A., Imamura, R., Ogura, T., and Hiraga, S. (1991). The new gene mukB codes for a 177 kd protein with coiled-coil domains involved in chromosome partitioning of E. coli. Embo J. *10*, 183–193.

Nishitani, H., Lygerou, Z., Nishimoto, T., and Nurse, P. (2000). The Cdt1 protein is required to license DNA for replication in fission yeast. Nature *404*, 625–628.

Nishiyama, T., Ladurner, R., Schmitz, J., Kreidl, E., Schleiffer, A., Bhaskara, V., Bando, M., Shirahige, K., Hyman, A.A., Mechtler, K., et al. (2010). Sororin mediates sister chromatid cohesion by antagonizing Wapl. Cell *143*, 737–749.

Nishiyama, T., Sykora, M.M., Huis in 't Veld, P.J., Mechtler, K., and Peters, J.-M. (2013). Aurora B and Cdk1 mediate Wapl activation and release of acetylated cohesin from chromosomes by phosphorylating Sororin. Proc. Natl. Acad. Sci. U.S.a. *110*, 13404–13409.

Nora, E.P., Goloborodko, A., Valton, A.-L., Gibcus, J.H., Uebersohn, A., Abdennur, N., Dekker, J., Mirny, L., and Bruneau, B. (2017). Targeted degradation of CTCF decouples local insulation of chromosome domains from higher-order genomic compartmentalization. bioRxiv 095802.

Nora, E.P., Lajoie, B.R., Schulz, E.G., Giorgetti, L., Okamoto, I., Servant, N., Piolot, T., van Berkum, N.L., Meisig, J., Sedat, J., et al. (2012). Spatial partitioning of the regulatory landscape of the X-inactivation centre. Nature *485*, 381–385.

Novak, B., Tyson, J.J., Gyorffy, B., and Csikasz-Nagy, A. (2007). Irreversible cell-cycle transitions are due to systems-level feedback. Nat. Cell Biol. *9*, 724–728.

Oehler, S., Eismann, E.R., Krämer, H., and Müller-Hill, B. (1990). The three operators of the lac operon cooperate in repression. Embo J. *9*, 973–979.

Ouyang, Z., Zheng, G., Song, J., Borek, D.M., Otwinowski, Z., Brautigam, C.A., Tomchick, D.R., Rankin, S., and Yu, H. (2013). Structure of the human cohesin inhibitor Wapl. Proc. Natl. Acad. Sci. U.S.a. *110*, 11355–11360.

Ouyang, Z., Zheng, G., Tomchick, D.R., Luo, X., and Yu, H. (2016). Structural Basis and IP6 Requirement for Pds5-Dependent Cohesin Dynamics. Mol. Cell *62*, 248–259.

Panizza, S., Tanaka, T., Hochwagen, A., Eisenhaber, F., and Nasmyth, K. (2000). Pds5 cooperates with cohesin in maintaining sister chromatid cohesion. Curr. Biol. *10*, 1557–1564.

Parelho, V., Hadjur, S., Spivakov, M., Leleu, M., Sauer, S., Gregson, H.C., Jarmuz, A., Canzonetta, C., Webster, Z., Nesterova, T., et al. (2008). Cohesins functionally associate with CTCF on mammalian chromosome arms. Cell *132*, 422–433.

Rankin, S., Ayad, N.G., and Kirschner, M.W. (2005). Sororin, a substrate of the anaphase-promoting complex, is required for sister chromatid cohesion in vertebrates. Mol. Cell *18*, 185–200.

Rao, H., Uhlmann, F., Nasmyth, K., and Varshavsky, A. (2001). Degradation of a cohesin subunit by the N-end rule pathway is essential for chromosome stability. Nature *410*, 955–959.

Rao, S.S.P., Huntley, M.H., Durand, N.C., Stamenova, E.K., Bochkov, I.D., Robinson, J.T., Sanborn, A.L., Machol, I., Omer, A.D., Lander, E.S., et al. (2014). A 3D map of the human genome at kilobase resolution reveals principles of chromatin looping. Cell *159*, 1665–1680.

Rao, S., Huang, S.-C., Hilaire, B.G.S., Engreitz, J.M., Perez, E.M., Kieffer-Kwon, K.-R., Sanborn, A.L., Johnstone, S.E., Bochkov, I.D., Huang, X., et al. (2017). Cohesin Loss Eliminates All Loop Domains, Leading To Links Among Superenhancers And Downregulation Of Nearby Genes. bioRxiv 139782.

Rees, D.C., Johnson, E., and Lewinson, O. (2009). ABC transporters: the power to change. Nat. Rev. Mol. Cell Biol. *10*, 218–227.

Remeseiro, S., Cuadrado, A., Kawauchi, S., Calof, A.L., Lander, A.D., and Losada, A. (2013). Reduction of Nipbl impairs cohesin loading locally and affects transcription but not cohesion-dependent functions in a mouse model of Cornelia de Lange Syndrome. Biochim. Biophys. Acta *1832*, 2097–2102.

Revenkova, E., Focarelli, M.L., Susani, L., Paulis, M., Bassi, M.T., Mannini, L., Frattini, A., Delia, D., Krantz, I., Vezzoni, P., et al. (2009). Cornelia de Lange syndrome mutations in SMC1A or SMC3 affect binding to DNA. Hum. Mol. Genet. *18*, 418–427.

Rohatgi, S., Clark, D., Kline, A.D., Jackson, L.G., Pié, J., Siu, V., Ramos, F.J., Krantz, I.D., and Deardorff, M.A. (2010). Facial diagnosis of mild and variant CdLS: Insights from a dysmorphologist survey. Am. J. Med. Genet. A *152A*, 1641–1653.

Roig, M.B., Löwe, J., Chan, K.-L., Beckouët, F., Metson, J., and Nasmyth, K. (2014). Structure and function of cohesin's Scc3/SA regulatory subunit. FEBS Lett. *588*, 3692–3702.

Rolef Ben-Shahar, T., Heeger, S., Lehane, C., East, P., Flynn, H., Skehel, M., and Uhlmann, F. (2008). Eco1-dependent cohesin acetylation during establishment of sister chromatid cohesion. Science *321*, 563–566.

Rollins, R.A., Morcillo, P., and Dorsett, D. (1999). Nipped-B, a Drosophila homologue of chromosomal adherins, participates in activation by remote enhancers in the cut and Ultrabithorax genes. Genetics *152*, 577–593.

Rowland, B.D., Roig, M.B., Nishino, T., Kurze, A., Uluocak, P., Mishra, A., Beckouët, F., Underwood, P., Metson, J., Imre, R., et al. (2009). Building sister chromatid cohesion: smc3 acetylation counteracts an antiestablishment activity. Mol. Cell *33*, 763–774.

Sanborn, A.L., Rao, S.S.P., Huang, S.-C., Durand, N.C., Huntley, M.H., Jewett, A.I., Bochkov, I.D., Chinnappan, D., Cutkosky, A., Li, J., et al. (2015). Chromatin extrusion explains key features of loop and domain formation in wild-type and engineered genomes. Proc. Natl. Acad. Sci. U.S.a. *112*, E6456–E6465.

Schmitz, J., Watrin, E., Lénárt, P., Mechtler, K., and Peters, J.-M. (2007). Sororin is required for stable binding of cohesin to chromatin and for sister chromatid cohesion in interphase. Curr. Biol. *17*, 630–636.

Sekiya, T., Muthurajan, U.M., Luger, K., Tulin, A.V., and Zaret, K.S. (2009). Nucleosome-binding affinity as a primary determinant of the nuclear mobility of the pioneer transcription factor FoxA. Genes Dev. *23*, 804–809.

Shimomura, O., Johnson, F.H., and Saiga, Y. (1962). Extraction, purification and properties of aequorin, a bioluminescent protein from the luminous hydromedusan, Aequorea. J Cell Comp Physiol *59*, 223–239.

Shirayama, M., Toth, A., Galova, M., and Nasmyth, K. (1999). APC(Cdc20) promotes exit from mitosis by destroying the anaphase inhibitor Pds1 and cyclin Clb5. Nature *402*, 203–207.

Skibbens, R.V., Corson, L.B., Koshland, D., and Hieter, P. (1999). Ctf7p is essential for sister chromatid cohesion and links mitotic chromosome structure to the DNA replication machinery. Genes Dev. *13*, 307–319.

Skibbens, R.V. (2009). Establishment of sister chromatid cohesion. Curr. Biol. *19*, R1126–R1132.

Sprague, B.L., Pego, R.L., Stavreva, D.A., and McNally, J.G. (2004). Analysis of binding reactions by fluorescence recovery after photobleaching. Biophysical Journal *86*, 3473–3495.

Stewart-Ornstein, J., and Lahav, G. (2016). Dynamics of CDKN1A in Single Cells Defined by an Endogenous Fluorescent Tagging Toolkit. Cell Rep *14*, 1800–1811.

Stigler, J., Çamdere, G.Ö., Koshland, D.E., and Greene, E.C. (2016). Single-Molecule Imaging Reveals a Collapsed Conformational State for DNA-Bound Cohesin. Cell Rep *15*, 988–998.

Stillman, B. (1993). DNA replication. Replicator renaissance. Nature *366*, 506–507.

Strunnikov, A.V., Larionov, V.L., and Koshland, D. (1993). SMC1: an essential yeast gene encoding a putative head-rod-tail protein is required for nuclear division and defines a new ubiquitous protein family. J. Cell Biol. *123*, 1635–1648.

Sudakin, V., Ganoth, D., Dahan, A., Heller, H., Hershko, J., Luca, F.C., Ruderman, J.V., and Hershko, A. (1995). The cyclosome, a large complex containing cyclin-selective ubiquitin ligase activity, targets cyclins for destruction at the end of mitosis. Mol. Biol. Cell *6*, 185–197.

Sumara, I., Vorlaufer, E., Gieffers, C., Peters, B.H., and Peters, J.M. (2000). Characterization of vertebrate cohesin complexes and their regulation in prophase. J. Cell Biol. *151*, 749–762.

Talbert, P.B., and Henikoff, S. (2006). Spreading of silent chromatin: inaction at a distance. Nat Rev Genet *7*, 793–803.

Tanaka, T.U., Stark, M.J.R., and Tanaka, K. (2005). Kinetochore capture and bi-orientation on the mitotic spindle. Nat. Rev. Mol. Cell Biol. *6*, 929–942.

Tedeschi, A., Wutz, G., Huet, S., Jaritz, M., Wuensche, A., Schirghuber, E., Davidson, I.F., Tang, W., Cisneros, D.A., Bhaskara, V., et al. (2013). Wapl is an essential regulator of chromatin structure and chromosome segregation. Nature *501*, 564–568.

Terakawa, T., Bisht, S., Eeftens, J.M., Dekker, C., Haering, C.H., and Greene, E.C. (2017). The condensin complex is a mechanochemical motor that translocates along DNA. Science *11*, eaan6516.

Terekawa, T., Bisht, S., Eeftens, J., Dekker, C., Haering, C., and Greene, E. (2017). The Condensin Complex Is A Mechanochemical Motor That Translocates Along DNA.

Teves, S.S., An, L., Hansen, A.S., Xie, L., Darzacq, X., and Tjian, R. (2016). A dynamic mode of mitotic bookmarking by transcription factors. Elife *5*, 1213.

Toth, A., Ciosk, R., Uhlmann, F., Galova, M., Schleiffer, A., and Nasmyth, K. (1999). Yeast cohesin complex requires a conserved protein, Eco1p(Ctf7), to establish cohesion between sister chromatids during DNA replication. Genes Dev. *13*, 320–333.

Uhlmann, F., and Nasmyth, K. (1998). Cohesion between sister chromatids must be established during DNA replication. Curr. Biol. *8*, 1095–1101.

Uhlmann, F., Lottspeich, F., and Nasmyth, K. (1999). Sister-chromatid separation at anaphase onset is promoted by cleavage of the cohesin subunit Scc1. Nature *400*, 37–42.

Uhlmann, F., Wernic, D., Poupart, M.A., Koonin, E.V., and Nasmyth, K. (2000). Cleavage of cohesin by the CD clan protease separin triggers anaphase in yeast. Cell *103*, 375–386.

Uhlmann, F. (2016). SMC complexes: from DNA to chromosomes. Nat. Rev. Mol. Cell Biol. *17*, 399–412.

Unal, E., Heidinger-Pauli, J.M., Kim, W., Guacci, V., Onn, I., Gygi, S.P., and Koshland, D.E. (2008). A molecular determinant for the establishment of sister chromatid cohesion. Science *321*, 566–569.

Uphoff, S., Sherratt, D.J., and Kapanidis, A.N. (2014). Visualizing protein-DNA interactions in live bacterial cells using photoactivated single-molecule tracking. J Vis Exp.

van de Linde, S., Löschberger, A., Klein, T., Heidbreder, M., Wolter, S., Heilemann, M., and Sauer, M. (2011). Direct stochastic optical reconstruction microscopy with standard fluorescent probes. Nat Protoc *6*, 991–1009.

van den Berg, D.L.C., Azzarelli, R., Oishi, K., Martynoga, B., Urbán, N., Dekkers, D.H.W., Demmers, J.A., and Guillemot, F. (2016). Nipbl Interacts with Zfp609 and the Integrator Complex to Regulate Cortical Neuron Migration. Neuron *0*.

Vietri Rudan, M., and Hadjur, S. (2015). Genetic Tailors: CTCF and Cohesin Shape the Genome During Evolution. Trends Genet. *31*, 651–660.

Walter, J., Schermelleh, L., Cremer, M., Tashiro, S., and Cremer, T. (2003). Chromosome order in HeLa cells changes during mitosis and early G1, but is stably maintained during subsequent interphase stages. J. Cell Biol. *160*, 685–697.

Wang, H., Yang, H., Shivalila, C.S., Dawlaty, M.M., Cheng, A.W., Zhang, F., and Jaenisch, R. (2013). One-step generation of mice carrying mutations in multiple genes by CRISPR/Cas-mediated genome engineering. Cell *153*, 910–918.

Wang, X., Brandão, H.B., Le, T.B.K., Laub, M.T., and Rudner, D.Z. (2017). Bacillus subtilis SMC complexes juxtapose chromosome arms as they travel from origin to terminus. Science *355*, 524–527.

Watrin, E., Schleiffer, A., Tanaka, K., Eisenhaber, F., Nasmyth, K., and Peters, J.-M. (2006). Human Scc4 is required for cohesin binding to chromatin, sister-chromatid cohesion, and mitotic progression. Curr. Biol. *16*, 863–874.

Webb, C.D., Teleman, A., Gordon, S., Straight, A., Belmont, A., Lin, D.C., Grossman,

A.D., Wright, A., and Losick, R. (1997). Bipolar localization of the replication origin regions of chromosomes in vegetative and sporulating cells of B. subtilis. Cell *88*, 667–674.

Wells, J.N., Gligoris, T.G., Nasmyth, K.A., and Marsh, J.A. (2017). Evolution of condensin and cohesin complexes driven by replacement of Kite by Hawk proteins. Current Biology *27*, R17–R18.

Wendt, K.S., Yoshida, K., Itoh, T., Bando, M., Koch, B., Schirghuber, E., Tsutsumi, S., Nagae, G., Ishihara, K., Mishiro, T., et al. (2008). Cohesin mediates transcriptional insulation by CCCTC-binding factor. Nature *451*, 796–801.

Wilhelm, L., Bürmann, F., Minnen, A., Shin, H.-C., Toseland, C.P., Oh, B.-H., and Gruber, S. (2015). SMC condensin entraps chromosomal DNA by an ATP hydrolysis dependent loading mechanism in Bacillus subtilis. Elife *4*, 11202.

Wutz, G., Varnai, C., Nagasaka, K., Cisneros, D.A., Stocsits, R., Tang, W., Schoenfelder, S., Jessberger, G., Muhar, M., Hossain, J.M., et al. (2017). CTCF, WAPL and PDS5 proteins control the formation of TADs and loops by cohesin.

Yang, H., Wang, H., Shivalila, C.S., Cheng, A.W., Shi, L., and Jaenisch, R. (2013). One-step generation of mice carrying reporter and conditional alleles by CRISPR/Cas-mediated genome engineering. Cell *154*, 1370–1379.

Yeeles, J.T.P., Deegan, T.D., Janska, A., Early, A., and Diffley, J.F.X. (2015). Regulated eukaryotic DNA replication origin firing with purified proteins. Nature *519*, 431–435.

Zhang, N., Kuznetsov, S.G., Sharan, S.K., Li, K., Rao, P.H., and Pati, D. (2008). A handcuff model for the cohesin complex. J. Cell Biol. *183*, 1019–1031.

Zuin, J., Franke, V., van Ijcken, W.F.J., van der Sloot, A., Krantz, I.D., van der Reijden, M.I.J.A., Nakato, R., Lenhard, B., and Wendt, K.S. (2014). A cohesin-independent role for NIPBL at promoters provides insights in CdLS. PLoS Genet. *10*, e1004153.